USDA United States Department of Agriculture

Forest Service

Rocky Mountain Research Station

General Technical Report RMRS-GTR-263

December 2011

High Resolution Interpolation of Climate Scenarios for the Conterminous USA and Alaska Derived from General Circulation Model Simulations

Linda A. Joyce, David T. Price, Daniel W. McKenney, R. Martin Siltanen, Pia Papadopol, Kevin Lawrence, and David P. Coulson

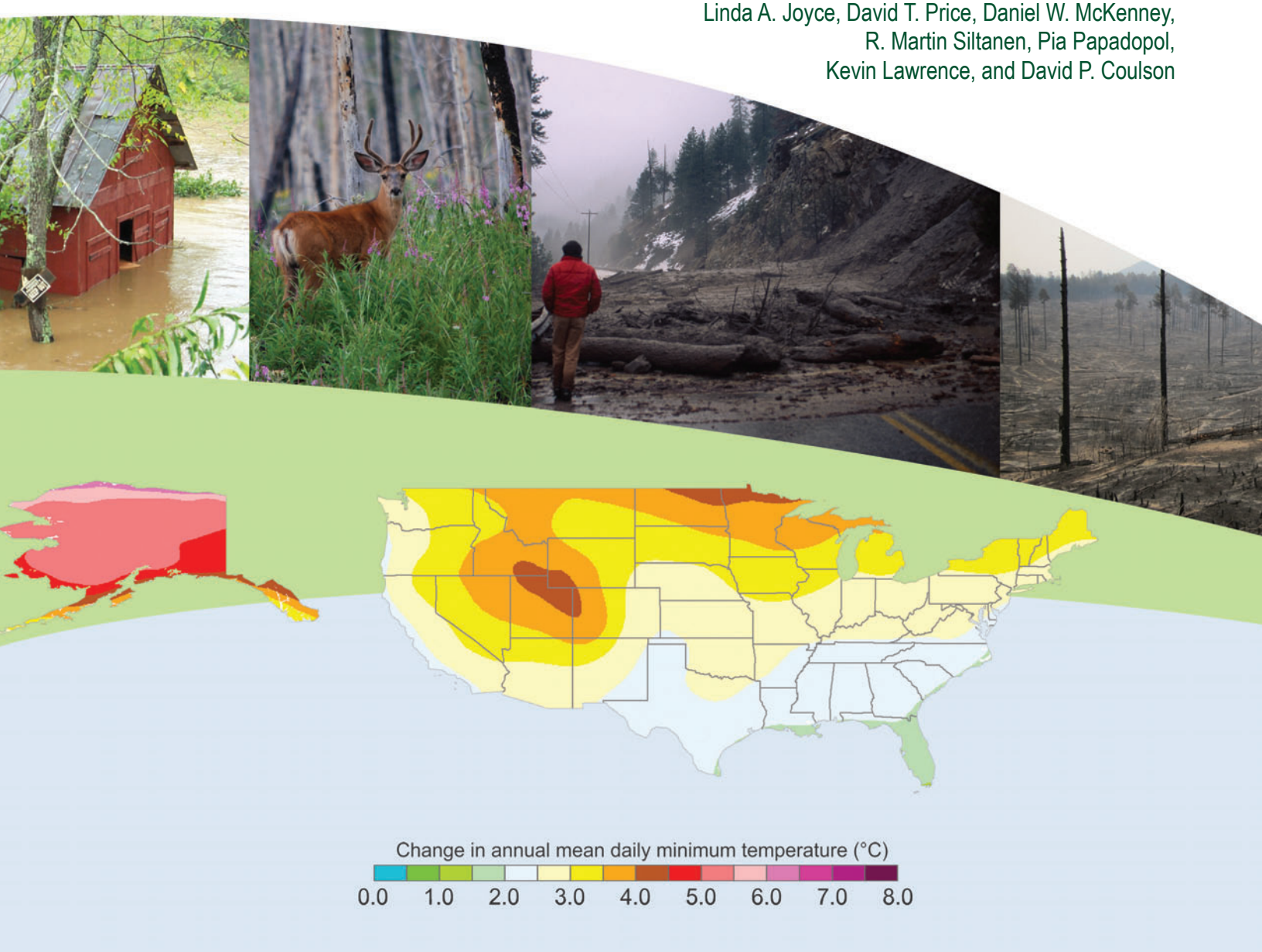

Published in partnership with the Canadian Forest Service, Northern Forestry Centre and Great Lakes Forestry Centre

Natural Resources Canada

Ressources naturelles Canada

Joyce, Linda A.; Price, David T.; McKenney, Daniel W.; Siltanen, R. Martin; Papadopol, Pia; Lawrence, Kevin; and Coulson, David P. 2011. **High Resolution Interpolation of Climate Scenarios for the Conterminous USA and Alaska Derived from General Circulation Model Simulations**. Gen. Tech. Rep. RMRS-GTR-263. Fort Collins, CO: U.S. Department of Agriculture, Forest Service, Rocky Mountain Research Station. 87 p.

Abstract

Projections of future climate were selected for four well-established general circulation models (GCM) forced by each of three greenhouse gas (GHG) emissions scenarios, namely A2, A1B, and B1 from the Intergovernmental Panel on Climate Change (IPCC) Special Report on Emissions Scenarios (SRES). Monthly data for the period 1961–2100 were downloaded mainly from the web portal of Third Coupled Model Intercomparison Project (Phase 3) of the Program for Climate Model Diagnosis and Intercomparison (PCMDI) and subsets of data covering North America were extracted. Climate variables included monthly mean daily maximum and minimum temperatures, precipitation, incident surface solar radiation, wind speed, and specific humidity. All variables were expressed as changes relative to the simulated monthly means for 1961–1990, which corrected for GCM bias in reproducing past climate and allowed future projected trends to be compared directly. The downscaling procedure used the ANUSPLIN software package to fit a two-dimensional spline function to each month's change data for each climate variable at a spatial resolution of 5 arcminutes (0.0833º) longitude and latitude. The A2 emission scenario invariably generated the greatest warming by 2100 and the B1 the least. Alaska is projected to undergo the greatest regional increases in temperature and precipitation. Differences across the projections were generally greater from the different GHG forcings than those resulting from the different GCMs, although the consistency varied spatially. Gridded datasets are publicly available. The downscaled change factors from this study are being used with historical climatology developed from the PRISM climate data set to develop the climate projections for the RPA scenarios in the USDA FS RPA assessment. A companion report and data set will be issued by Natural Resources Canada (Canadian Forest Service) for Canada.

Keywords: climate scenario, GCM, downscaling, interpolation, ANUSPLIN, National Center for Atmospheric Research, NCAR, Community Climate System Model, CCSM, Canadian Centre for Climate Modelling and Analysis, CCCma, Coupled Global Climate Model, CGCM, Commonwealth Scientific and Industrial Research Organisation, CSIRO, Climate System Model, Centre for Climate System Research, CCSR, National Institute for Environmental Studies, NIES, Model for Interdisciplinary Research on Climate, MIROC

You may order additional copies of this publication by sending your mailing information in label form through one of the following media. Please specify the publication title and number.

Publishing Services

Telephone	(970) 498-1392
FAX	(970) 498-1122
E-mail	rschneider@fs.fed.us
Web site	http://www.fs.fed.us/rmrs
Mailing Address	Publications Distribution Rocky Mountain Research Station 240 West Prospect Road Fort Collins, CO 80526

Authors

Linda A. Joyce, USDA Forest Service Rocky Mountain Research Station, Fort Collins, CO, USA

David T. Price, Natural Resources Canada, Canadian Forest Service, Northern Forestry Centre, Edmonton, AB, Canada

Daniel W. McKenney, Natural Resources Canada, Canadian Forest Service, Great Lakes Forestry Centre, Sault Ste Marie, ON, Canada

R. Martin Siltanen, Natural Resources Canada, Canadian Forest Service, Northern Forestry Centre, Edmonton, AB, Canada

Pia Papadopol, Natural Resources Canada, Canadian Forest Service, Great Lakes Forestry Centre, Sault Ste Marie, ON, Canada

Kevin Lawrence, Natural Resources Canada, Canadian Forest Service, Great Lakes Forestry Centre, Sault Ste Marie, ON, Canada

David P. Coulson, USDA Forest Service Rocky Mountain Research Station, Fort Collins, CO, USA

Acknowledgments

We acknowledge the modeling groups, the Program for Climate Model Diagnosis and Intercomparison, and the World Climate Research Programme's (WCRP) Working Group on Coupled Modelling for their roles in contributing and willingness to share the WCRP Coupled Model Intercomparison Project phase 3 (CMIP3) multi-model dataset through the web-based data portal. Support of this dataset is provided by the Office of Science, U.S. Department of Energy.

Further, we greatly appreciate the availability of data provided by:

- The Canadian Centre for Climate Modelling and Analysis
- The U.S. National Center for Atmospheric Research, and G Strand of the U.S. University Corporation for Atmospheric Research
- The Australian Commonwealth Scientific and Industrial Research Organisation, particularly M. Collier, M. Dix, and T. Hirst of the Marine and Atmospheric Research Division
- In Japan, the Center for Climate System Research, together with the University of Tokyo, the National Institute for Environmental Studies, and the Frontier Research Center for Global Change.

This research uses data provided by the Community Climate System Model (CCSM) project (www.ccsm.ucar.edu), supported by the Directorate for Geosciences of the National Science Foundation and the Office of Biological and Environmental Research of the U.S. Department of Energy. Any redistribution of CCSM data must include this data acknowledgment statement. Similarly, the authors request that any users of the scenario data presented in this report also provide appropriate acknowledgments to the respective modeling groups, as identified above.

We also acknowledge the support of the USDA Forest Service for this research.

We greatly appreciate the time and effort by reviewers: Louis Iverson, Nicholas Crookston, Alisa Gallant, Peter Thornton, Jorge Ramirez, Robert Bailey, Roger Simmons, and Ray Drapek; for editorial review: Lane Eskew; for graphics: Suzy Stephens; and for layout: Nancy Chadwick.

***Cover photo credits**:*

The Land Trust for the Little Tennessee River Valley, Macon County, NC., September 2004.

David P. Coulson, USFS. Deer on the White River near Trappers Lake, CO, 2011.

Karen Wattenmaker. Mud slide on the Lowman Road. Boise National Forest, ID, 1996. http://www.forestphoto.com/asset-bank/action/viewHome

C.D. Allen, USGS. View is of the headwaters of Sanchez Canyon in the Jemez Mountains on the Santa Fe National Forest, NM, 2011.

The cover figure is the change in annual mean daily minimum temperature (°C) from the 1961-1990 period to the 2041-2070 period for the A1B scenario.

Executive Summary

Researchers from the USDA Forest Service and the Canadian Forest Service (CFS) collaborated in the production of a suite of downscaled climate scenarios covering the continental United States and Canada to support the national assessment required by the U.S. Forest and Rangelands Renewable Resource Planning Act of 1974 (RPA). Each scenario was derived from a simulation carried out with a state-of-art general circulation model (GCM) for which results were available from the World Climate Research Programme's Coupled Model Intercomparison Project Phase 3 (CMIP3) through the Program for Climate Model Diagnosis and Intercomparison. The following four GCMs were selected on the basis of data available in 2008 and because they were well-recognized within the global GCM community: the Third Generation Coupled Global Climate Model, version 3.1, medium resolution (CGCM31MR), developed by the Canadian Centre for Climate Modelling and Analysis; Mark 3.5 Climate System Model (CSIROMK35) developed by the Australian Commonwealth Scientific and Industrial Research Organisation; the Model for Interdisciplinary Research on Climate, version 3.2, medium resolution (MIROC32MR) developed by the Japanese Centre for Climate System Research; and the Community Climate Model version 3.0 (NCARCCSM3) developed by the U.S. National Center for Atmospheric Research.

Monthly time-series data were obtained for each GCM, representing both the 20th century (1961–2000) and three scenarios of greenhouse gas (GHG) emissions for the 21st century developed for the Intergovernmental Panel on Climate Change (IPCC) Third and Fourth Assessment Reports, namely A2, A1B, and B1 of the Special Report on Emission Scenarios (SRES) (Nakićenović and others 2000). When these scenarios are used in global models, the potential future global mean surface warming ranges from a minimum of 1.8 °C associated with the B1 scenario, 2.8 °C for the A1B, to 3.4 °C in the A2 for 2090–2100 relative to 1980–1999 (IPCC 2007). In each case, data for simulated climate variables were downloaded and computer programs used to extract and manipulate subsets covering Canada and the continental United States (i.e., including Alaska but excluding Hawaii). The climate variables included monthly mean daily maximum and minimum temperatures, precipitation, incident surface solar radiation, and wind speed. Two other variables, monthly mean specific humidity and sea-level barometric pressure, were used to calculate monthly mean vapor pressure as a sixth variable. Each monthly value at each GCM grid node was normalized either by subtracting (temperature variables) or dividing by (other climate variables) the mean of that month's values for the 30-year period 1961–1990. The normalized data (or "deltas") were formatted for input to the ANUSPLIN thin-plate spline software of Hutchinson and co-workers at the Australian National University (Hutchinson 2010). ANUSPLIN was used to fit a unique two-dimensional spline "surface" function to each month's data for each of the six normalized climate variables. The fitted spline functions were, in turn, used to create gridded data sets for each monthly variable covering North America at a spatial resolution of 5 arcminutes (0.0833º) longitude and latitude on a geographic projection. Data for Alaska and the continental United States were extracted.

The normalization and interpolation procedures effectively removed model biases associated with the individual GCMs and allowed direct comparison of the downscaled projections for different GHG scenarios and different GCMs. This approach is consistent with requirements outlined in U.S. Forest Service memorandum ("Draft NEPA Guidance on Consideration of the Effects of Climate Change and Greenhouse Gas Emissions," released February 18, 2010, http://www.fs.fed.us/emc/nepa/climate_change/index.htm).

The downscaled data were analyzed, partly as a form of quality assessment and partly to demonstrate how the data can be used for national and regional studies of the impacts of climate change. The analysis explored spatial patterns of the climate projections across the United States, temporal patterns for specific variables at the regional scales, and the outlook for each region through tabular summaries of the future changes in the six climate variables at the regional scale. In the spatial analysis, results for selected variables were plotted as national maps of 30-year means for the three periods 2011–2040, 2041–2070, and 2071–2100 (or 2071–2099 in the case of NCARCCSM3), where the normalized data (deltas) were added to (for temperature variables) or multiplied by (for other variables) spatially interpolated climatological data for the 1961–1990 period. Temporal dynamics of the historical observed data (1961-2008) within regions were compared with the simulated historical data for each GCM as well as comparing future projections across the GCMs by climate variable for the 2001-2100 period. The conterminous states were divided into seven regions, based on the ecoregions (ecoclimatic divisions) identified in Bailey's (1995), with Alaska forming an eighth region. Area-weighted ecoregional means of the downscaled data were calculated for every monthly value for every climate variable in each of the 12 scenarios (four climate models with three SRES scenarios), and used to calculate seasonal and annual means and totals. These data were summarized by region for each climate variable and each GHG forcing scenario to create scatterplots comparing projected changes for the 2050s and 2090s. Summarized data for all four GCMs were averaged and further summarized in a comprehensive set of tables, to compare results of individual variables across regions and scenarios.

The MIROC32MR GCM projected a distinctly warmer and drier future under the A2 and A1B forcing scenarios for much of the eastern and southern United States, but in other respects the maps of projections for temperature and precipitation indicated the GCMs behaved rather similarly. Differences were generally too small (e.g., less than 1 °C), given the range of each variable at the continental scale, to allow them to be visually discriminated for the same forcing scenario and the same 30-year period. Accordingly a series of maps of the change fields was created. Each map showed the distribution of mean temperature increase (°C) or change in precipitation ratio relative to 1961–1990 for each of the three 30-year periods according to each GCM forced by the A1B emissions scenario. In these cases, the range of values was much narrower, which allowed a much easier comparison of the climate impacts according to each model.

The generally greater warming detected for MIROC32MR was confirmed all the way north into Montana and South Dakota, but ranking changes projected by the other three GCMs was difficult. For specific states (Nebraska and South Dakota), CGCM31MR projected the least warming, followed by CSIROMK35 and NCARCCSM3. In the south, however, NCARCCSM3 projected the least warming (though CGCM31MR was very similar). CSIROMK35 projected generally smaller temperature increases in the northwest, with CGCM31MR and NCARCCSM3 projecting progressively greater increases.

For precipitation, the southeastern states were projected to be markedly drier according to MIROC32MR compared to all other models, with this trend clearly apparent as early as 2010–2040 in the A1B scenario. In this region, Arkansas provided a ranking for precipitation change, with NCARCCSM3 projecting a general increase, CGCM31MR a smaller increase, and CSIROMK35 a slight decrease, by 2070–2099. NCARCCSM3 also projected precipitation declines in the west, particularly in the coastal states, and CGCM31MR indicated decreases in the southwest but slight increases in Oregon and Washington. CSIROMK35 projected large increases in precipitation inland, but smaller increases were projected by CGCM31MR in Montana, South Dakota, Nebraska, and Iowa. All models projected increases in precipitation for Alaska, particularly in the north.

The results of the analysis confirmed that the GCMs generally were in agreement, particularly with respect to temperature, precipitation, and solar radiation, both in terms of their relative responses to the different scenarios, and in the magnitudes of the changes projected for the 21st century. This is not to say the results agreed in all cases, but the different projections all were often consistent among the four models. Further, when historical records of temperature and precipitation were compared subjectively to the GCM results for the period 1961–2008, the magnitude and periodicity of interannual variations, as well as the overall trends in means, appeared very similar for all GCMs in all seasons and all regions. There was less consistency among the models in their projections of changes in interannual variability over the 21st century, but the differences were congruent among seasons.

Projections of changes in mean vapor pressure generally were consistent with projected increases in mean temperature, and often reflected the associated projected increases in seasonal and annual precipitation. Interestingly, increases in vapor pressure, particularly in summer, often were matched with the slight reductions in solar radiation, consistent with a warmer atmosphere holding more water vapor and hence creating generally cloudier conditions.

Wind speed data generally showed agreement among the models, projecting little change in either the interannual variability or in mean wind speeds under any of the GHG forcing scenarios. (Note this applied only at monthly time scales; changes in the distribution of wind speeds at daily or hourly time-scales were not investigated.)

In summary, the suite of 12 climate scenarios provides a range of potential future climates for assessing possible effects of a changing climate on natural resources, ecosystems, human infrastructure and communities. Each should be considered a "plausible" scenario for a specific set of assumptions captured in each GCM and in each of the emissions scenarios. The results are interpolated changes calculated with respect to 1961-1990 means, and gridded to a common format to facilitate handling and comparison among scenarios. The interpolated deltas for each monthly variable and grid will be made available through the archive website at the USDA FS Rocky Mountain Research Station website, as will the climate projections for each variable at the monthly time scale and the grid spatial scale (http://www.fs.fed.us/rm/data_archive/).

Table of Contents

Tables

High Resolution Interpolation of Climate Scenarios for the Conterminous USA and Alaska Derived From General Circulation Model Simulations

Linda A. Joyce, David T. Price, Daniel W. McKenney, R. Martin Siltanen, Pia Papadopol, Kevin Lawrence, and David P. Coulson

Introduction

The U.S. Forest and Rangeland Renewable Resources Planning Act (RPA) of 1974 requires a comprehensive assessment of the state of the U.S. renewable resources at 10-year intervals. This Act was amended in 1990 to require the U.S. Department of Agriculture to:

1. Assess impacts of climate change on the condition of renewable resources on forest and rangelands, and
2. Identify rural and urban forestry opportunities to mitigate the buildup of atmospheric carbon dioxide.

While previous RPA Assessments had examined the impact of climate change on forest production and the forest sector (Joyce 2007), the 2010 RPA National Renewable Resource Assessment uses an expanded framework for exploring the many drivers of change that affect natural resource production. In this framework, population, economics and climate projections are used to provide a range of future scenarios in which to explore future natural resource production. The RPA scenarios are based on the emissions scenarios developed in the Special Report on Emission Scenarios (SRES) (Nakićenović and others 2000) and used in the IPCC Third and Fourth Assessments Reports. Specifically, the emissions scenarios selected were SRES A2, A1B, and B2 (USDA FS, in review). While six emissions scenarios were developed in SRES, scenarios A2, A1B, and B1 have been the focus of model intercomparions studies (Meehl and others 2007) and the IPCC report (Randall and others 2007). Thus, no climate projections driven by the B2 scenario were available as part of the archiving efforts associated with the projections used in the Fourth Assessment; hence, B2 projection data was obtained from models used in the Third Assessment report (Joyce and others, in process).

As reported in the Intergovernmental Panel on Climate Change (IPCC) Fourth Assessment Report (AR4, e.g., http://www.ipcc.ch/ipccreports/ar4-wg1.htm), projections of the future global climate have been developed by numerous general circulation model (GCM) research groups around the world, using greenhouse gas (GHG) forcing scenarios recommended in the SRES (Nakićenović and others 2000). We focus here on the development of a suite of high resolution climate projections for the North American land surface (and enclosed water bodies) using a subset of the available AR4 GCM results for the A1B and A2 scenarios, with the specific aim of supporting the 2010 RPA assessment. The downscaled change factors from this study are being used to develop the climate projections of the RPA scenarions for the USDA FS RPA Assessment (USDA FS, in press). Downscaled projections for the AR4 B1 scenario are included in this study. We anticipate the products will be of great value to many other studies of the impacts of climate change at regional to continental scales.

There are several major limitations in using the GCM data that are directly available from recognized climate data archives, such as the IPCC Data Distribution Centre (IPCC-DDC, http://www.ipcc-data.org/) and the Program for Climate Model Diagnosis and Intercomparison (PCMDI, http://www-pcmdi.llnl.gov/). These limitations include the very coarse spatial resolution inherent in GCM output (typically to a separation of 100-400 km between grid nodes at mid-latitudes) and the need to extract data from huge global data sets for application to smaller regions. Further problems include determining which scenarios are representative of the range of future climates projected for North America and bringing the data into a common format to allow easy comparison when used for studies assessing the impacts of climate change.

This report provides a detailed description of the process to "downscale" the results of four different GCMs, operating at a range of spatial resolutions and forced by three different emissions scenarios, to a common spatial resolution. The downscaling approach described here follows that reported by Price and others (2004) and McKenney and others (2006c) and uses the ANUSPLIN thin-plate smoothing spline-interpolation technique, a method developed at the Australian National University over the last two decades (Hutchinson 2010). Results of this analysis covered Canada, Alaska, and the conterminous 48 states of the United States. Individual grid cells measured 5 arcminute (0.0833°) latitude and longitude, or approximately 10 km north-to-south.[1] Change factors (deltas) for each climate variable are reported as monthly departures from simulated monthly means for the 1961–1990 period. Data for six standard climate variables were developed in this way for the period from 1961 to 2100 (or 2099 in the case of the GCM developed by the National Center for Atmospheric Research): monthly mean daily maximum and minimum temperature, precipitation, solar radiation, vapor pressure, and wind speed. The advantage of this approach is that different historical climatologies can be used to construct projections of future climate. For this report, the historical climatology developed by McKenney and others (2007) was used. For the RPA scenarios, the historical climatology of PRISM is being used to construct climate projection data (e.g., Coulson and others 2010).

The data are available for state and other federal agencies, as well as private sector groups (e.g., forest and tourism industries, non-governmental organizations, and consultants), to use in studies of the effect of climate change on systems ranging from wildland management to agriculture to human health throughout the continental United States. The projection data sets are available at the USDA FS Rocky Mountain Research Station archive website [http://www.fs.fed.us/rm/data_archive/dataaccess/contents_datatype.shtml#MetClimate].

A companion report (Price and others 2011) provides a similar analysis for Canada to document the data sets available for climate change impacts research in that country. All data sets are freely available for use by researchers and others, on request from the authors at the CFS Northern Forestry Centre and Great Lakes Forestry Centre.

Objectives

1. Create a consistent set of climate projections from the output generated by four well-established general circulation models for the conterminous United States and Alaska forced by SRES A2, A1B, and B1 greenhouse gas emissions scenarios as defined in the IPCC Special Report on Emissions Scenarios (Nakićenović and others 2000).
2. Provide results as ASCII text file format 5 arcminute (~10 km) resolution geographic grids, each consisting of the change factor (as absolute difference [for temperature] and as a ratio [for all other climate variables]) for monthly mean daily minimum and maximum temperature, precipitation, solar radiation, wind speed, and vapor pressure.
3. Provide results as ASCII text file format 5 arcminute resolution geographic grids, each consisting of the monthly value of a single climate variable (temperature, precipitation, solar radiation, wind speed and vapor pressure).
4. Analyze the data sets generated in Objectives 2 and 3 to demonstrate and interpret similarities and differences among the general circulation models and emission scenarios for distinct regions of the United States and to highlight any problems discovered as a result of the downscaling procedures.

Methods

Review of Spatial Downscaling of Global Climate Simulations

Various approaches to downscaling GCM output differ in their complexity. The more sophisticated approaches include *dynamical* and *statistical* downscaling. Of these, dynamical approaches typically use higher resolution atmospheric circulation models (generally referred to as regional climate models, RCM) that operate over a relatively large region bounded by GCM grid cells. The atmospheric processes occurring within the RCM domain are forced by boundary conditions generated by the GCM at its usual time step. Within the RCM domain, higher resolution representation of surface topography and more detailed parameterization of some processes are intended to allow the model to generate physically

[1] Although we refer to the resolution as 10 km, this is a nominal dimension. In reality, a 5 arcminute grid cell is an approximate square measuring about 9.25 km on a side at the equator. Further, the east-west dimension decreases with the cosine of the latitude (i.e., as meridians converge toward the poles).

consistent simulations of weather and climate that can be validated against observed data. The validated model should be able to project more realistic regional climate than can be obtained from the GCM alone. In general, RCMs are expensive to operate and do not provide continuous long-term projections for multiple GCM scenarios (but see latest results of the North American Regional Climate Change Assessment Program, http://www.narccap.ucar.edu/results/rcm3-gfdl-results.html).

In contrast to dynamical downscaling, statistical downscaling is based on relationships among multiple local scale and larger scale meteorological observations that are used to interpret or modify the GCM outputs (e.g., Hashmi and others 2009), often by generating a distribution of values for the location of interest. There are three broad statistical approaches: weather typing, weather generators, and modeling by regression models, the last of which are also known as transfer functions (IPCC-TGICA 2007; Hashmi and others 2009; see also http://www.cics.uvic.ca/scenarios/index.cgi?More_Info-Downscaling_Background). Weather typing is based on statistical relationships between observed meteorological variables and a classification of synoptic weather patterns. The GCM-simulated changes in frequency and spatial distributions of these weather patterns are used to project changes in the same meteorological variables. Challenges with this approach include the known problem of underpredicting climate variability to varying degrees, a reflection of the choice of variables and predictor domain since only part of the regional and local climate variability is related to the large-scale climate variations (Fowler and others 2007). Additionally, the stationary relationship between the local observed variables and regional weather patterns has been shown questionable in the observed record (Fowler and others 2007), hence it also may not hold in the future (e.g., Conway and Jones 1998), which is a concern given the expectation of "novel" climates (e.g., Williams and others 2007).

Weather generators (e.g., Semenov and Barrow 1997; Wilks and Wilby 1999) are used to simulate the occurrence of high frequency climatic events, at daily or hourly time scales, typically for weekly or monthly climate statistics. Hence, such tools are not germane to spatial downscaling of GCM projections of monthly climate data, but they may be useful in impact studies that make use of data that have been spatially downscaled by another method.

Statistical transfer functions represent a range of linear or non-linear regression methods (the latter including approaches such as artificial neural networks and genetic algorithms) to relate large scale meteorological or climatic data (observed or generated by a GCM) to small scale climate variables (e.g., Wilby and others 2002, see also the bias-corrected spatial disaggregation approach [http://gdo-dcp.ucllnl.org/downscaled_cmip3_projections/dcpInterface.html#Welcome]). While some of these techniques are quite powerful, and many provide the capacity to estimate daily values (rather than monthly means) coupled with physically based predictions of changes in variability and the occurrence of extreme events, Hashmi and others (2009) noted the following limitation:

> *...there is no universal single statistical downscaling technique that works very well under all circumstances. According to the "Guidelines for Use of Climate Scenarios Developed from Statistical Downscaling Methods" (IPCC-TGICA 2004), the user should carefully select the downscaling method according to the nature of problem and predictands involved.*

Simpler and more transparent methods include using the GCM output directly (e.g., from the closest grid node) and spatial interpolation to finer resolution from latitude and longitude coordinates. Such methods have been adopted for interpolating both climate observations and GCM scenario output to fine spatial resolutions over large regions where it is generally impractical to apply statistical downscaling methods. Typically, the GCM data are normalized to a historical reference period so that bias in the GCM's estimates of observed values can be removed, an approach sometimes referred to as the *delta method*. Because GCMs typically have very low horizontal resolution (see Figure 1), their representation of topographic effects on local climate is necessarily poor. For this reason, the normalized and interpolated GCM data ("delta values") should be combined with observed climatological data for the reference period interpolated to the same resolution. This approach provides a more localized correction to the climate scenario.

Interpolation of Climate Data Using ANUSPLIN

In this study, the monthly data values of GCM output were treated as simulated records of a 'virtual climate station' located at GCM grid-node coordinates and were used to develop an interpolated surface of the climatology at the spatial scale of interest using the ANUSPLIN software developed at the Australian National University by Hutchinson and co-workers (e.g., Hutchinson 2010). This software has been used widely for estimating observed climate data as grids (or at specific locations), often, but not always, identified by latitude, longitude, and

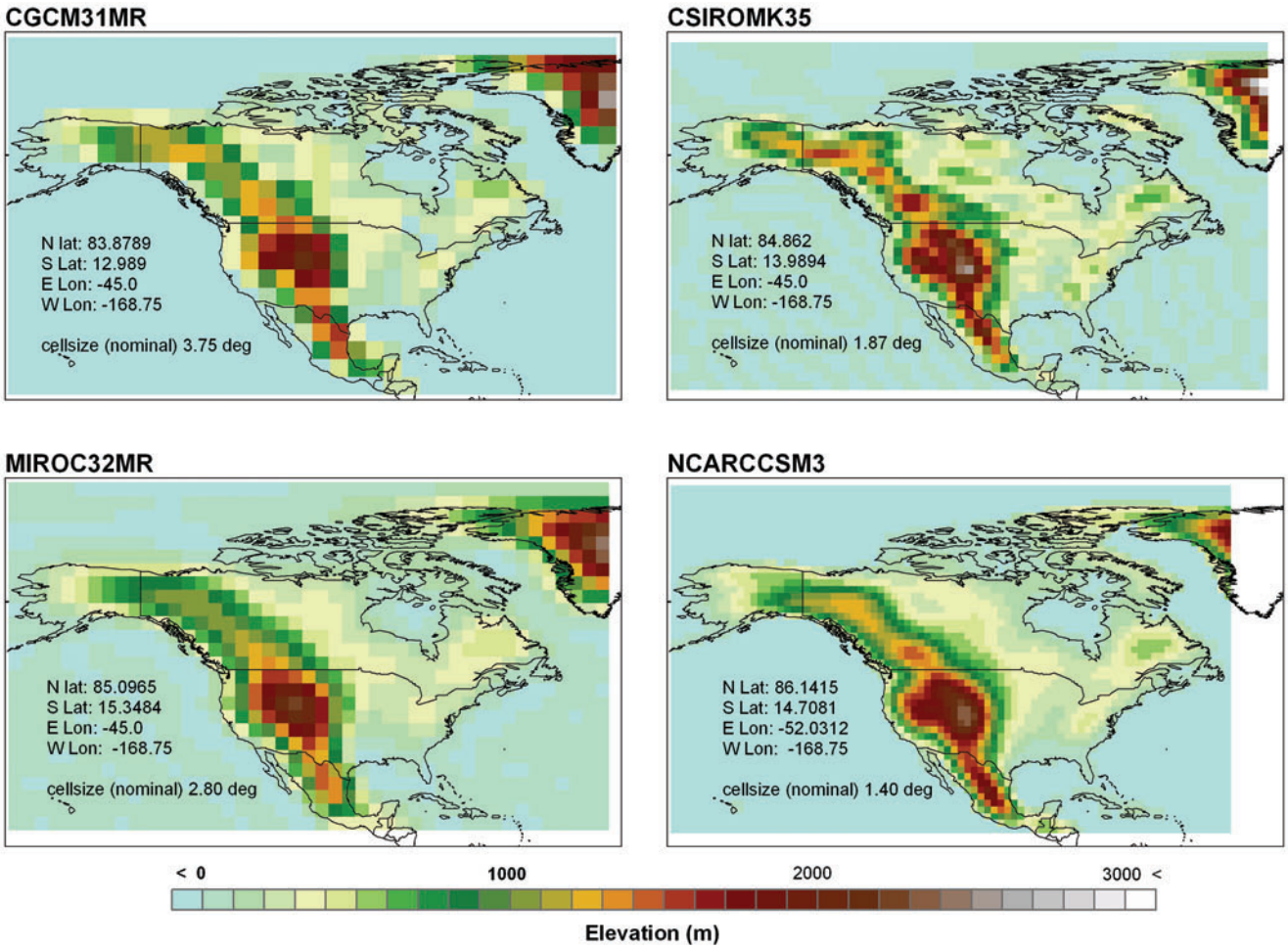

Figure 1. Comparison of grid cell elevations for the four GCMs used in this study from which simulation data were used in the downscaling procedures. Note the differences in horizontal resolution, from CGCM31MR (coarsest) to NCARCCSM3 (finest), and also the peak elevations achieved in the CSIROMK35 grid are higher than those in the NCARCCSM3 grid because the NCARCCSM3 elevation grid is more highly smoothed. For CSIROMK35 and MIROC32MR, some ocean pixels have nonzero values. Latitude and longitude values represent the boundaries of the area for the downscaling analysis with each model. CGCM31MR = Third Generation Coupled Global Climate Model, version 3.1, medium resolution; CSIROMK35 = Commonwealth Scientific and Industrial Research Organisation Climate System Model, Mark 3.5; MIROC32MR = Model for Interdisciplinary Research on Climate, version 3.2; NCARCCSM3 = Community Climate System Model, version 3.0.

elevation. The software has been applied in many individual countries (e.g., Hutchinson 1995, 1998a, 1998b), including Canada (Price and others 2000; McKenney and others 2001, 2004; Hutchinson and others 2009), United States (Rehfeldt 2006) and globally (New and others 2002; Hijmans and others 2005).

The theory of ANUSPLIN has been described elsewhere (e.g., Hutchinson and Gessler 1994; Hutchinson 1995, 1998a, 1998b, 2010; Hutchinson and others 2009), and briefly in McKenney and others (2004), and will not be discussed in detail here. Thin-plate splines can be described as a multi-dimensional nonparametric curve-fitting technique although ANUSPLIN can be configured in other ways. For interpolation of climate data, the target climate variable generally is modeled as a function of various spatially varying dimensions (typically position, as represented by latitude and longitude, and topography, as represented by appropriately scaled elevation). ANUSPLIN has been applied to many climate variables at temporal resolutions ranging from a single day, to a month, and extending to long-term mean, such as a 30-year monthly normal.

Price and others (2000) and McKenney and others (2001) showed that ANUSPLIN performs extremely well for mean values of monthly temperature, precipitation, observed over periods of 30 years or more. ANUSPLIN also has been successfully used to carry out interpolations of monthly time-series data and time series at shorter time scales (weeks to days) (McKenney and others 2006b; Hutchinson and others 2009). It is recognized, however, that the inherently patchy nature of precipitation (both in time and space) generally reduces the confidence of precipitation models as compared with temperature models (Kang and Ramírez 2010). McKenney and coworkers in the CFS have invested considerable effort (in close collaboration with Hutchinson at Australian National University) to develop high resolution climatologies covering the continental United States and Canada (e.g., McKenney and others 2006b, 2007; Hutchinson and others 2009).

Price and others (2001, 2004) and Price and Scott (2006) were the first to report the use of ANUSPLIN as a method of downscaling GCM climate projections. The improvements by McKenney and Hutchinson (e.g., McKenney and others 2006a, 2006b) were extended to interpolate time series of GCM output data as functions of grid node latitude and longitude, with treatment of the data values simulated for each grid node as if they were climate observations at the grid node location. Interpolated climate scenarios, derived from GCM data produced for the IPCC Third Assessment Report, were documented in Price and others (2004) and McKenney and others (2006c). A range of climate data products has since been developed and made widely available both from the CFS Great Lakes Forestry Centre based in Ontario and the CFS Northern Forestry Centre in Alberta.

Price and others (2001) carried out several experiments to investigate various ANUSPLIN models and settings for spatial interpolation of GCM output, in particular relating to the use of elevation as a third independent variable. Diagnostics produced by ANUSPLIN in those tests showed relatively little impact of GCM grid-cell elevation on the resulting spline function, likely because elevation typically is averaged across an entire GCM grid cell such that high mountains are reduced to relatively lower-altitude plateaus. Hence the influence of elevation on, for example, temperature, precipitation, and wind speed currently is not well captured in GCMs. This concern will need to be revisited as the spatial resolution of GCMs increases. In the present study, the four GCMs generated climate output at scales ranging from 300–400 km (e.g., Canadian Third Generation Coupled Global Climate model, version 3.1, medium resolution, CGCM31MR) to 100–150 km (e.g., Community Climate System model, version 3.0, of the U.S. National Center for Atmospheric Research, NCARCCSM3). For these reasons, the interpolations of all GCM results presented here use only longitudinal and latitudinal gradients with a "fixed signal." It should be noted that each downscaled GCM projection is reported as *change factors* (i.e., delta values) from the means of the data simulated by the same GCM for 1961–1990, as a way of normalizing the data for any inherent bias between the model and reality (i.e., to remove bias in projected means, although not necessarily in the projected interannual variation). The intention is that these change factors will be combined with interpolated normals of *observed* climate for the period 1961–1990—which necessarily should account for topographic/elevation effects. In this way, the effects of local spatial variability on real climate are captured and can be combined with the trends in climate projected by the GCMs.

The simulated climate variables to be interpolated in this study were monthly means of daily surface temperature (minimum and maximum, denoted T_{min} and T_{max}, respectively), global downward solar radiation, wind speed, and monthly precipitation. Monthly mean atmospheric vapor pressure was estimated from the simulated monthly mean specific humidity and sea-level barometric pressure. The monthly values (including calculated vapor pressure data) were converted to monthly *change factors* with the means of the simulated monthly values for the 30-year period 1961–1990 used as a reference point. In the case of T_{min} and T_{max}, the change factor was computed as the arithmetic *difference* between the monthly value and the corresponding 30-year mean of the same temperature variable for that month. For all other variables, the change factor was the *ratio* of the monthly value to mean for that month over the period 1961–1990.

The change factors were interpolated using the ANUSPLIN software to create time series for the period over which the AR4 simulations were carried out (generally from 1961 to 2100). An ANUSPLIN model was generated for each monthly variable, which was used to create gridded data covering North America at a spatial resolution of 5 arcminutes. It should be noted that the grids are simply a convenient expression of the fitted spline function mapped over the region of interest. The spline functions have been archived and can, in principle, be used to estimate monthly values at any location given only latitude and longitude.

Selection of Forcing Scenarios for GHG Emissions

The choice of GHG emissions scenarios (used to "force" a GCM's simulation of future climate) was limited to three global economic-demographic storylines, as described in the SRES (Nakićenović and others 2000) and used in the IPCC AR4 reports: A2, A1B, and B1 (see also http://www.ippc.ch/publications_and_data/ar4/wg1/en/contents.html). When these scenarios are used in global models, the potential future global mean surface warming ranges from 1.8 °C associated with the B1 scenario, 2.8 °C for the A1B, and 3.4 °C for the A2 scenario for 2090–2100 relative to 1980–1999 (IPCC 2007).

In addition, output from each GCM was downloaded for an additional scenario, the 20C3M scenario. This fourth scenario represents the model's attempt to simulate historical climate for the 20th century, on the basis of known atmospheric forcings (GHG concentrations, ozone depletion, aerosols including those caused by volcanic eruptions, and variations in solar output). For most climate models, 20C3M scenario results were made available only for the period 1961–2000, which is sufficient to allow the 1961–1990 period as a reference point for normalizing the future scenario data (see below).

For the current project, results were selected from the Coupled Model Intercomparison Project Phase 3 (CMIP3) data at the Program for Climate Model Diagnosis and Intercomparison web portal at https://esg.llnl.gov:8443/index.jsp,as simulated by each of the following GCMs (see Figure 1 for comparison of resolution; note "T" values reported in parentheses refer to the triangular truncation of the spectral transformations of each model's horizontal spherical harmonic functions; see also Appendix 1.):

- CGCM31MR – Third Generation Coupled Global Climate Model, version 3.1, medium resolution (T47), developed by the Canadian Centre for Climate Modelling and Analysis http://www.cccma.bc.ec.gc.ca/models/cgcm3.shtml
- CSIROMK35 – Climate System Model, Mark 3.5 (T63), developed by the Commonwealth Scientific and Industrial Research Organisation, Australia http://www.cmar.csiro.au/e-print/open/gordon_2002a.pdf; http://www-pcmdi.llnl.gov/ipcc/model_documentation/CSIRO-Mk3.5.htm
- MIROC32MR – Model for Interdisciplinary Research on Climate, version 3.2, medium resolution (T42), developed by the Japanese Center for Climate System Research, University of Tokyo, National Institute for Environmental Studies, and Frontier Research Center for Global Change http://www.ccsr.u-tokyo.ac.jp/kyosei/hasumi/MIROC/tech-repo.pdf
- NCARCCSM3 – Community Climate System Model, version 3.0 (T85), developed by the U.S. National Center for Atmospheric Research http://www.ccsm.ucar.edu/models/ccsm3.0/

The use of these distinct and well-established GCMs ensured the downscaled scenarios met recommended criteria for selecting and using scenarios for climate change impacts studies (IPCC-TGICA 2007), including:

- Consistency of global projections and representative of the potential range of future regional climate change;
- Physically plausible and consistent, because multiple climate variables including radiation, humidity, and wind speed were to be interpolated for each GCM scenario separately and provided in each data set;
- Applicable for impacts assessment, because the downscaled scenario data were reported as change factors that can be referenced to locally observed climate data.

At the time this work commenced, many climate modeling groups were carrying out simulations for the various SRES scenarios; however, relatively few of these groups had made data sets available for all three scenarios. This restricted the choice of GCMs quite severely, and it proved necessary to locate some data from sources other than the CMIP3 database for three of the four models selected (see Table 1). Furthermore it was critically important that when locating simulation results from different sources, they be from the same realization of each model for each GHG forcing scenario. Table 2 summarizes the realizations (runs) that were selected for each GCM from the CMIP3 database.

Downloading, extraction, and processing GCM data:

Standardized procedures for processing the GCM data sets were developed following those reported in Price and others (2004). These procedures were built around interpolation of GCM output data using ANUSPLIN, where the monthly data values were treated as simulated records obtained from a "virtual climate station" located at the GCM grid node coordinates.

Because the conversion and extraction processes, described in the following paragraphs, had to be carried out many times (approximately 40 repetitions for each GCM), the processing programs were run on multiple Linux-based computers, controlled by Unix shell

Table 1. General circulation model (GCM) data sets for scenarios from the Fourth Assessment Report of the Intergovernmental Panel on Climate Change used to create input files for interpolation by ANUSPLIN software.

GCM[1]	SRES scenario	Monthly variables[2]	Source[3]	Time period
CGCM31MR	20C3M, A2. A1B, B1	tas,pr, rsds, uas, vas, hur, huss, psl	CMIP3	1961–2100
CGCM31MR	20C3M, A2, A1B, B1	tasmin, tasmax	CCCma	1961–2100
CSIROMK35	20C3M, A2, A1B, B1	tas, tasmin, tasmax, pr, rsds, uas, vas, hur, huss (except B1), psl	CMIP3	1961–2100
CSIROMK35	B1	Huss	CSIRO	2001–2100
MIROC32MR	20C3M, A2, A1B, B1	tas, tasmin, tasmax, pr, rsds, uas, vas, hur, huss, psl	CMIP3	1961–2100
NCARCCSM3	20C3M, A1B, B1	tas, tasmin, tasmax, pr, rsds, hur, huss, uas, vas, psl	CMIP3	1961–2099
NCARCCSM3	A2	tas, tasmin, tasmax, pr, rsds, uas, vas, hur, huss, psl	ESG	1961–2099

[1] CGCM31MR = Third Generation Coupled Global Climate Model, version 3.1, medium resolution; CSIROMK35 = Commonwealth Scientific and Industrial Research Organisation Climate System Model, Mark 3.5; MIROC32MR = Model for Interdisciplinary Research on Climate, version 3.2; NCARCCSM3 = Community Climate System Model, version 3.0.

[2] **Simulated climate variables (as defined by Program for Climate Model Diagnosis and Intercomparison):**
tas – mean 2-m air temperature (K)
tasmin – mean daily minimum 2-m air temperature (K)
tasmax – mean daily maximum 2-m air temperature (K)
pr – monthly precipitation (kg m^{-2} s^{-1})
rsds – surface downwelling shortwave radiation (W m^{-2})
uas – zonal wind velocity (m s^{-1})
vas – meridional wind velocity (m s^{-1})
hur – relative humidity (%)
huss – surface specific humidity (kg kg^{-1})
psl – sea level pressure (Pa).

[3] Most data were downloaded from the WCRP Coupled Model Intercomparison Project Phase 3 (CMIP3) at the data portal hosted by the Program for Climate Model Diagnosis and Intercomparison at httsp://eqg.llnl.gov:83443/index.jsp. This "multi-model data set" is archived by the Program for Climate Model Diagnosis and Intercomparison. The major advantage to using CMIP3 data was their standardization of format, variable names, units, and other aspects, which facilitated comparison among models. The Canadian Centre for Climate Modelling and Analysis (CCCma) website serves data for CGCM31MR and other Canadian climate models (http://www.cccma.bc.ec.gc.ca/data/cgcm3/cgcm3.shtml). Daily Tmin and Tmax data for CGCM31MR were obtained from this source because they were not available from CMIP3. The University Corporation for Atmospheric Research (UCAR), Earth System Grid (ESG) data portal (http://www.earthsystemgrid.org) serves data standardized to the specifications of the US national Center for Atmospheric Research model. The complete and consistent NCARCCSM3 data set for the A2 scenario was only available from ESG. CSIRO = Commonwealth Scientific and Industrial Research Organisation.

scripts. These scripts (developed in-house) were edited specifically for each GCM, to account for the different spatial resolutions covering the North American domain (as shown in Figure 1) and for other differences in the contents of the data files.

The following major steps were used in preprocessing the data for interpolation by ANUSPLIN.

Step 1. Global orography datasets for each GCM were downloaded and used to create sets of grid cell coordinates, which were stored in three individual comma-separated value (CSV) format files: elevs_world.csv, lats_world.csv, and lons_world.csv. Elevation data contained in elevs_world.csv needed to be "naturally oriented" (i.e., west-to-east and north-to-south). The global grids for all

Table 2. Realization (or run) numbers for each general circulation model and greenhouse gas forcing scenario in the Coupled Model Intercomparison Project (CMIP3) catalog that was selected for interpolation using ANUSPLIN in this study.

Model and scenario	Run number	Time Stamp[1]
CGCM31MR[2]		
20C3M	Run 5	reformatted 2005-05-12—22:21:09
A2	Run 5	reformatted 2005-05-12—22:21:09
A1B	Run 5	reformatted 2005-05-12—22:21:09
B1	Run 5	reformatted 2005-05-12—22:21:09
CSIROMK35[3]		
20C3M	Run 1	2006-09-20—05:09
A2	Run 1	2006-09-20—04:09
A1B	Run 1	2006-11-04—10:04
B1	Run 1	2006-09-20—04:09
MIROC32MR[4]		
20C3M	Run 3	reformatted 2004-10-14—20:53:37
A2	Run 3	reformatted 2004-12-14—00:22:38
A1B	Run 3	reformatted 2004-12-14—00:02:09
B1	Run 3	reformatted 2004-12-14—00:53:41
NCARCCSM3[5]		
20C3M	b30.030e (Run 5)	2004-10-18—12:38:54 MDT
A2	b30.042e (Run 5)	2004-11-28—15:15:39
A1B	b30.040e (Run 5)	2004-12-09—12:52:07 MST
B1	b30.041e (Run 5)	2005-01-26—11:05:29 EST

[1] Date and time information extracted from available metadata for the run. MDT = mountain daylight time, MST = mountain standard time, EST = eastern standard time.
[2] CGCM31MR = Third Generation Coupled Global Climate Model, version 3.1, medium resolution.
[3] CSIROMK35 = Commonwealth Scientific and Industrial Research Organisation Climate System Model, Mark 3.5.
[4] MIROC32MR = Model for Interdisciplinary Research on Climate, version 3.2.
[5] NCARCCSM3 = Community Climate System Model, version 3.0.

four GCMs were flipped north-to-south (which meant that the processing programs had to invert them), with the west-most column at 0° longitude. The longitude coordinates stored in lons_world.csv were converted to their negative equivalent (e.g., 240.0° = 120.0° W = -120.0°). Given that the data sets provided global coverage, latitude values for the southern hemisphere stored in lats_world.csv were also converted to their negative equivalents. These CSV data files were copied to the working directory used to extract data for the North American rectangle (Figure 1).

Step 2. GCM data files (for each climate variable and each of the four scenarios) were downloaded generally in NetCDF format. The downloaded files were renamed to a systematic format to ensure models and scenarios were uniquely identified and to facilitate subsequent manipulation.

Step 3. Global data for each climate variable was extracted from the NetCDF files using a script (developed in-house) called nc-readvar_to_asg.txt, which then called program nc-readvar to convert data for each variable to ASCII with GRIB-format headers (a single line at the top of the data for each monthly time step, containing information about the time step and grid dimension information, as described at http://cera-www.dkrz.de/IPCC_DDC/info/Readme.grbconv). These output files were called "ASCII grids," to reflect the use of ASCII text and to refer to the data content organized on a standard geographic grid. The files were identified with the same names as used for the input NetCDF files but with the extension "asg" suffix to replace the extension "nc."

Step 4. Data for wind speed were extracted for those GCMs with data files containing multiple atmospheric pressure levels. Further scripts were used to call several

programs, described below, to extract the required data and combine them with the GCM grid node elevations to obtain estimates of wind velocity at the surface elevation of the GCM. Scripts called merge_ua.txt, and combine_merge_ua.txt were used for the zonal (U) component of wind velocity. Scripts called merge_va.txt, and combine_merge_va.txt were used for the meridional (V) wind velocity component. These programs used to extract data and their specific functions were as follows:

nc-readvar	Extract data from NetCDF file at multiple pressure levels and convert to ASCII grids for each month;
cat	Concatenate ASCII data from multiple months and a single pressure level into a single time series;
asg2nc	Convert an ASCII time series into a NetCDF file containing the time series for a single pressure level; and
nc_merge	Merge data from multiple pressure levels into a single surface (i.e., where the grid-cell elevations are sufficiently high to penetrate above the bottom atmospheric pressure levels in the GCM data file). This program has switches (--or --inclusive) to allow retention of existing surface level values as they are merged with data from progressively higher atmospheric levels.

For all GCMs, the *U* and *V* wind velocity component vectors of wind velocity were combined to calculate mean wind speed (u) using the hypotenuse calculation:

$$u = \sqrt{U^2 + V^2} \quad [1]$$

Another script, extract_merged_to_asg.txt, which again called nc-readvar, was run to create ASCII files with GRIB headers from the merged data.

Step 5. Data for the North American rectangles (including the western part of Greenland, Figure 1) were extracted from the global NetCDF data files using a script called do_gcm_subsetXXxYY.txt and from the merged global ASCII files using a script called do_gcm_subsetXXxYY_merged.txt, where XX and YY are the longitudinal and latitudinal grid dimensions, respectively, of the GCM-specific rectangle. The do_gcm_subsetXXxYY.txt script first converted the NetCDF file into ASCII format. Both scripts then called the program gcm_subset to extract the desired North American spatial subset from the global ASCII files. Most GCM grids were "flipped" meaning the data are organized with the southern-most grid cells at the top, so it was necessary to check for flipping and reverse as appropriate. The gcm_subset program defaults to handle the flipped grid orientation correctly, but flipping can be suppressed with a -F switch. Output files generated by gcm_subset had a suffix added to the input file name of the generic format ".XXxYY.subset." For each GCM, gcm_subset also produced the corresponding subsets of the elevs-world.csv, lats-world.csv, and lons-world.csv files that were needed to generate the grid-node coordinate information when formatting the data for input to ANUSPLIN.

Because the spatial domains, grid resolutions, and output variables differed among the four GCMs, some model-specific details are provided in the following paragraphs (see also Figure 1 and Appendix I):

CGCM31MR. The global domain consists of 96 longitudinal × 48 latitudinal cells, yielding nominal grid-cell dimensions of 3.75° longitude by 3.75° latitude at the equator. Although the longitudinal angular dimensions are constant for all grid cells in common with most GCMs, the latitudinal angular dimensions vary with latitude. Within this model, generation of a subset for North America produced a rectangular grid of 20 cells north-to-south and 34 cells east-to-west with northerly and southerly boundaries at 83.8789° N and 12.989° N, respectively, and westerly and easterly boundaries at 168.75° W and 45.0° W, respectively. For CGCM31MR, the variables tasmax and tasmin (defined in Table 1) were available only as daily data. These daily files were downloaded, spatial subsets were created, and the data were averaged for each month to obtain the monthly mean daily values before continuing with Step 6.

CSIROMK35. The global domain consists of 192 longitudinal × 96 latitudinal cells, yielding a nominal grid-cell size of 1.875° longitude × 1.865° latitude at the equator. Generation of a subset for North America produced a rectangular grid of 39 cells north-to-south and 67 cells east-to-west with boundaries at 84.862° N, 13.9894° N, 168.75° W and 45.0° W, respectively.

MIROC32MR. The global domain consists of 128 longitudinal cells × 64 latitudinal cells, yielding a nominal grid-cell size of 2.81° longitude × 2.79° latitude at the equator. Generation of a subset for North America produced a rectangular grid of 26 cells north-to-south and 45 cells east-to-west, with boundaries at 85.0965° N, 15.3484° N, 168.75° W and 45.0° W, respectively.

NCARCCSM3. The global domain consists of 256 longitudinal cells × 128 latitudinal cells, yielding a nominal grid-cell size of 1.40625° longitude × 1.400768° latitude at the equator. Generation of a subset for North America produced a rectangular grid of 52 cells north-to-south and 84 cells east-to-west, with boundaries at 86.1415° N, 14.7081° N, 168.75° W and 52.0312° W, respectively.

Step 6. The subsets of monthly GCM data grids were converted into the columnar format used for input to ANUSPLIN: annual data blocks, each comprising fields for the latitude, longitude, and elevation of the grid node followed by 12 monthly climate values, sorted by lines in latitude and longitude order. This procedure was carried out using program gcm_processor, called by a script named gcmprocessor_GCM_XXxYY.txt, where "GCM" represents the name of the GCM and "XXxYY" represents the longitudinal and latitudinal dimensions (i.e., number of grid cells) of its North American rectangle, respectively. The main function of gcm_processor was to normalize the GCM data in a two-pass procedure. On the first pass, gcm_processor was run using the GCM's twentieth century (20C3M) results as input, to calculate 30-year means for each month during the simulated period 1961–1990. On the second pass, these calculated means were then used to convert the GCM output from projections of absolute values to change factors *relative to the 1961–1990 means*. These means were applied to the GCM projections (A2, A1B, B1). In the case of temperature variables, the change factors were calculated by *subtracting* the means from the monthly values. For all other climate variables, the change factors were calculated by *dividing* the monthly values by the simulated 1961–1990 means. The multi_gcmproc.txt script called multiple instances of gcmprocessor_GCM_XXxYY.txt so that data for all climate variables for a single GHG emissions scenario could be handled in a single process. Specific versions of both batch files were created for each GCM and emissions scenario, which also accounted for the period of the simulation (1961–2099 for NCARCCSM3; 1961–2100 for the other three GCMs). Each output file generated by multi_gcmproc.txt contained data for a single climate variable and a single year, because ANUSPLIN treats each month of each year as an independent data set.

Step 7. In the particular case of simulated atmospheric humidity, the preferred measure was vapor pressure (denoted e), which required conversion from other humidity terms simulated by the GCMs. After much searching, complete error-free data sets of simulated specific humidity (denoted H_s) at surface elevation were obtained, though data for only 10 of the 12 GCM projections were available from the CMIP3 database. One exception was the NCARCCSM3 model forced by the A2 emissions scenario, for which there were acknowledged errors, including the complete absence of data for the 2070s, and some very high values occurring every January at several locations around the globe (including all grid cells at the South Pole and two small groups of adjacent cells in North America). The use of surface relative humidity instead of H_s to calculate vapor pressure was considered, but these data also were also missing for the 2070s decade.

Subsequently, a complete time series of surface H_s data was located at the Earth System Grid data portal of the University Corporation for Atmospheric Research, although this data set also had the problem with extreme values at two locations in North America and elsewhere. To overcome this problem, a new routine was added to gcm_processor, which scanned all of the data in each month for values that were excessively high (values of 650,000 to 750,000 rather than the typical values, on the order of 0.001 kg kg^{-1}). Whenever the scanning algorithm located a grid cell containing an over-range value, the value was replaced by the mean of the values in the adjacent grid cells, excluding any that were themselves over-range. Because the search algorithm worked from northwest to southeast, the means of some grid cells were derived from interpolated means in adjacent cells to the north and west. Under the circumstances, this seemed like a necessary but minor compromise to provide the consistent data set needed for the ANUSPLIN interpolation to be carried out successfully.

Precipitation amounts simulated by GCMs are often highly correlated with the simulated humidity in the same or adjacent grid cells. However, no precipitation data that were clearly over range were found in the NCARCCSM3 data for the months affected by the specific humidity problem.

A second exception was the CSIROMK35 when forced by the A1B scenario. In this case, surface H_s data were unavailable from PCMDI, but were obtained directly from the Commonwealth Scientific and Industrial Research Organisation, Australia.

Because vapor pressure depends on elevation, sea-level pressure data (also simulated by each GCM) were used to provide barometric corrections for grid-cell elevation. A second custom program, anu_hum, was written to perform the conversion of humidity data extracted for each GCM to the format required for input to ANUSPLIN. This program read monthly change factors for H_s and the corresponding change factors for sea-level pressure, recombining these values with the 1961–1990 means

calculated in Step 6. The appropriate data were used to calculate monthly values of e, which were exported to new output files, also in ANUSPLIN input format.

Vapor pressure was derived from the values for H_s and sea-level pressure simulated by each GCM. Steps for the conversion algorithm were as follows:

1. Read specific humidity (H_s, kg kg^{-1}), and sea-level pressure (P(0), kPa) for each GCM gridpoint.
2. Adjust sea-level pressure to "surface pressure" at the elevation given by the GCM orography data, using the equation of Jensen and others (1990):

$$P(z) = P(0)\ (1.0 - 0.0065z/293.0)^{5.26} \qquad [2]$$

where $P(z)$ is the atmospheric pressure (kPa) at elevation z (m).

3. Calculate surface vapor pressure at elevation z, $e(z)$, from specific humidity, H_s, and surface pressure, P(z), using the following equation:

$$e(z) = P(z)\ H_s/[0.622 + H_s(1.0 - 0.622)] \qquad [3]$$

where 0.622 is the ratio of the molecular weights of water vapor to air (e.g., Monteith and Unsworth 2008) and e and $P(z)$ are in kilopascals.

Consideration was given to limiting the calculated values of surface vapor pressure to the lesser of the value obtained from [3] and saturation at T_{min} (or at T_{mean}) for the same time step and GCM grid node, since it is generally unlikely that monthly mean e would exceed saturation. However, computing saturation at T_{min} produced many instances where this assumption did not hold. The justifications for not limiting the vapor pressure values were:

(i) Although unlikely, it is possible that diurnal changes in e, coupled with the curvilinear response of saturation vapor pressure to temperature, would cause a situation in which monthly mean e exceeds saturation at T_{min} or T_{mean}.

(ii) There are likely to be differences among the GCMs in their simulation of variability and trends in vapor pressure. Limiting these values to saturation at temperatures simulated by each GCM could mask some of these differences and cause any comparison of the calculated values to be misleading.

(iii) As for precipitation, solar radiation and wind speed data, projected changes in monthly mean vapor pressure were normalized as *ratios* of the simulated 1961–1990 monthly means. These ratios necessarily required that the future and the reference point data be computed in the exactly same way; hence even if the absolute values simulated by the GCM violated the assumption of ($e \leq e^*(T_{min})$, the actual vapor pressure data obtained from each downscaled scenario would depend on the historical climatology temperature and vapor pressure data that are to be combined with the change factors.

(iv) The responsibility for determining whether the simulated climate variables are physically consistent should remain with the user of the downscaled data. It is safer, and potentially less confusing, for users of the data to account for situations where vapor pressure exceeds saturation (if needed) than it is for them to assume this will never happen.

For these reasons, the final change factors for vapor pressure were not arbitrarily limited to saturation at monthly T_{min} or T_{mean}.

Step 8. The files of normalized monthly change factors for each GCM variable (i.e., four GCMs × three scenarios × six variables, for 72 files in total) were submitted to the CFS Great Lakes Forestry Centre for interpolation using ANUSPLIN. At Great Lakes Forestry Centre, ANUSPLIN models were developed for each month of normalized data, with the data being treated as anomalies (deltas) relative to the 1961–1990 means. A fixed signal model, rather than a standard optimization model, was used because the input data were anomalies, rather than actual climate values (McKenney and others 2006c). We note there are no inherent statistical relationship between these anomalies and the independent variables of longitude and latitude. A fixed signal of 60% of the data points (GCM grid-cell values) produced reasonable results (e.g., avoiding singularities ["bulls eyes"] in the resultant climate change scenario models). The LAPGRD program (part of the ANUSPLIN package) was used to generate the data grids from a 30 arc-second digital elevation model of North America. This model was constructed by staff at the Great Lakes Forestry Centre using the U.S. Geological Survey GTOPO30 digital elevation model coverage for the United States. (http://eros.usgs.gov/#/Find_Data/Products_and_Data_Available/GTOPO30_info) and a Canadian digital elevation model (see Lawrence and others 2007). Log files containing summary statistics were also generated by LAPGRD. The monthly grids of interpolated change factors were generated in ARC/INFO ASCII format, with a cell size of 5 arcminute (300 arc-second) latitude x 5 arcminute (300 arc-second) longitude (about 9.25 km^2 at the equator), covering the domain from 168º W to 52º W and from 25º N to 85º N (1392 columns x 720 rows). This

grid resolution matches that of many other climate data products previously produced at CFS (McKenney and others 2007). The generated monthly files were bundled and transmitted back to CFS Northern Forestry Centre via FTP for post-processing.

Step 9. "Subset rectangles" were extracted from the North American grids for Alaska, the conterminous 48 States and Canada, by means of macros running in ARC/INFO and were packaged for final distribution.

The normalization procedures carried out in Step 6 removed biases in the individual GCMs. That is, any tendency for a GCM model to over or underestimate historical climate, defined as the 1961–1990 mean, was removed and only the change relative to that period was retained. The interpolations carried out in Step 9 allowed direct comparison of the downscaled projections for different scenarios and different GCMs (which operate at different spatial resolutions). These steps were consistent with requirements outlined in a recent USDA Forest Service memorandum, "Draft NEPA Guidance on Consideration of the Effects of Climate Change and Greenhouse Gas Emissions," which was released on 18 February 2010.

Use of Historical Climatology

The interpolation procedure applied to the GCM output data did not account for topographic effects because the representation of surface orography in global-scale GCMs is typically is poor (although as Figure 1 shows, the horizontal resolution varied substantially among the four GCMs). Observed climate normals for the period 1961–1990 were interpolated to the same grid resolution accounting for topographic effects (see McKenney and others 2007). The interpolated change factors for each GCM can be combined with these or other interpolated grid data of observed climate, so that spatial variability in future climate attributable to topography is retained while the climate-change trends simulated by the GCMs are captured. This approach is only considered an approximation of future climate, however, as there may be interactions between topography and climate change that alter the course of the local projection. Consequently, there are many other larger sources of errors in the GCM projections that errors associated with this combination approach are unlikely to be important (see also the Discussion).

Because the interpolated GCM scenario data are consistent with IPCC selection criteria (see http://www.ipcc-data.org/ddc_scen_selection.html) and have been converted to change factors referenced to the 30-year monthly means for the simulated 1961–1990 period, they can be combined with gridded climate normals for the same 30-year period to create "absolute" values for the future projections of climate. This approach preserves the characteristics of current climate while superimposing the climate change signals simulated by each GCM for each GHG forcing scenario. A key advantage is that the user is free to combine these interpolated scenario data with *any* climatological data set (although of course these data should be for an appropriate variable[2] averaged over the 1961–1990 period). A further advantage is that for change factors expressed as ratios (i.e., for climate variables other than temperature), the units of the historical climatology will always be retained in the combined data.

As previously noted, the CFS has constructed continental scale gridded climatologies derived from climate station records collected across Canada and the continental United States since 1901. These data, including grids of 30-year normals and historical monthly models are freely available in various formats. In addition, historical continent-wide dailey models have been constructed (Hutchinson and others 2009). Several other historical climatologies are available for the conterminous United States. As part of the VEMAP project (http://www.cgd.ucar.edu/vemap/) monthly and daily climate variables were developed for the 1895-1993 period at the 0.5 degree latitude by 0.5 degree longitude grid size (Kittel and others 2004). Climate variables include: precipitation, minimum and maximum temperature, total incident solar radiation, daylight-period irradiance, vapor pressure, and daylight-period relative humidity. PRISM data for the 1895 to present time period is available at the 4 km grid cell size (Daly and others 1994; Gibson and others, 2002; see also http://www.prism.oregonstate.edu/) and were used with the change factors from this study to develop the climate projections for the RPA scenarios (USDA Forest Service, in process). Climate variables include monthly mean maximum temperature, monthly mean minimum temperature and monthly precipitation. For the 1971-2000 period, PRISM gridded data of the same variables are available at the 800 m grid cell (http://www.prism.oregonstate.edu/). Climatologies for the United States have also been developed by Rehfeldt (2006) and DAYMET (see http://www.daymet.org/default.jsp).

[2] Examples of appropriate variables include: radiation expressed in W m^{-2} or MJ m^{-2} d^{-1}; wind speed in m s^{-1}, miles per hour or knots; and precipitation in mm d^{-1} or inches per month

Analysis of Interpolated Climate Variables

This section describes the methods used to analyze the interpolated GCM data. The objective was to carry out a comprehensive survey of the results obtained for the Alaska and the conterminous United States, including the following aspects:

- Compare and contrast the large-scale trends (spatial and temporal) seen in the 12 high-resolution GCM projections that were produced;
- Demonstrate the kinds of analyses that can be performed with the data that might be applied to specific regions of the United States (other than the regions identified for the current project);
- Highlight the consistencies and inconsistencies among the different GCMs;
- Perform quality control on the interpolated data products by locating apparent errors; and
- Identify problems with GCMs and/or with particular GHG forcing scenarios.

The 12 projections (three scenarios and four GCMs) each generated projected changes in monthly climate over a 100-year period for six distinct climate variables (i.e., maximum temperature, minimum temperature, precipitation, solar radiation, wind speed and vapor pressure). We analyzed this data in three different ways: spatial and temporal patterns at the scale of the United States, interannual variations at the regional scale, and a more in-depth look at the future regional patterns.

Spatial and Temporal Patterns

First, spatial variability of three key variables for 30-year periods (2011–2040, 2041–2070 or 2071–2100) was compared and contrasted among the different GCMs and GHG emissions scenarios for the conterminous United States and Alaska. Initially, maps were developed to display the change factors applied to the interpolated 1961-1990 normals. However, the differences among the projections often were very subtle, because the spatial variations in projected changes are small compared with the strong climatic gradients that exist across the entire continent, resulting from latitudinal and elevation differences and from the east-to-west gradients caused by synoptic weather systems and the Rocky Mountains.

The approach subsequently adopted was to compare, for a single GCM, the 1961-1990 normals with projections for each of the 30-year periods for three key variables: annual mean daily maximum temperature, annual mean daily minimum temperature, and total annual precipitation. The GCM selected was the NCARCCSM3 forced by scenario A1B. The temperature maps were derived by adding the means of the interpolated change factors for each 30-year period to the interpolated 1961-1990 normals. For precipitation, the projections were derived by multiplying the means of the interpolated change factors for each 30-year period by the 1961-1990 normals. This analysis was followed by a comparison of the spatial variability of the change factors projected by each of the four GCMs for the A1B scenario for each of the 30-year periods: 2011–2040, 2041–2070 or 2071–2100. The change factors in these maps are relative to the 1961-1990 period. In these maps, all grid-cell means were weighted to account for the number of days in each month, including leap years, and, hence, can be compared with historical 30-year climate normals obtained from climate station observations. The last spatial comparison was of the change factors projected by each of the four GCMs for the A2 and B1 scenario for the last period: 2070-2100 (or 2099 in the case of NCARCCSM3).

Interannual Variations at the Regional Scale

Following the exploration of *spatial* differences in the projected trends, the more detailed analysis of the *temporal* changes involved the computation of seasonal and annual values, computed for each of eight regions. Data were spatially averaged for Alaska and seven other regions of the conterminous 48 states, the latter based on groupings of the major ecoclimatic divisions in the Bailey (1995) ecoregions classification for the United States (Figure 2) (termed "regions"). These regions stratify the conterminous United States in relatively homogenous ecoclimatic divisions, allowing the exploration of the effects of future climate change. Alaska was kept as a single region to keep the total number of regions examined small.

The seasonal and annual absolute data are *area-weighted* spatial averages of the monthly aggregated values. The area weightings were calculated as ratios for each grid cell, where the actual area was expressed relative to the mean area of all grid cells in the region, i.e.,

$$R_{Ai} = \frac{A_i}{A_{region}/N} \qquad [4]$$

where R_{Ai} is the area ratio for grid cell i, N is the number of grid cells in the region, A_i is the area of grid cell i and A_{region} is the total area of the region given by $\sum_{i=1}^{N} A_i$. The area A_i was calculated in steradians using the following equation:

$$A_i = \frac{\cos(\alpha + \delta/2) + \cos(\alpha - \delta/2)}{2} \delta^2 \qquad [5]$$

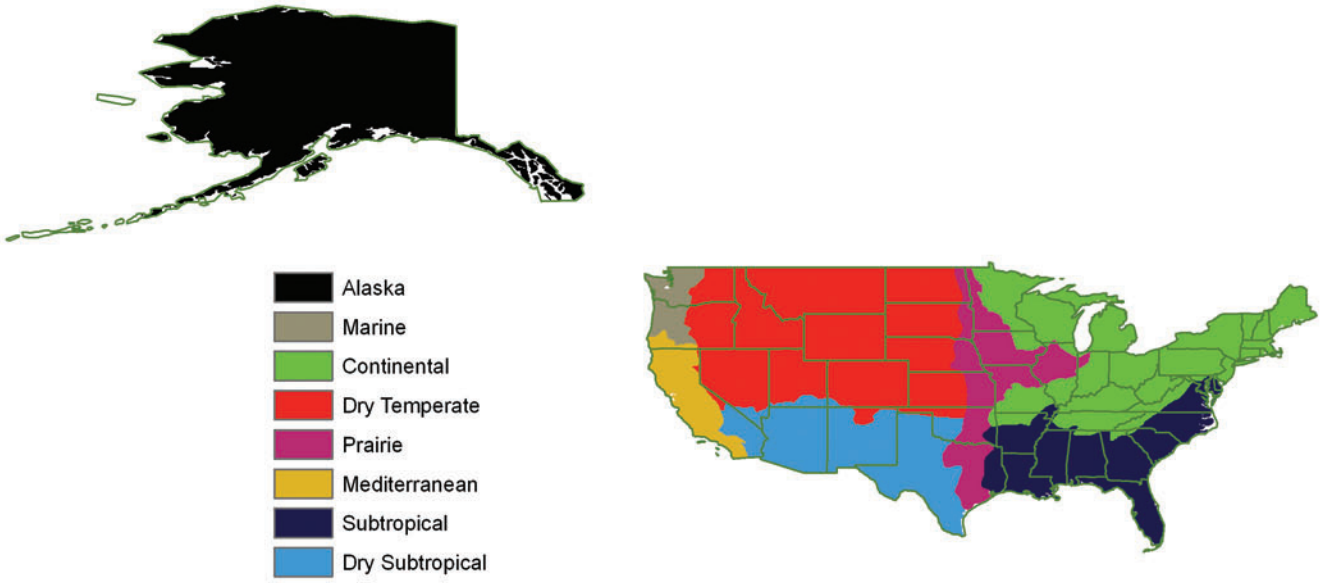

Figure 2. Regions of the conterminous United States used in the climate scenario analysis, derived from the Ecoregions map of Bailey (1995). The Alaska region was defined by state boundaries rather than ecoclimatic boundaries.

where angle α is the latitude at the grid cell centroid, and δ is the dimension of the grid cell (latitude and longitude) expressed in radians. The area in steradians can be converted to square kilometers using a value of 6371.2213 km per radian, assuming the earth is a perfect sphere (Kittel and others 1995), but this is unnecessary for [4].

The analysis included a systematic production of time-series data for annual and seasonal means of each monthly variable in every region for all four GCMs and all three scenarios, plus the 20th century simulations and observed temperature and precipitation data. Seasons were defined as three-month periods: spring (March-May), summer (June-August), fall (September-November), winter (December-February). Note the winter of 2100 (2099 for NCARCSM3) would, by this definition, contain only one month, and it was therefore omitted in the calculations of 30-year averages.

The first analysis examines the regional relationships between the spatially averaged regional change in annual mean daily minimum temperature and the regional annual precipitation ratio projected by each GCM for the 2040-2059 period and the 2080-2099 period, relative to the 1961-1990 period. These scatter plots demonstrate how the four GCMs, forced by each of the three SRES scenarios, differed in their projections of climatic change for each ecoregion across two periods into the future. These graphs also facilitate selecting scenarios that may be representative of the range of projected changes in climate (temperature and precipitation) for a particular region of the United States. The second analysis examined the interannual variation in each climate projection by graphing long-term time series of key annual or seasonal variables. The regional graphs enable comparison of projected trends in means and interannual variability, according to each GCM scenario, for a specified variable and region.

Climate Scenario Regional Outlook

We also summarized, in a set of comprehensive tables, the results for all variables and all scenarios in each of the eight regions identified in Figure 2. The time-series data were imported into a series of spreadsheets and used to generate summary tables providing key information about projected changes during the 21st century.

In these tables, the area-weighted mean for each climate variable is the mean of the values projected by the four GCMs and therefore represents a "best guess," assuming that the GCMs are equally skillful (or equally believable). Each table presents results for a total of six climate variables (maximum and minimum temperature, precipitation, global solar radiation, vapor pressure and wind speed) for a single region. For each variable, the data are organized across the table, in three sets of five columns. Each set of columns represents a single GHG emissions scenario (in the order A2, A1B, and B1), with the columns containing the means of the four GCM

projections of monthly values for spring, summer, fall, winter, and the entire year.

The rows of data are labeled in the left-most column according to the period represented. "Baseline 1980–2009" refers to the 30-year mean for the period 1980–2009. This period was selected as the baseline because it represents current climate and immediately precedes the three consecutive 30-year periods reported as projections for the future (starting with 2010). It is important to distinguish this 30-year period from the period 1961–1990, which was used as the reference period for combining scenario data with observed climate normals for 1961–1990. Although any differences between the periods 1961–1990 and 1980–2009 are probably small, there is evidence of a general warming trend over this entire period that is apparent in many of graphs shown previously (both in the observed temperature records and in the GCM projections). Notably, the baseline 1980–2009 mean values differed slightly among the three emissions scenarios, because data for the nine years from 2001 to 2009 originated from the different GHG simulations, which led to different calculated means.

The rows for "Change by 2010–2039," "Change by 2040–2069," and "Change by 2070–2099" give the mean net changes in the projected 30-year means relative to 1980–2009. In these rows, a positive value indicates an increase, and a negative value indicates a decrease. The rows for "100-year forcing" and "100-year variability (%)" represent the changes in 30-year means and 30-year standard deviations (SDs), respectively, between the periods 1970–1999 and 2070–2099. The changes in SD are reported as percentages relative to 100% for 1970–1999.

Calculation of Bioclimatic Indices for the Scenario Data

As an added set of products, 30-year models of mean changes in temperature and precipitation were also developed, for the purpose of projecting changes in various bioclimatic indicators (see Table 3). This required several additional steps. First, ANUSPLIN surfaces for the 30-year mean change fields from each GCM scenarios were created for the three future periods (2011–2040, 2041–2070 and 2071–2100). These surfaces were used to estimate projected mean changes at North American weather stations operating during the period 1961–1990. The mean changes were combined, in turn, with the station normals for the 1961–1990 period. This allowed for the generation of new ANUSPLIN surfaces of projected mean values for each future period. For these models, trivariate (position and elevation-dependent) splines were used. The statistical signals were good because there are statistically strong elevational dependencies in the 1961–1990 models, which remained in the derived ANUSPLIN models of future climate.

With these surfaces it was possible to generate several bioclimatic variables (e.g., length of growing season, precipitation during the growing season) that are often used in modeling in the fields of forestry, agricultural, and ecological impacts and hence have greater interest to some potential users. The derived variables are possible because a daily sequence of temperature and precipitation can be generated from the primary monthly surfaces. This is done through a Bessel interpolation whereby the daily sequence is forced to pass through the monthly means in a monotonic form (for details see Mackey and others 1996). It is important to understand that these data are intended to represent mean conditions and that in any given year, "noise" would influence the actual daily sequence of bioclimatic variables.

It is recognized that some users might desire estimates of bioclimatic variables at annual time steps, rather than 30-year averages. This created an additional challenge because of the previously noted caveat concerning the greater stochasticity of individual years. After due consideration, we decided to generate another resolution of model outputs that would allow the dissemination of some of the projected bioclimatic variables at annual time steps. Again, users should appreciate that these bioclimatic models do not account for stochasticity at daily and monthly timescales, but they do retain the interannual variations provided in the GCM projections. To make the data sets more manageable, these models were developed at the slightly coarser resolution of 900 arc seconds (~30 km).

Results

Spatial and Temporal Patterns

Maps showing the trends in annual mean daily $\underline{T_{max}}$ and $\underline{T_{min}}$ and precipitation are presented in Figures 3, 4 and 5, respectively. In each figure, the first set of maps (a) shows the trends in absolute measures (maximum temperature, minimum temperature, and precipitation, respectively) according to NCARCCSM3 forced by the A1B scenario for three future 30-year periods: 2011–2040, 2041–2070 or 2071–2100 (or 2071-2099 for NCARCCSM3). In each of Figures 3–5, maps b, c, and d show the changes relative to the means for 1961–1990, for each successive 30-year period, again forced by A1B.

Table 3. Variables derived from primary climate surfaces. Variables 1-19 are generated by ANUCLIM (Houlder and others 2000); variables 20-29 are generated by SEEDGROW (Mackey and others 1966)* (modified from McKenney and others 2006a). In all cases, the descriptions should be considered estimates rather than actual values.

No.	Variable	Description
1	Annual mean temperature	Annual mean of monthly mean temperatures
2	Mean diurnal temperature range	Annual mean of monthly mean daily temperature ranges
3	Isothermality	Variable 2 / variable 7
4	Temperature seasonality	Standard deviation of monthly mean temperature estimates expressed as a percentage of their mean
5	Maximum temperature of warmest period	Highest monthly maximum temperature
6	Minimum temperature of coldest period	Lowest monthly minimum temperature
7	Annual temperature range	Variable 5 – Variable 6
8	Mean temperature of wettest quarter	Mean temperature of three consecutive wettest months
9	Mean temperature of driest quarter	Mean temperature of three consecutive driest months
10	Mean temperature of warmest quarter	Mean temperature of three consecutive warmest months
11	Mean temperature of coldest quarter	Mean temperature of three consecutive coldest months
12	Annual precipitation	Sum of monthly precipitation values
13	Precipitation of wettest period	Precipitation of the wettest month
14	Precipitation of driest period	Precipitation of the driest month
15	Precipitation seasonality	Standard deviation of monthly precipitation estimates expressed as a percentage of their mean
16	Precipitation of wettest quarter	Total precipitation of three wettest months
17	Precipitation of driest quarter	Total precipitation of three driest months
18	Precipitation of warmest quarter	Total precipitation of three warmest months
19	Precipitation of coldest quarter	Total precipitation of three coldest months
20	Start of growing season	Date when daily mean temperature first meets or exceeds 5 °C for five consecutive days in spring
21	End of growing season	Date when daily minimum temperature first falls below -2 °C after 1 August
22	Growing season length	Variable 21 – Variable 20
23	Total precipitation in the three months before start of growing season	Total precipitation of three months prior to variable 20
24	Total growing season precipitation	Total precipitation during variable 22
25	Growing degree-days during growing season	Total degree days during variable 22, accumulated for all days where mean temperature exceeds 5 °C.
26	Annual minimum temperature	Annual mean of monthly minimum temperatures
27	Annual maximum temperature	Annual mean of monthly maximum temperatures
28	Mean temperature during growing season	Mean temperature during variable 22
29	Temperature range during growing season	Highest minus lowest temperature during variable 22

*The approach used by Mackey et al. (1996) creates a daily sequence of minimum and maximum temperature and precipitation with the values forced monotonically through the monthly values. The resulting values are intended to represent mean conditions only, as the weather in any given year would be expected to produce different results, because of interannual variability.

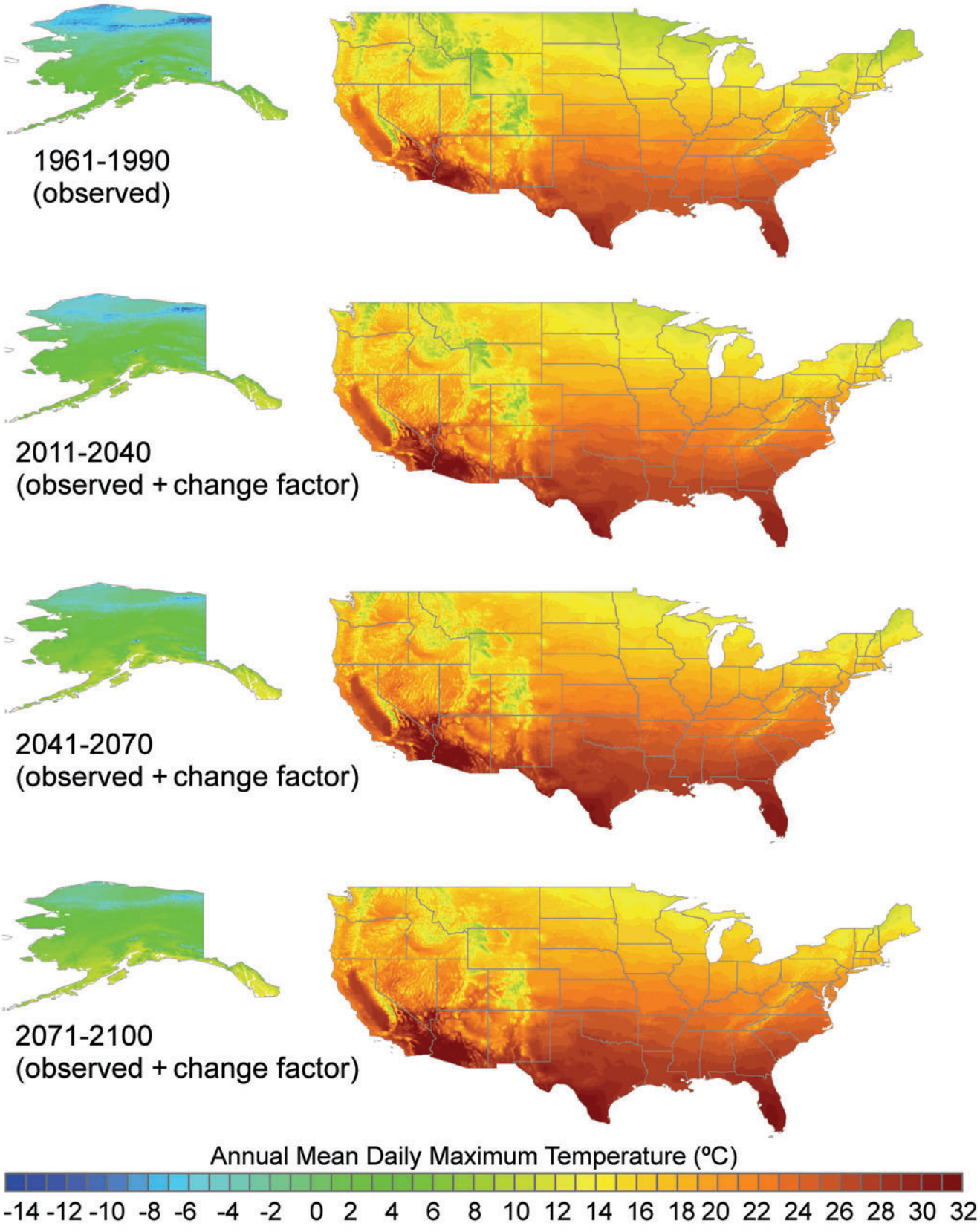

Figure 3a. Maps of annual mean daily maximum temperature derived from climate station records from the period 1961-1990 and projections according to the Community Climate System Model, version 3.0 (NCARCCSM3), forced by the A1B scenario, for 2011-2040, 2041-2070, and 2071-2099. The projections were derived by adding the means of the interpolated change factors for each 30-year period to the interpolated climate normal data shown in the 1961-1990 normals map (top).

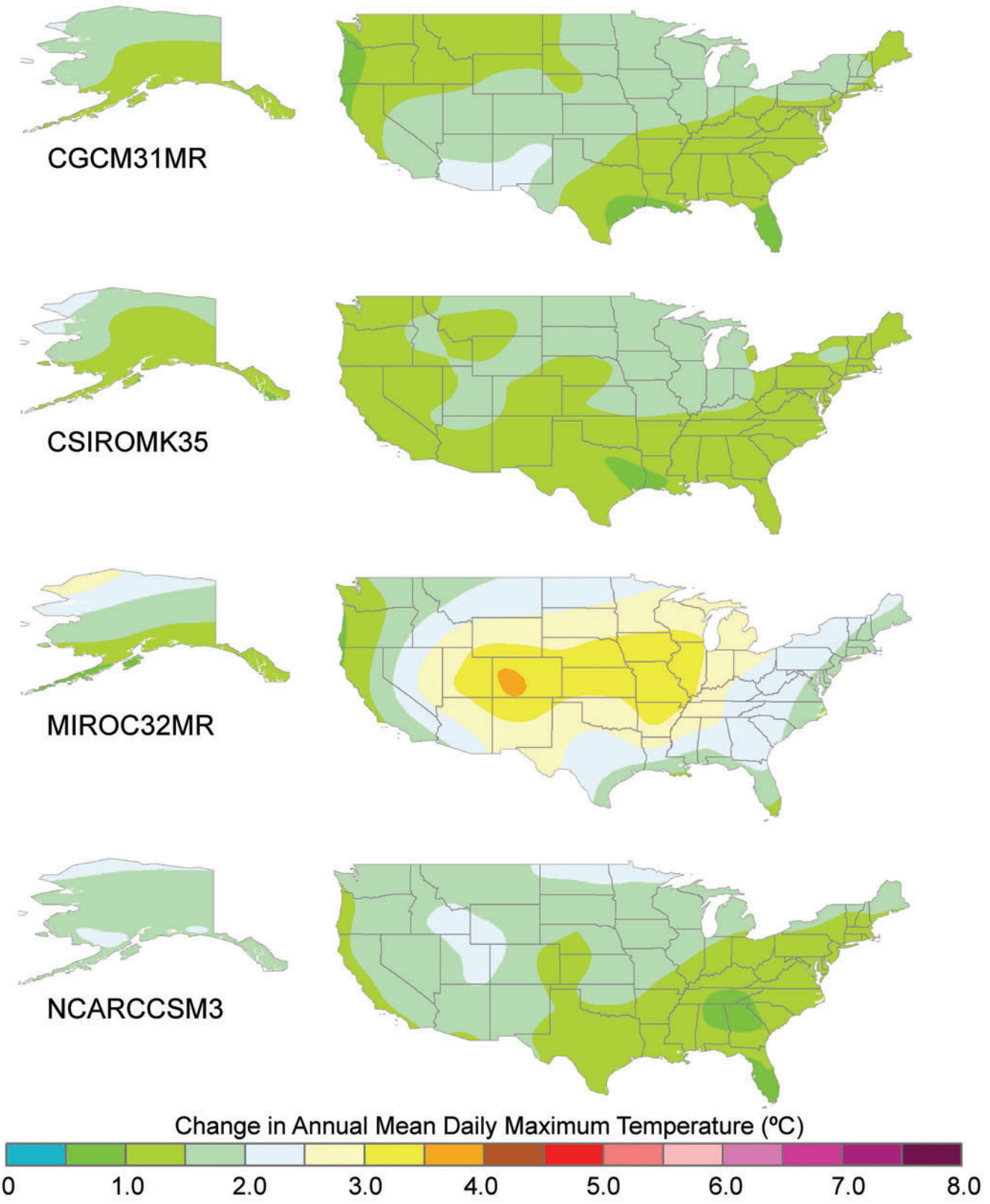

Figure 3b. Projected changes in annual mean daily maximum temperature for the period 2011–2040, relative to 1961–1990, for the A1B scenario according to the four general circulation models used in this study. CGCM31MR = Third Generation Coupled Global Climate Model, version 3.1, medium resolution; CSIROMK35 = Commonwealth Scientific and Industrial Research Organisation Climate System Model, Mark 3.5; MIROC32MR = Model for Interdisciplinary Research on Climate, version 3.2; NCARCCSM3 = Community Climate System Model, version 3.0.

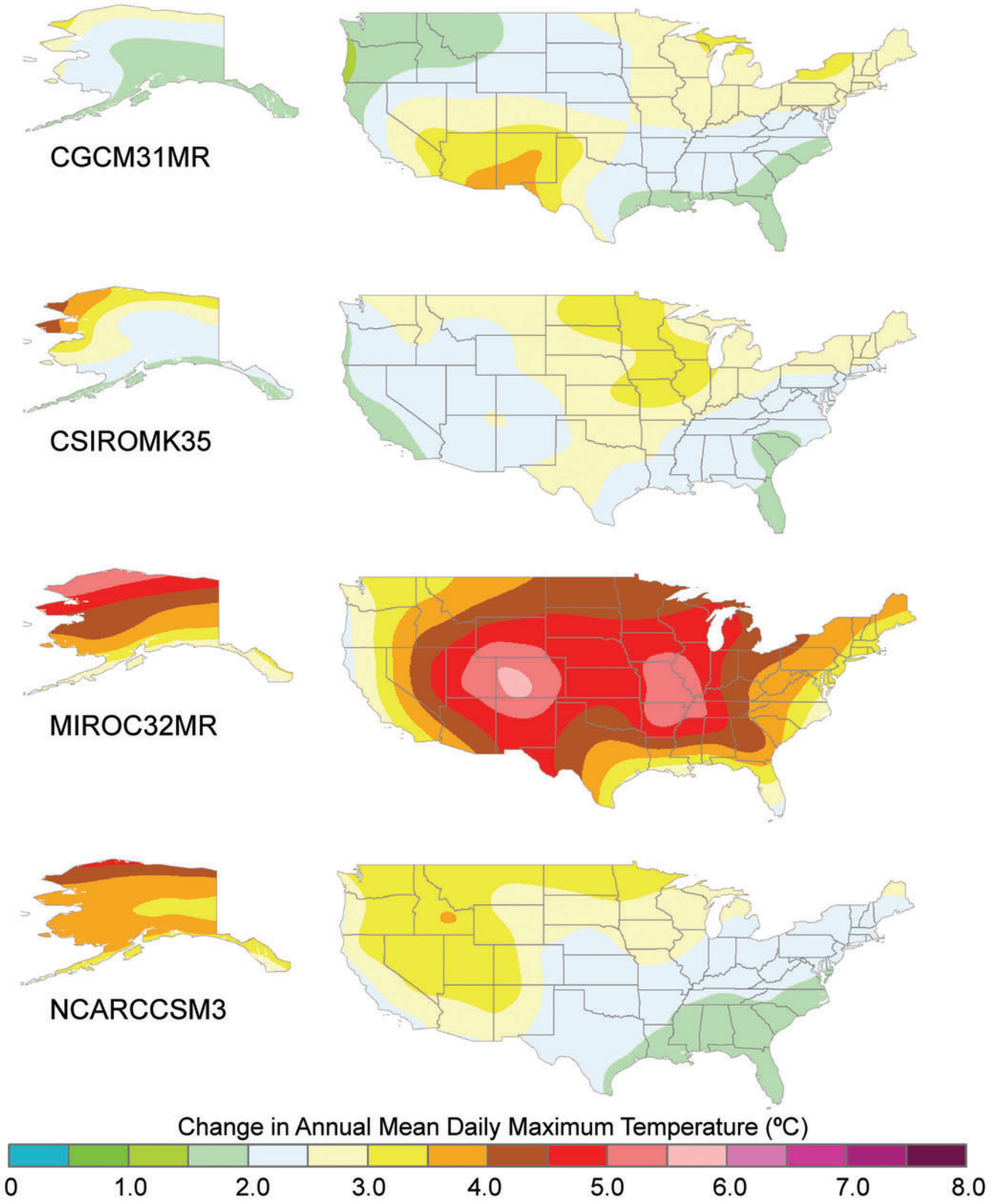

Figure 3c. Projected changes in annual mean daily maximum temperature for the period 2041–2070, relative to 1961–1990, for the A1B scenario according to the four general circulation models used in this study.

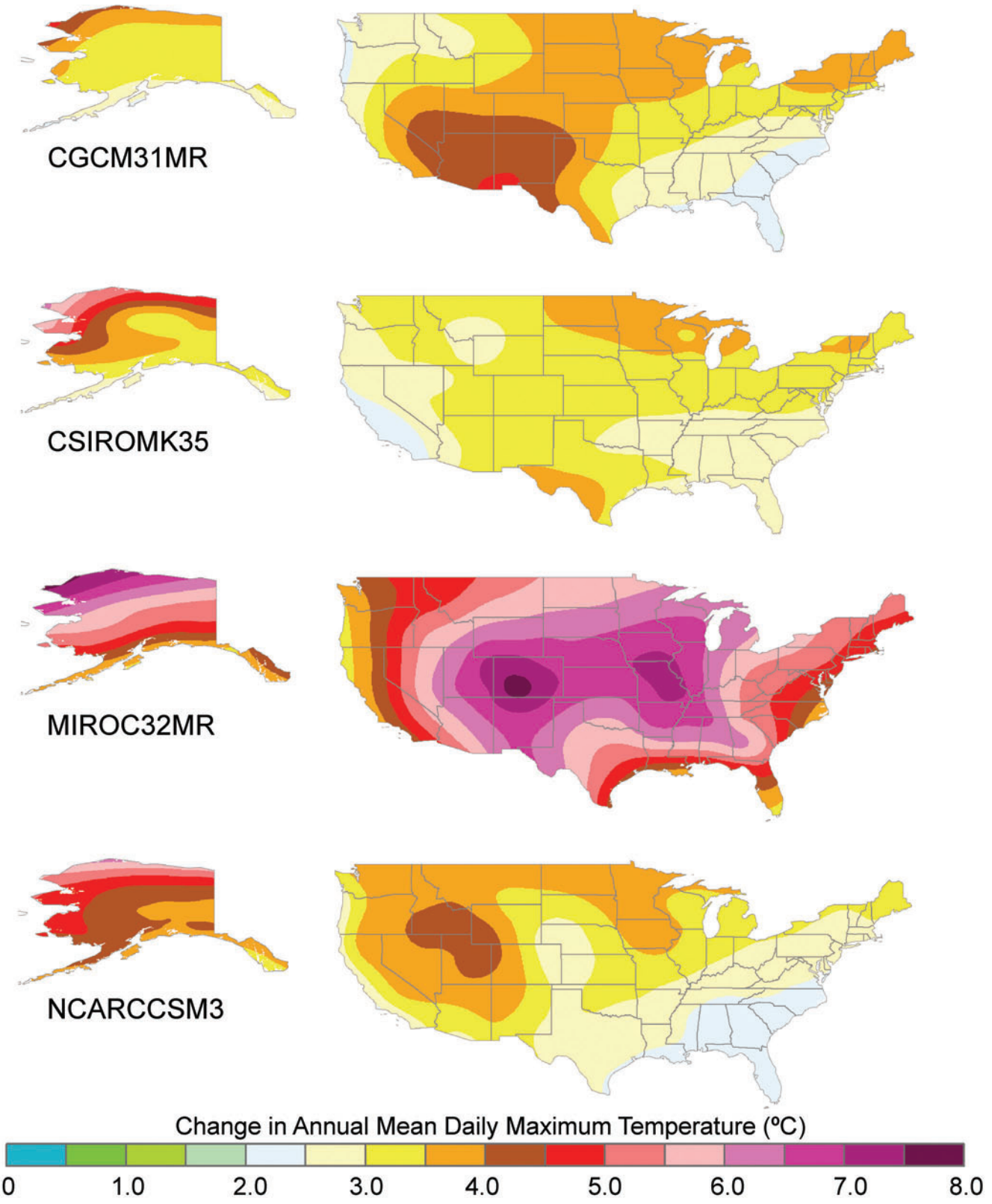

Figure 3d. Projected changes in annual mean daily maximum temperature for the period 2071-2100 (2071-2099 for NCARCCSM3), relative to 1961-1990, for the A1B scenario according to the four general circulation models used in this study.

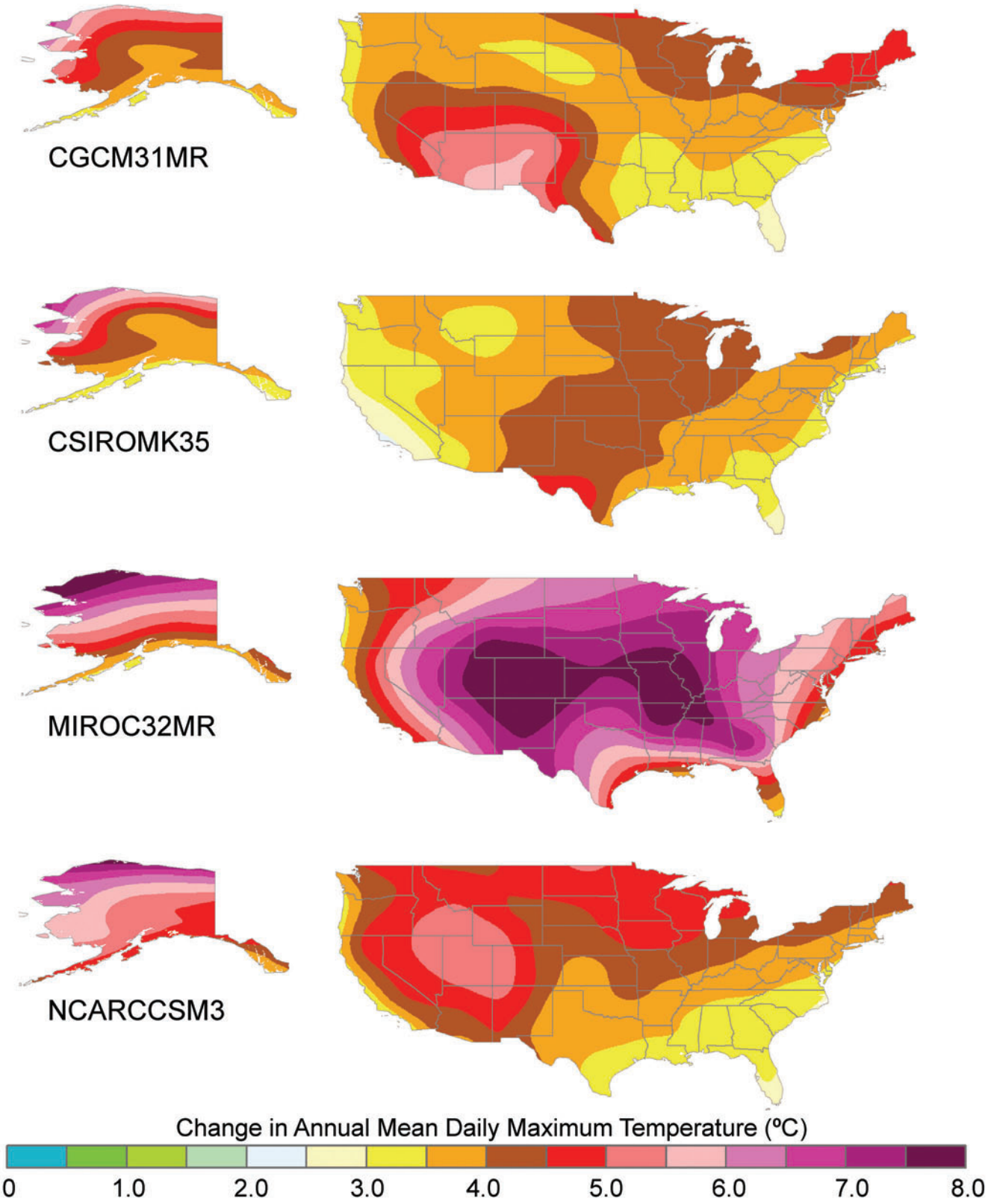

Figure 3e. Projected changes in annual mean daily maximum temperature for the period 2071-2100 (2071-2099 for NCARCCSM3), relative to 1961-1990, for the A2 scenario according to the four general circulation models used in this study.

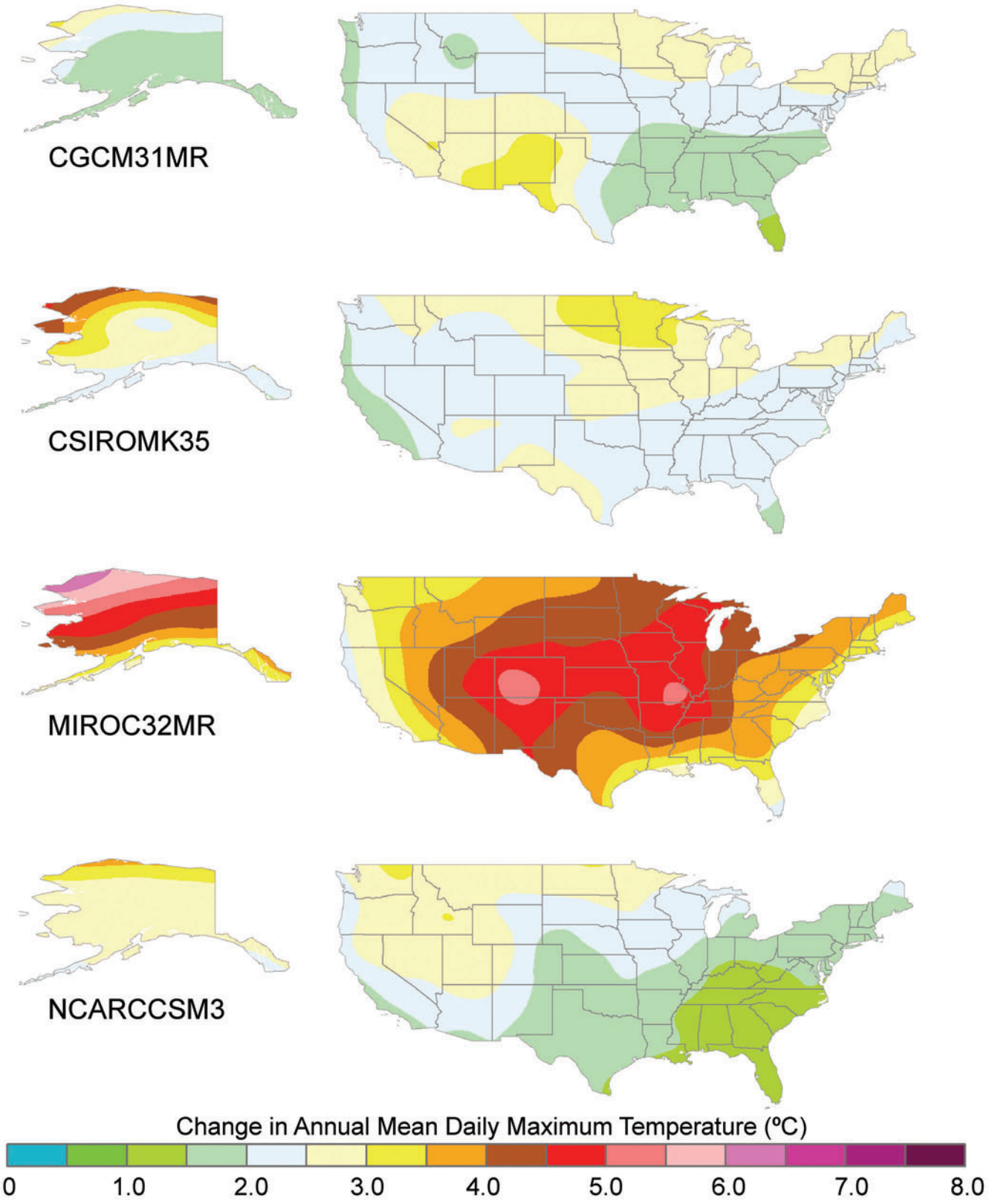

Figure 3f. Projected changes in annual mean daily maximum temperature for the period 2071-2100 (2071-2099 for NCARCCSM3), relative to 1961-1990, for the B1 scenario according to the four general circulation models used in this study.

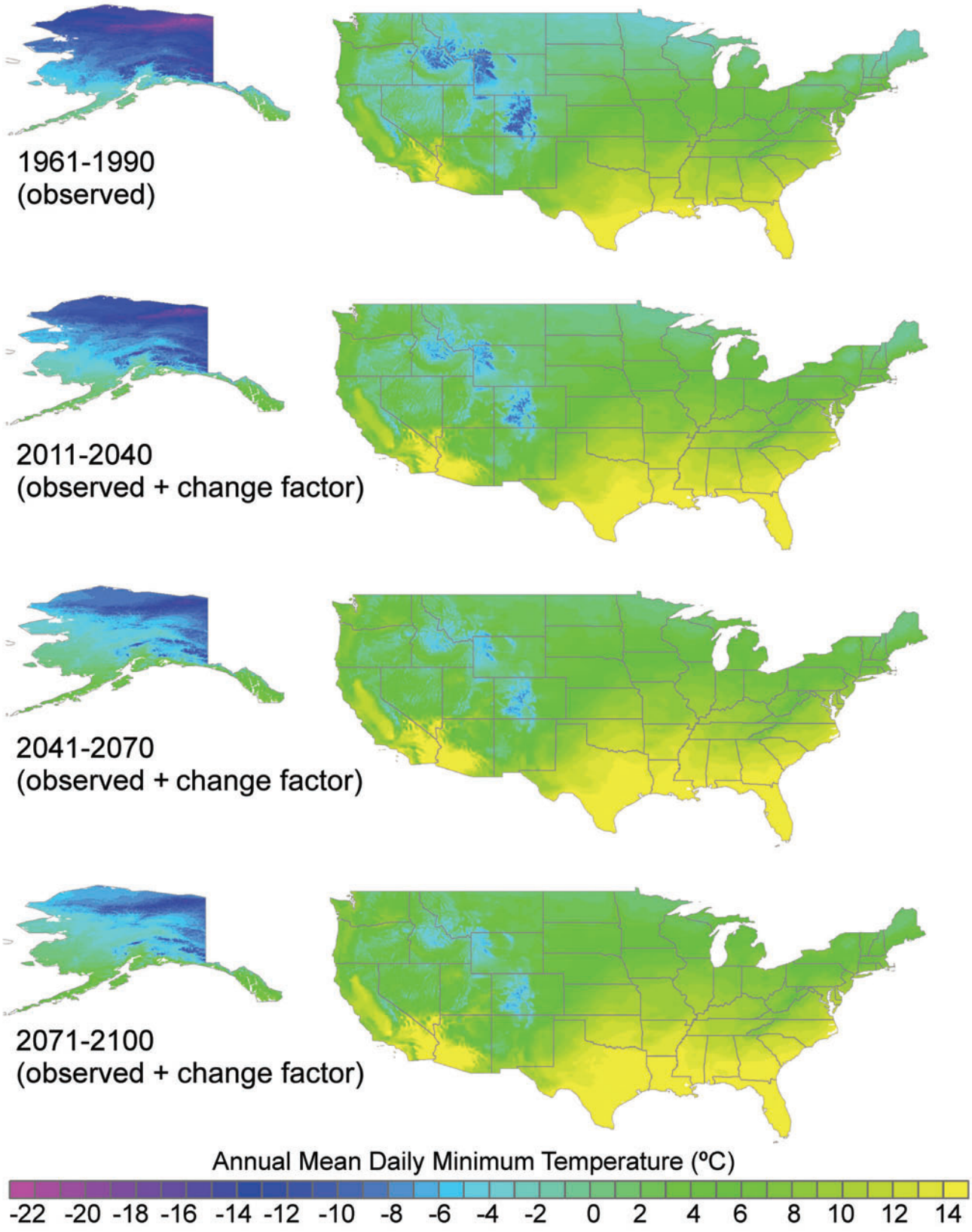

Figure 4a. Maps of annual mean daily minimum temperature derived from climate station records for the period 1961–1990 and projections according to the Community Climate System Model, version 3.0 (NCARCCSM3) forced by the A1B scenario, for 2011–2040, 2041–2070, and 2071–2099. The projections were derived by adding the means of the interpolated change factors for each 30-year period to the interpolated climate normal data shown in the 1961-1990 normals map (top).

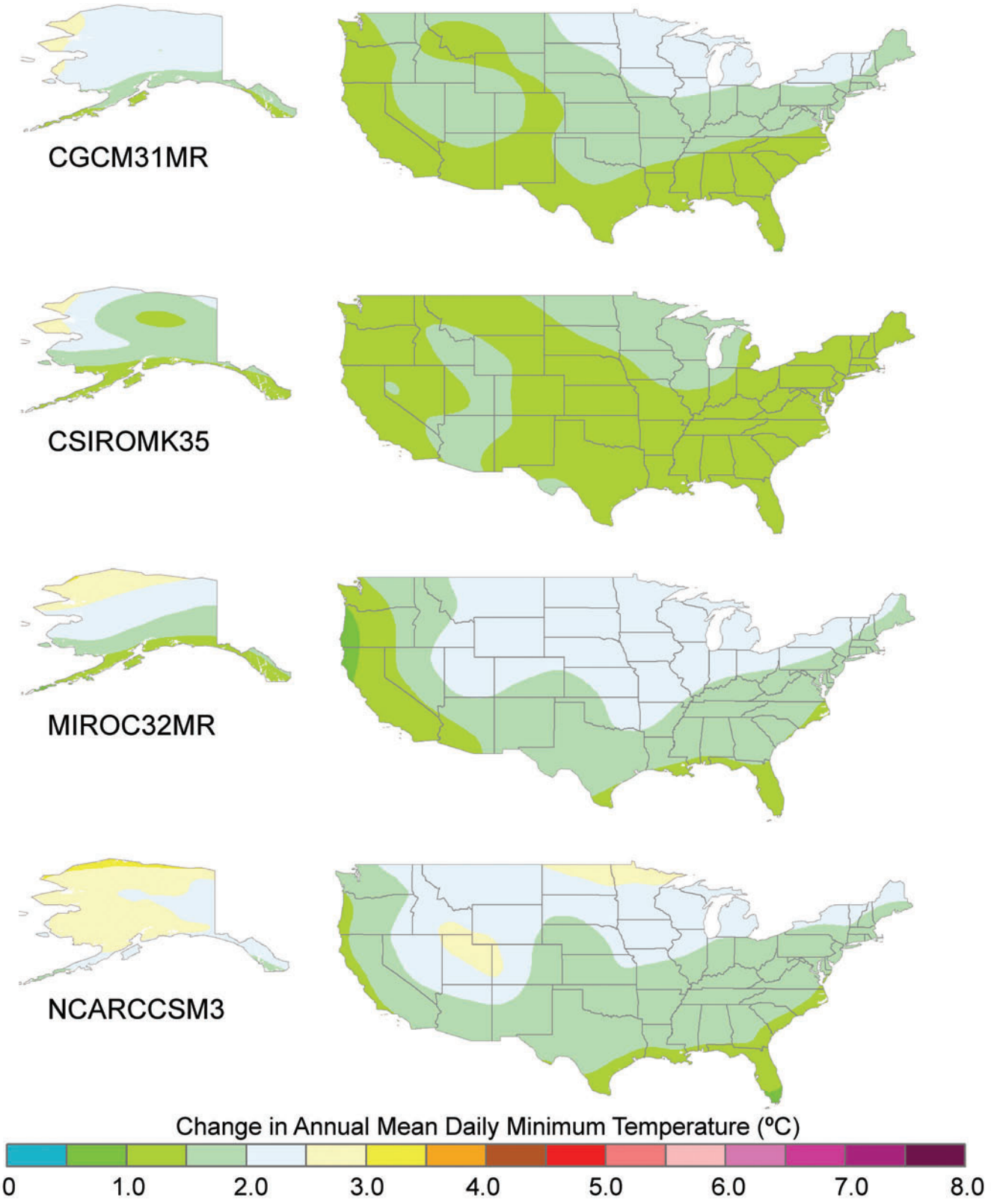

Figure 4b. Projected changes in annual mean daily minimum temperature for the period 2011-2040, relative to 1961-1990, for the A1B scenario according to the four general circulation models used in this study. CGCM31MR = Third Generation Coupled Global Climate Model, version 3.1, medium resolution; CSIROMK35 = Commonwealth Scientific and Industrial Research Organisation Climate System Model, Mark 3.5; MIROC32MR = Model for Interdisciplinary Research on Climate, version 3.2; NCARCCSM3 = Community Climate System Model, version 3.0.

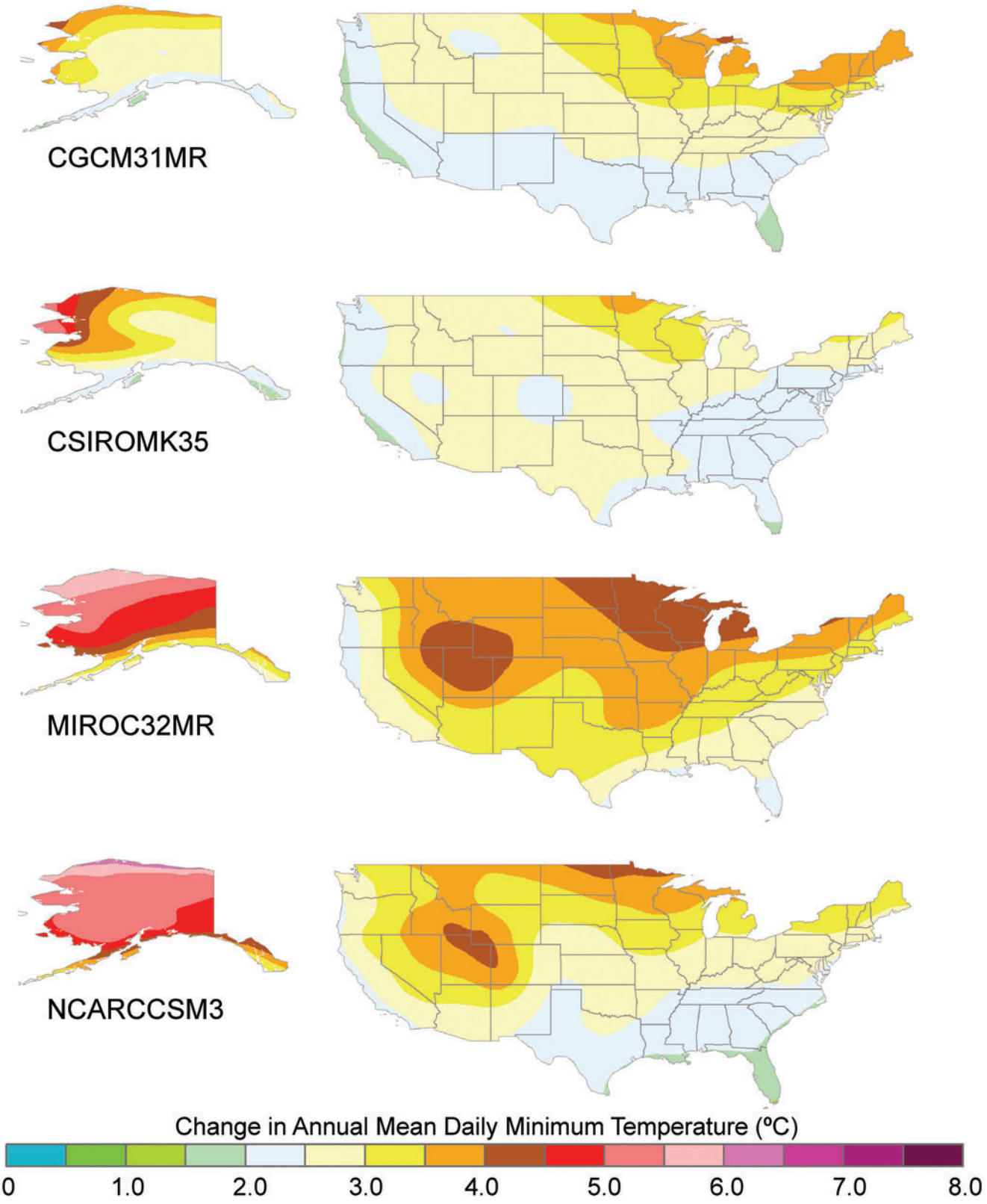

Figure 4c. Projected changes in annual mean daily minimum temperature for the period 2041-2070, relative to 1961-1990, for the A1B scenario according to the four general circulation models used in this study.

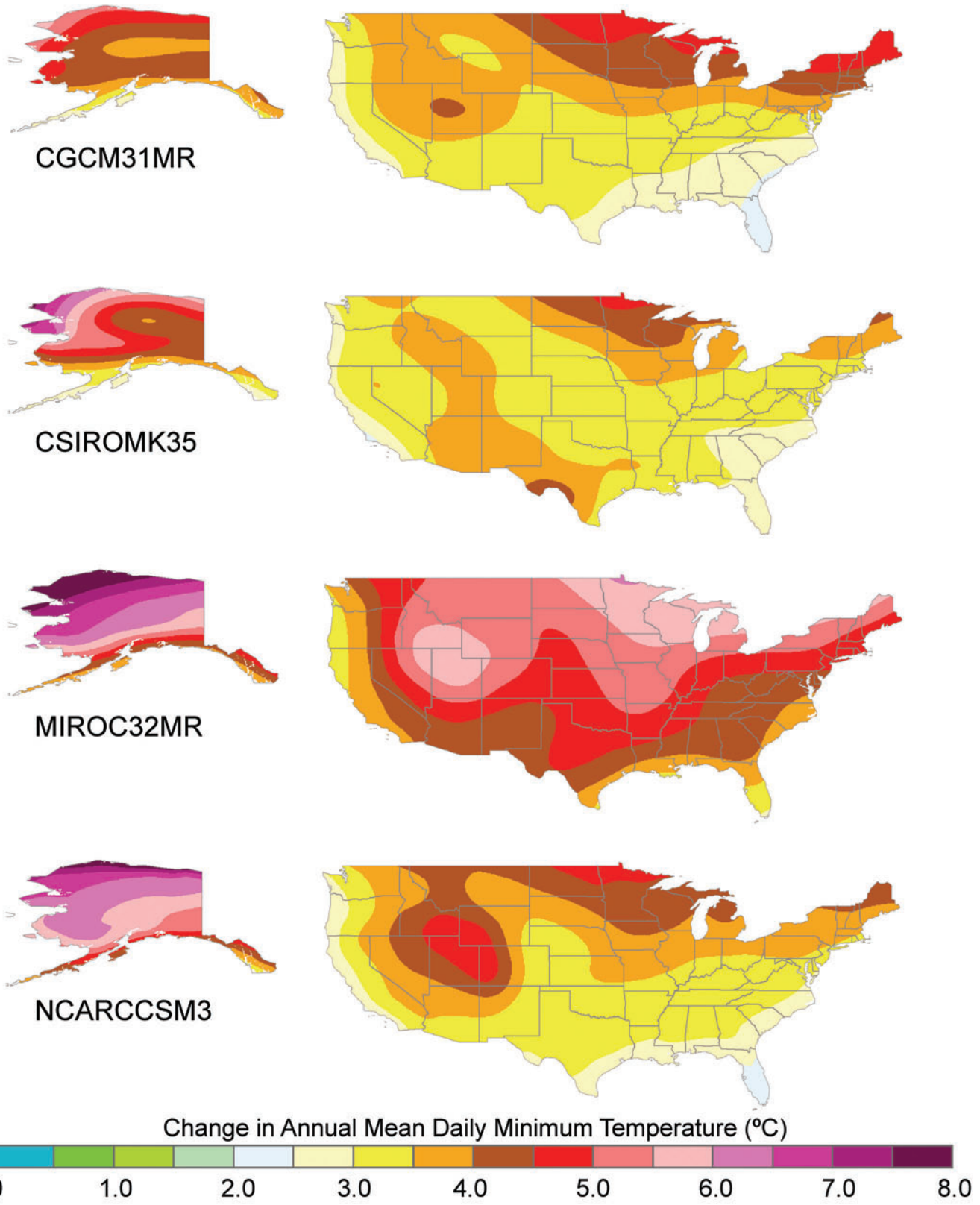

Figure 4d. Projected changes in annual mean daily minimum temperature for the period 2071-2100 (2071-2099 for NCARCCSM3), relative to 1961-1990, for the A1B scenario according to the four general circulation models used in this study.

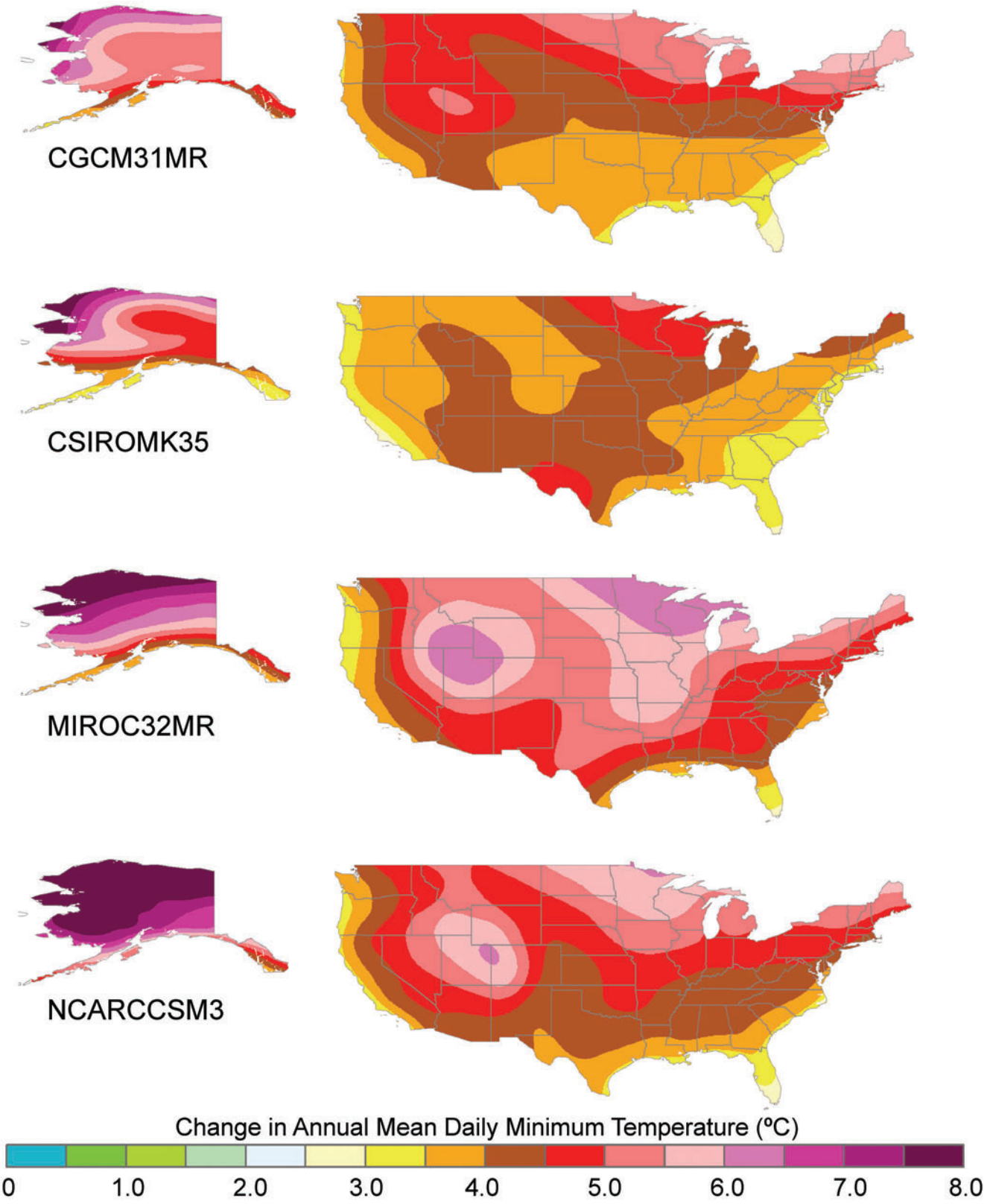

Figure 4e. Projected changes in annual mean daily minimum temperature for the period 2071-2100 (2071-2099 for NCARCCSM3), relative to 1961-1990, for the A2 scenario according to the four general circulation models used in this study.

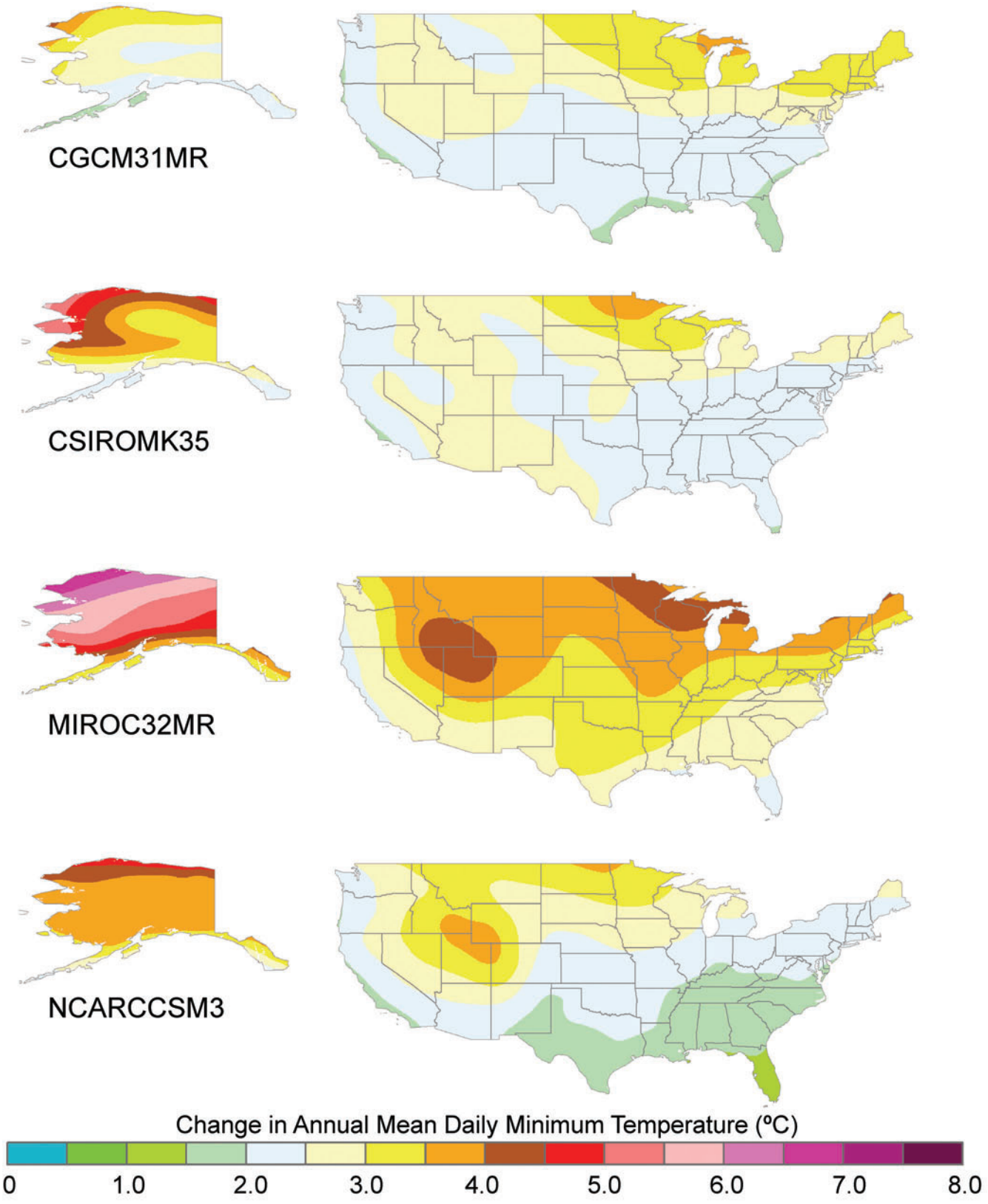

Figure 4f. Projected changes in annual mean daily minimum temperature for the period 2071-2100 (2071-2099 for NCARCCSM3), relative to 1961-1990, for the B1 scenario according to the four general circulation models used in this study.

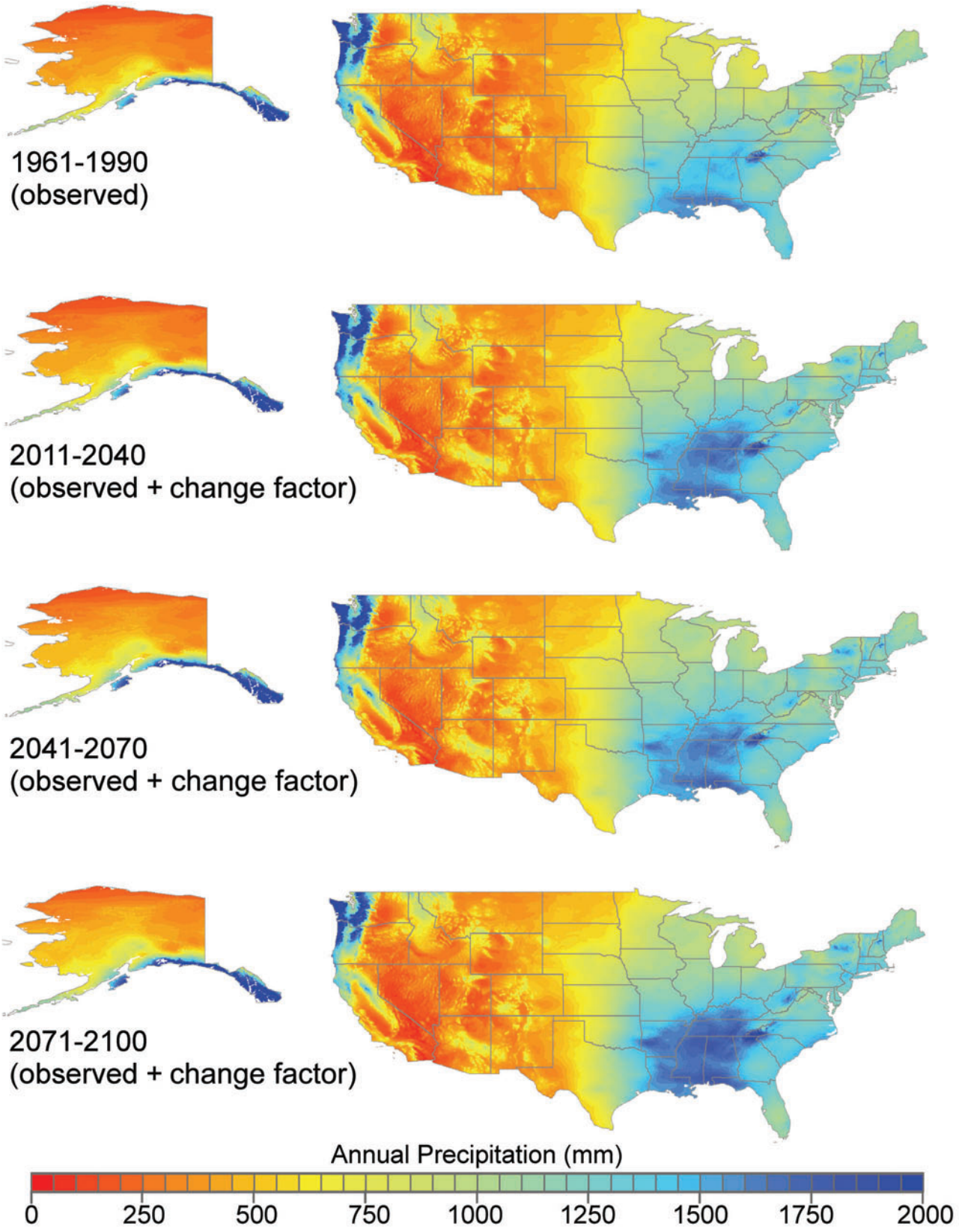

Figure 5a. Maps of annual total precipitation derived from climate station records for the period 1961–1990 and projections according to the Community Climate System Model, version 3.0 (NCARCCSM3) forced by the A1B scenario, for 2011–2040, 2041–2070, and 2071–2099. The projections were derived by multiplying the interpolated climate normal data shown in the top map by the means of the interpolated change factors for each 30-year period.

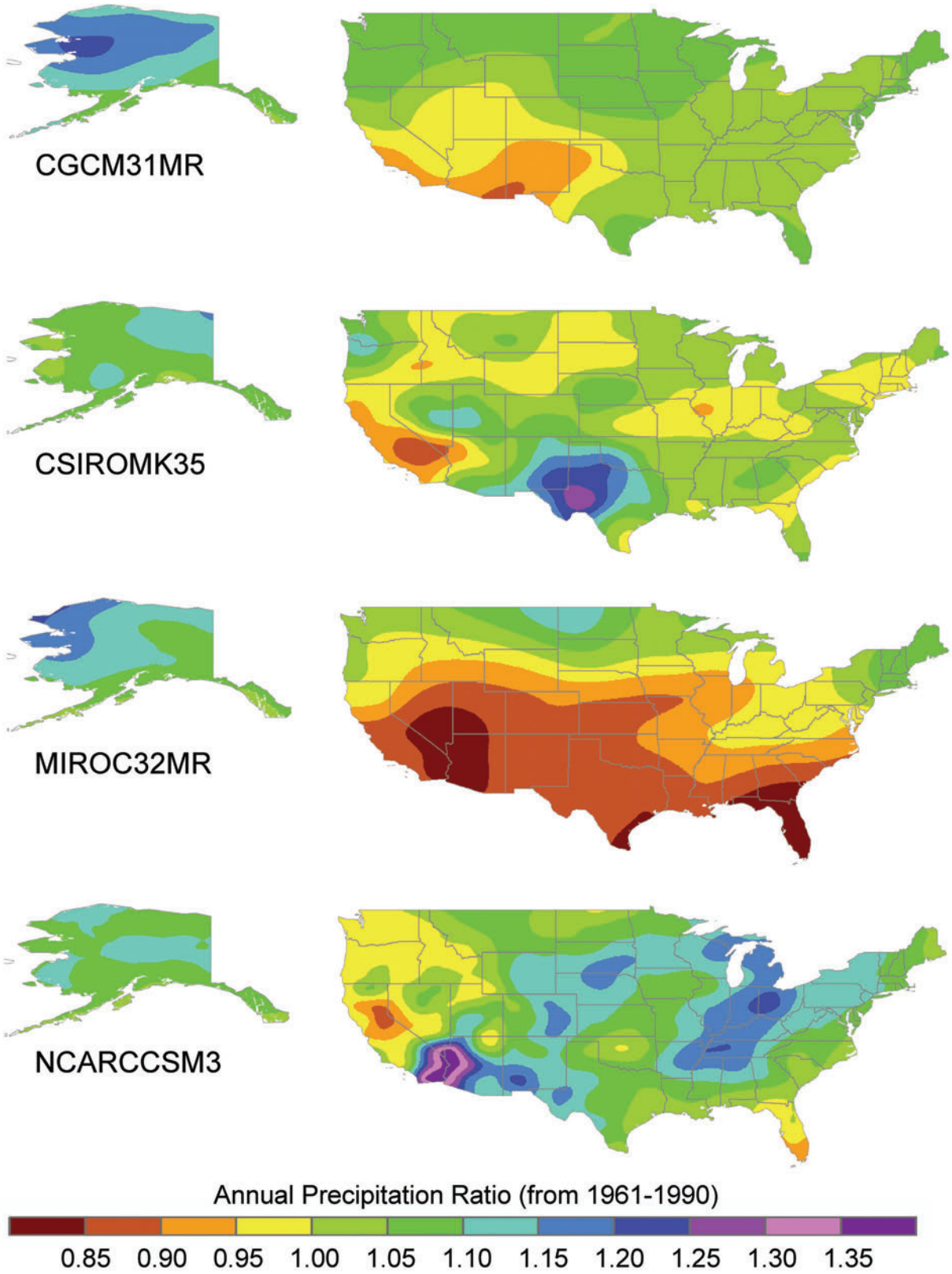

Figure 5b. Projected changes in annual total precipitation for the period 2011-2040, expressed as ratios relative to the means for 1961-1990, for the A1B scenario, according to the four general circulation models used in this study. CGCM31MR = Third Generation Coupled Global Climate Model, version 3.1, medium resolution; CSIROMK35 = Commonwealth Scientific and Industrial Research Organisation Climate System Model, Mark 3.5; MIROC32MR = Model for Interdisciplinary Research on Climate, version 3.2; NCARCCSM3 = Community Climate System Model, version 3.0.

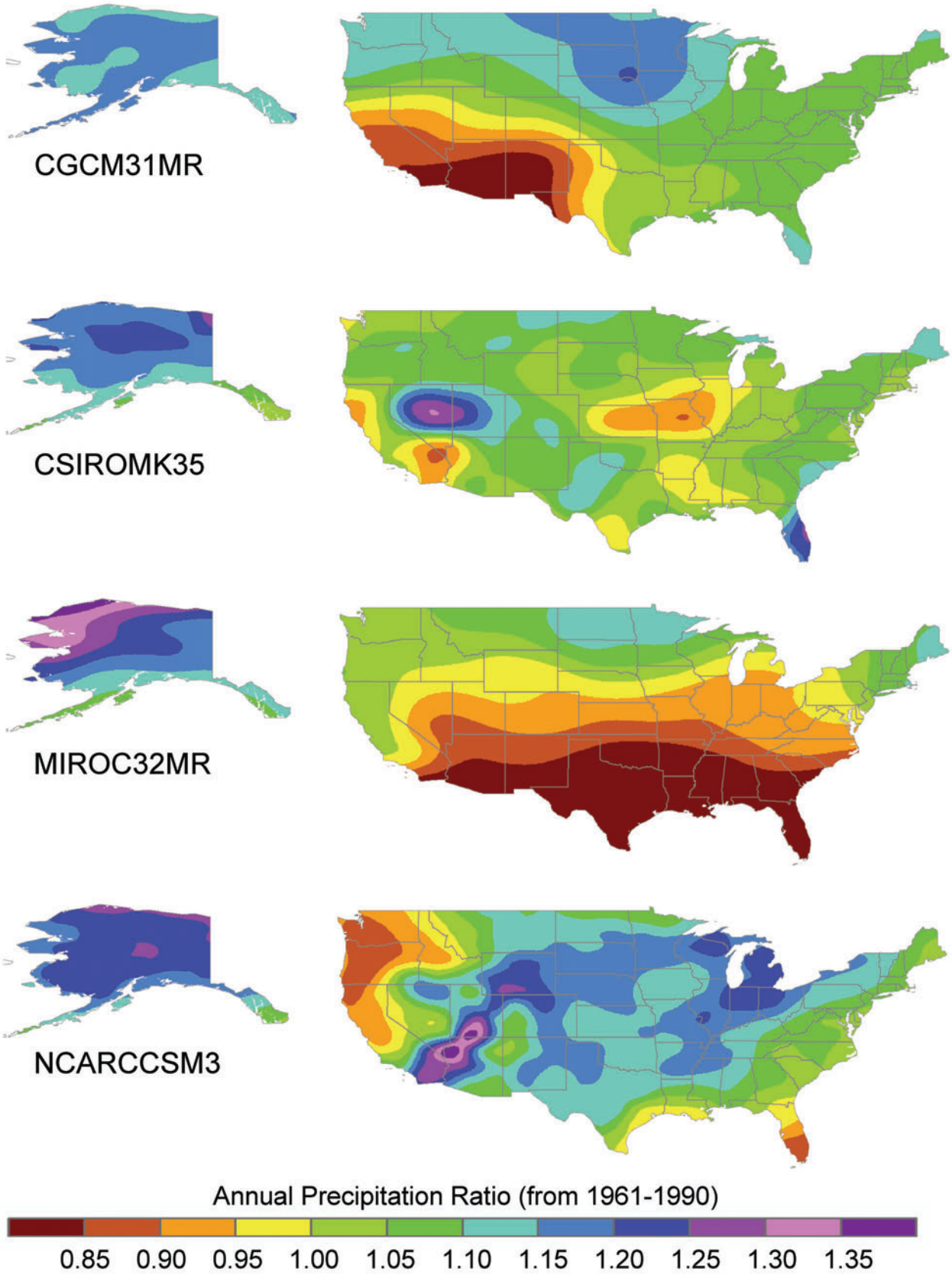

Figure 5c. Projected changes in annual total precipitation for the period 2041-2070, expressed as ratios relative to the means for 1961-1990, for the A1B scenario according to the four general circulation models used in this study.

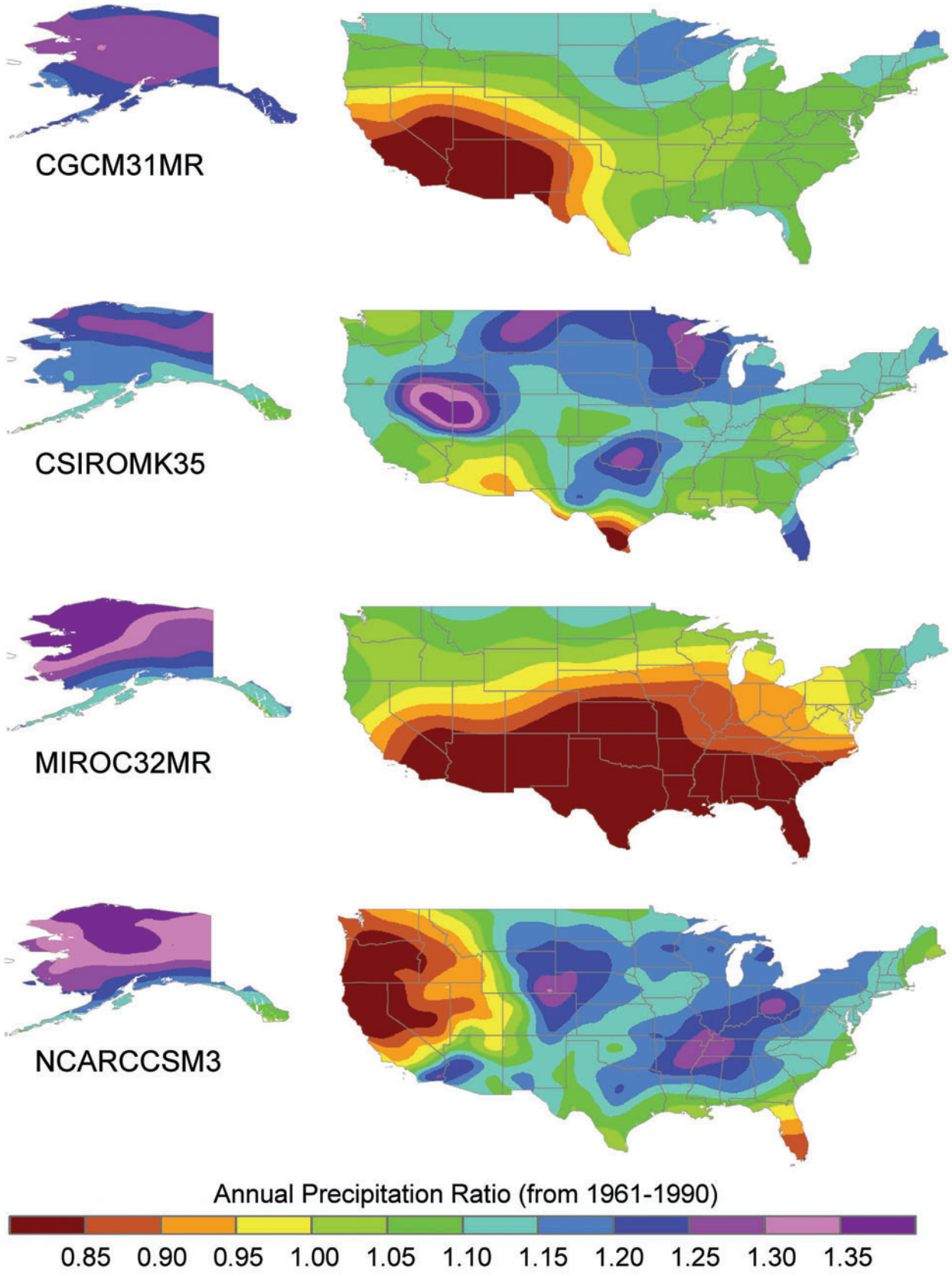

Figure 5d. Projected changes in annual total precipitation for the period 2071-2100 (2071-2099 for NCARCCSM3), expressed as ratios relative to the means for 1961-1990, for the A1B scenario according to the four general circulation models used in this study.

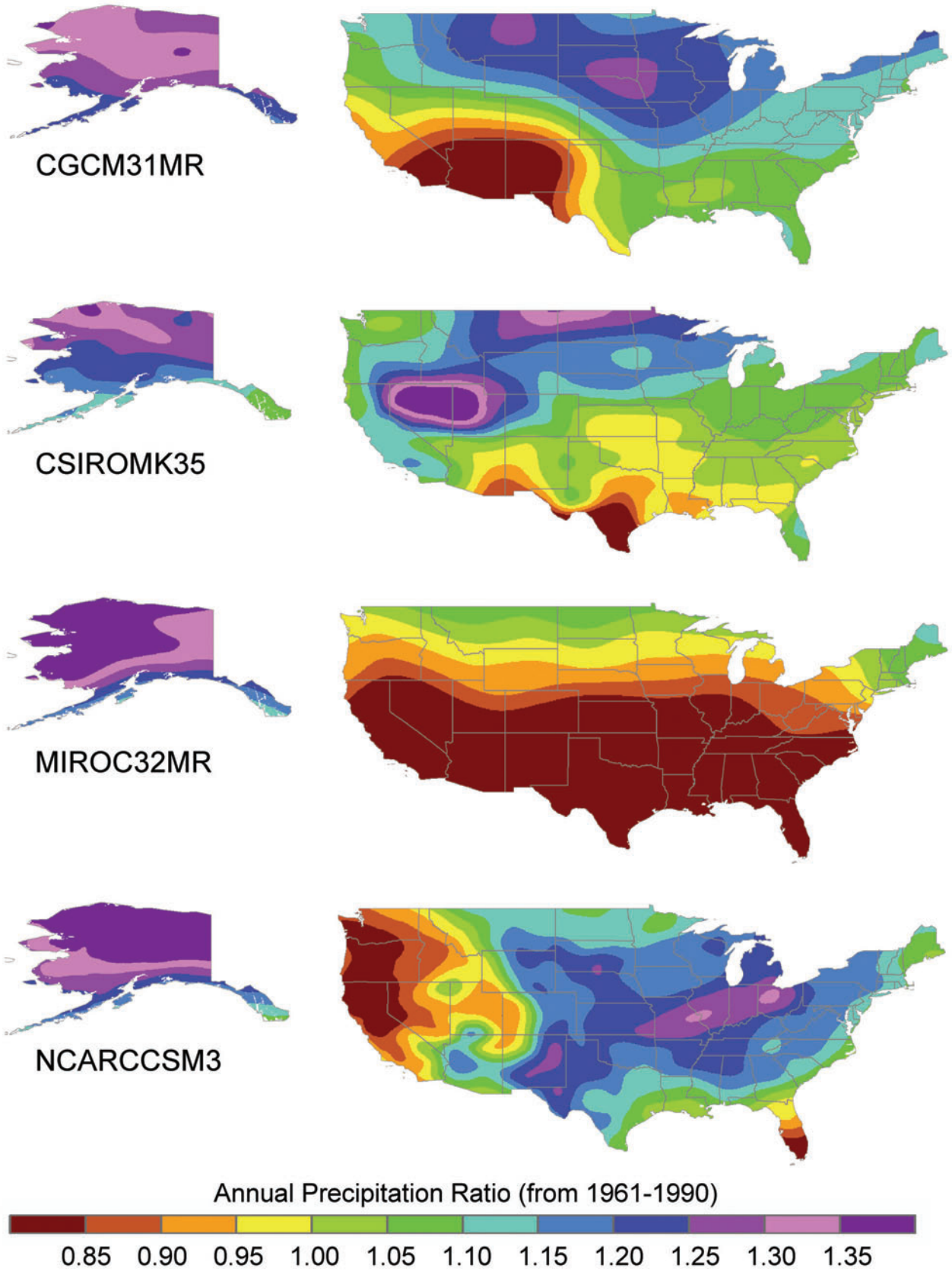

Figure 5e. Projected changes in annual total precipitation for the period 2071-2100 (2071-2099 for NCARCCSM3), expressed as ratios relative to the means for 1961-1990, for the A2 scenario according to the four general circulation models used in this study.

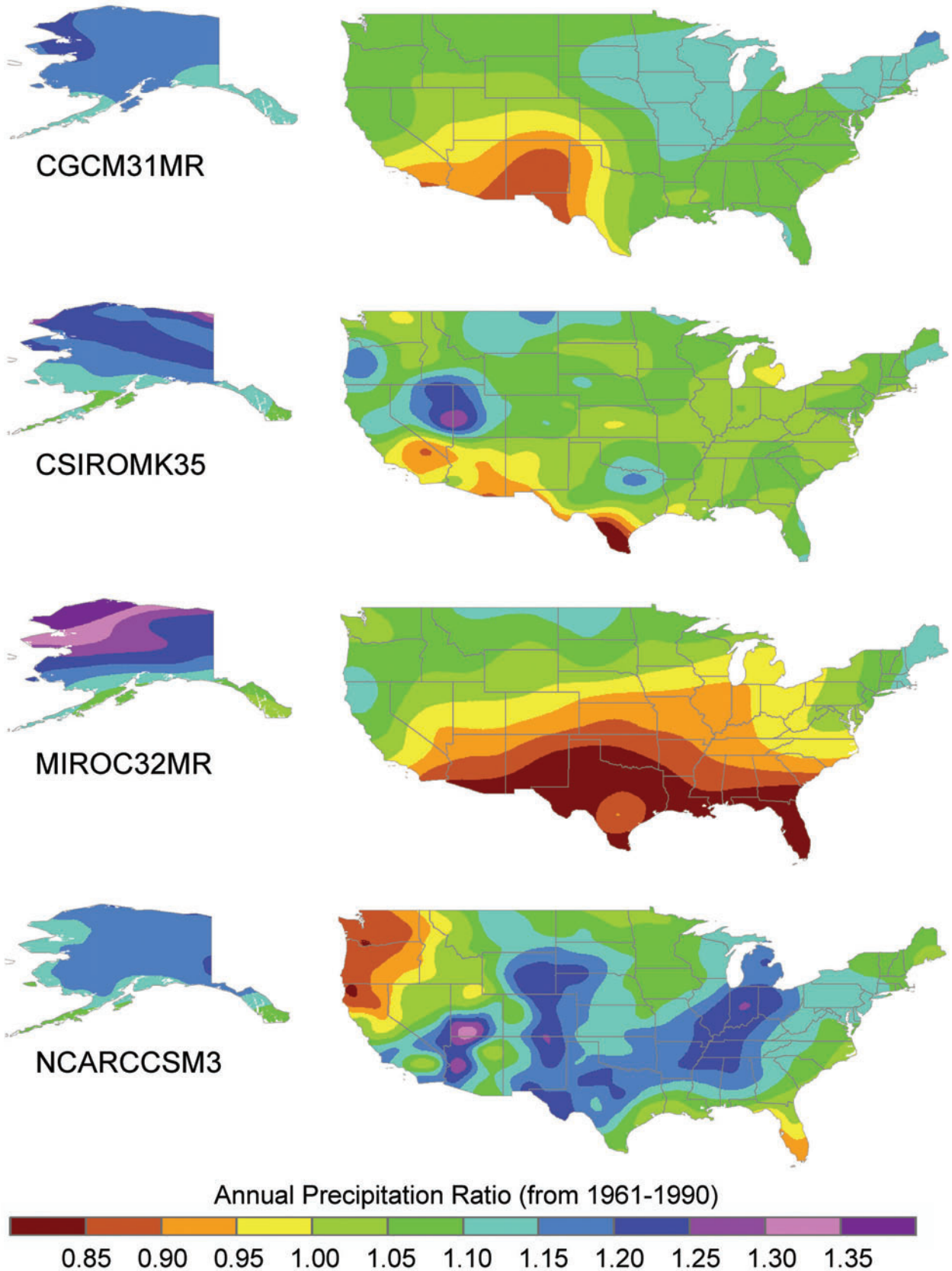

Figure 5f. Projected changes in annual total precipitation for the period 2071-2100 (2071-2099 for NCARCCSM3), expressed as ratios relative to the means for 1961-1990, for the B1 scenario according to the four general circulation models used in this study.

The final two sets of figures (e, f) show the changes for the period 2071–2099, relative to the 1961-1990 period, for each of the A2 and B1, which can be compared directly to the data for the A1B scenario in (d).

The four GCMs agreed fairly closely in their projections of temperature trends, as shown in Figures 3b and 4b for the first 30-year period. By the second 30-year period, differences between the models became increasingly greater for the A1B scenario (Figures 3c and 4c). By the 2071-2099 period, not surprisingly the A2 scenario projected the greatest warming across the country and the B1 the least (Figures 3d, 3e, and 3f, 4d, 4e, and 4f). In general, the B1 projection for each period was qualitatively rather similar to the A1B but for the preceding 30-year period (compare 3f with 3c).

Of the four models, MIROC32MR projected noticeably greater warming in annual mean daily maximum temperature than the other three models during the 21st century (Figures 3b-f). This pattern was most obvious for Alaska and the western states, and by 2099, for the midwestern states. For annual mean daily minimum temperature and the A1B and A2 scenarios, NCARCCSM3 was often within a degree of the projection by MIROC32MR for much of the United States. Comparing the minimum temperature projections with the maximum temperatures across the models (Figures 3d, 3e, 3f, and 4d, 3e, 3f), there was generally a greater increase in minimum temperature by 2099 for all models within each scenario, except MIROC32MR. Here, the projections for maximum temperature by MIROC32MR exceeded the projected changes in minimum temperature.

Ranking the other three models subjectively was difficult. Within the states of Nebraska and South Dakota, there was a noticeable gradation across results for the A2 scenario in 2070–2099 (Figures 3e and 4e): CGCM31MR projected the least warming, followed by CSIROMK35, NCARCCSM3 and MIROC32MR. However, the subjective ranking of these three models was reversed for southern Texas, where NCARCCSM3 projected the least warming (though CGCM31MR is very similar for T_{min}). In the A1B and the A2 scenario, CSIROMK35 projected generally smaller temperature increases in the northwestern states, notably Oregon and Washington, with CGCM31MR and NCARCCSM3 projecting progressively greater increases. Patterns changed for B1; CGCM31MR projected the least change in the northwestern states.

For annual precipitation, increases and decreases were across the United States (Figure 5). For the first 30-year period, CGCM31MR and MIROC32MR both established a drier pattern in the southwest and southern regions, respectively (Figure 5b) and this pattern intensified in the second and third 30-year period (Figures 5c and 5d). The states across the South became markedly drier by 2099 according to MIROC32MR compared to other models, with this trend apparent as early as 2011–2040 in the A1B scenario (Figure 5b). In contrast, NCARCCSM3 projected increases in precipitation from the southwest to the north of midwestern region in the first 30-year period (Figure 5b) and this intensified in the second 30-year period (Figure 5c). Within Alaska, all models and all scenarios projected increases in annual precipitation, particularly in the north (Figure 5 d, e, f).

The spatial patterns of precipitation change as projected within each model by 2099 were similar across the scenarios A1B and A2 (Figures 5d and 5e). For B1, the patterns of increase and decrease in precipitation were similar by model to A1B and A2, but less in magnitude. For example, MIROC32MR showed large areas of the southern United States with declines in precipitation for both A1B and A2 (Figures 5d and 5e); the pattern for B1 still showed declines in the southern United States but of less intensity. Similarly, NCARCCSM3 showed greater increases in precipitation in the midwestern states for both the A1B and A2, relative to the increases seen in B1.

Within each scenario, the geographic pattern of precipitation change varied by model. NCARCCSM3 showed major decreases throughout the western coastal states, while CGCM31MR indicated decreases in the southwestern states (for example, Figure 5d). CSIROMK35 projected large increases inland, notably in Nevada and Utah, and also in northern Montana and North Dakota; CGCM31MR projected increases in Montana, South Dakota, Nebraska, and Iowa. For the B1 scenario across all models, precipitation remained the same or a slight increase; declines were seen in the southwest (CGCM31MR), central south (MIROC32M) and Pacific Northwest (NCARCCSM3).

Comparison of Projections of Changes in Temperature and Precipitation

The four GCMs, forced by each of the three SRES scenarios, differ in their projections of climate change for each ecoregion. The scatter-plots presented in Figure 6 show mean changes in annual mean daily minimum temperature and precipitation ratio for 20-year periods centered on 2050 and 2090 (i.e., approximately 40 and 80 years from present day), referenced to the 1961–1990 period. Plots such as these, have been used when selecting specific GCM scenarios to be representative of the range of projected changes in climate (temperature and precipitation) for a particular region. The plots show some expected trends and a few surprising differences.

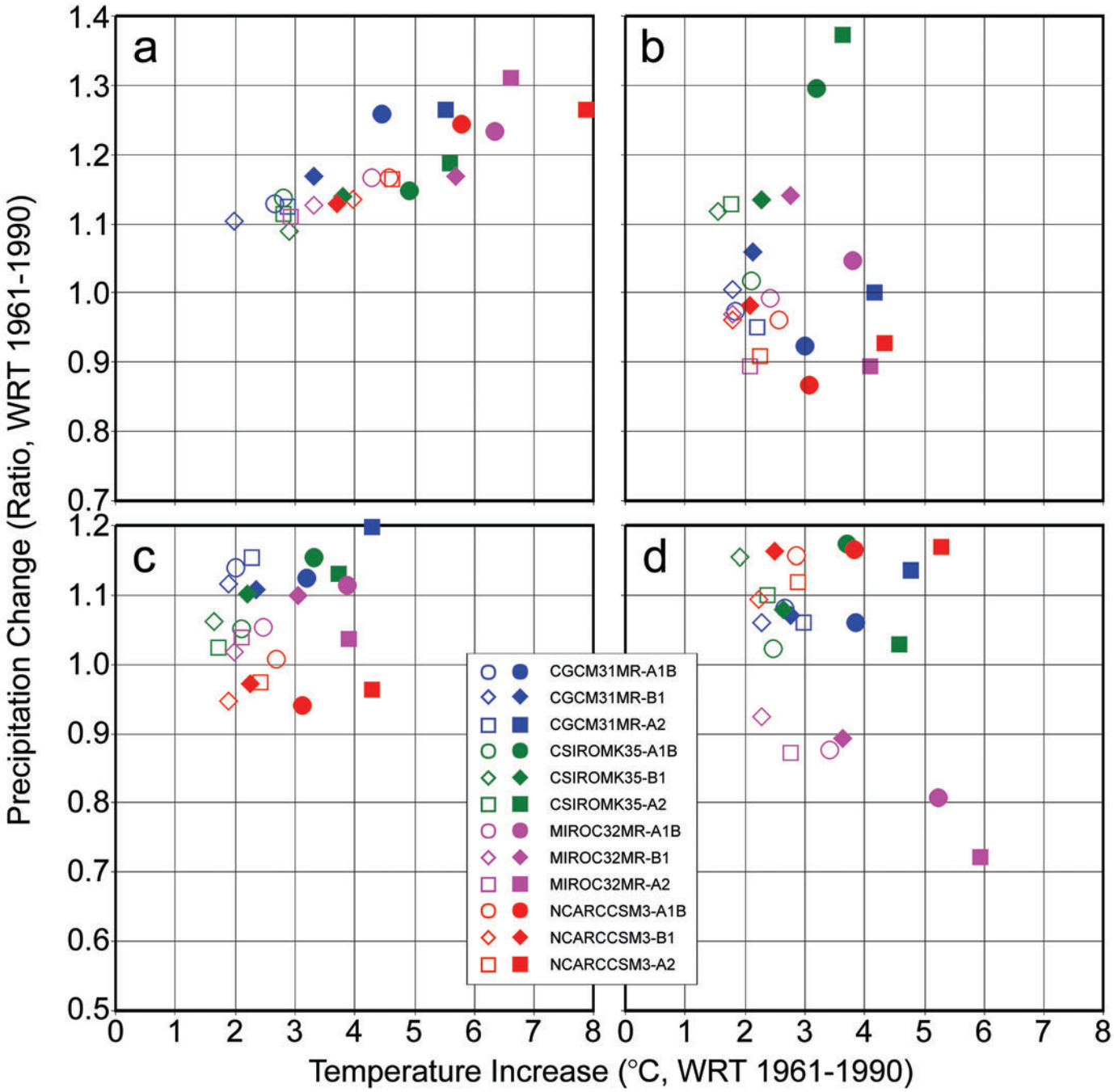

Figure 6. Scatter plots showing the changes in annual mean daily minimum temperature (*x*-axis) and annual precipitation ratio (*y*-axis) projected by each general circulation models, as forced by each greenhouse gas emissions scenario (A1B, B1, A2), relative to means for 1961–1990. Open symbols represent mean changes for 2040–2059, and closed symbols represent mean changes for 2080–2099. Each scatter plot shows area-weighted means for a specific region of the continental United States: (a) Alaska, (b) Mediterranean ecoregion, (c) Marine ecoregion, and (d) Prairie ecoregion. Note the change in the *y*-axis range of precipitation ratios between panels (a) and (b) compared to (c) and (d).

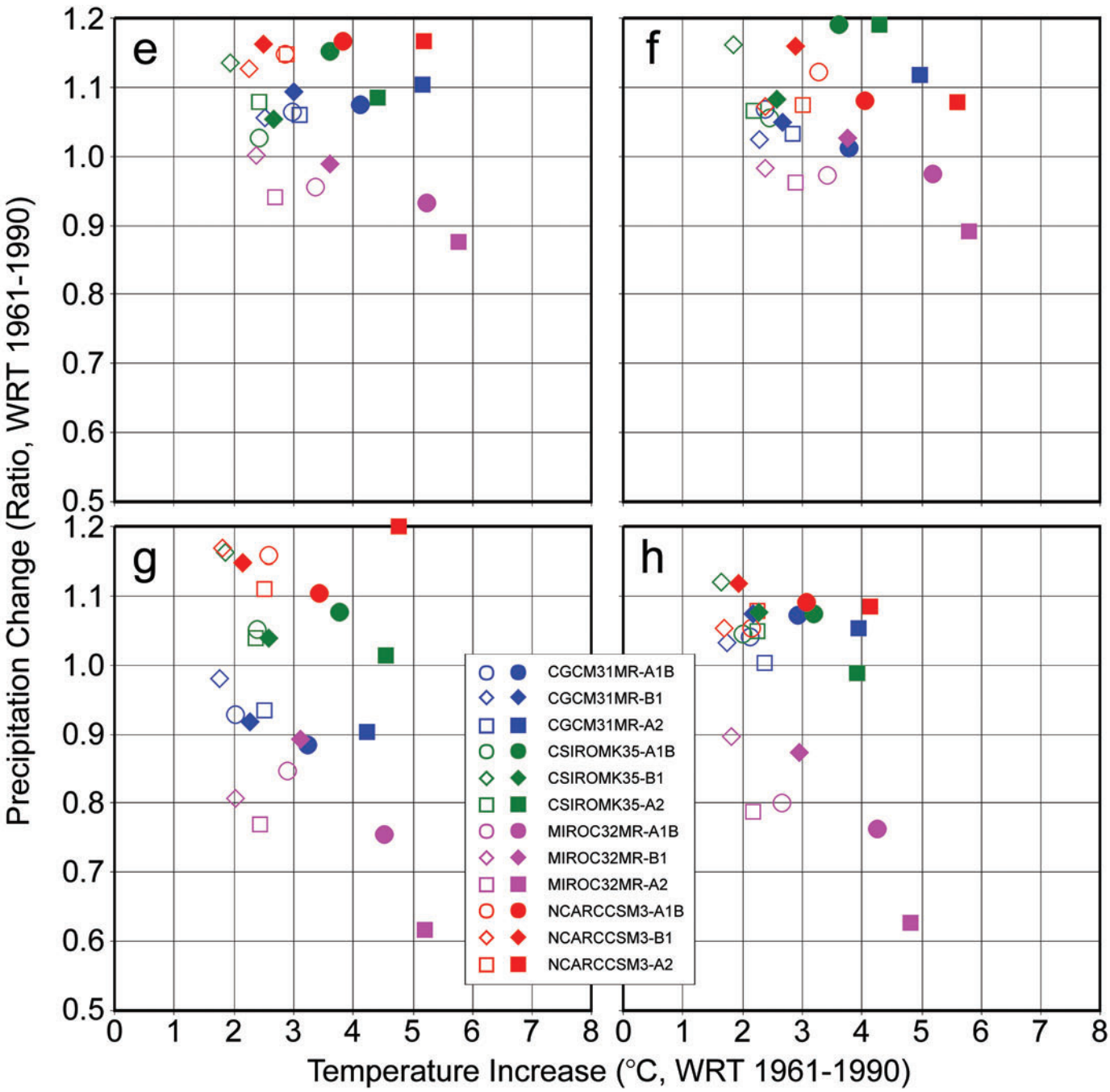

Figure 6 (cont). Scatter plots showing the changes in annual mean daily minimum temperature (*x*-axis) and annual precipitation ratio (*y*-axis) projected by each general circulation model, as forced by each greenhouse gas emissions scenario (A1B, B1, A2), relative to means for 1961–1990. Open symbols represent mean changes for 2040–2059, and closed symbols represent mean changes for 2080–2099. Each scatter plot shows area-weighted means for a specific region of the continental United States: (e) Continental ecoregion, (f) Dry Temperate ecoregion, (g) Dry Subtropical ecoregion, and (h) Subtropical ecoregion.

In general the projected warming was greater for the 2090s than the 2050s, but with increasing divergence among the GCMs. In the 2060s, projected changes clumped along the precipitation axis with temperature changes ranging from 1.5 to 3 ºC across all of the regions but precipitation changes ranging from decreases greater than 20 percent to increases of 20 percent. In the 2090s, a more scattered picture of the changes in temperature and precipitation developed and the results varied greatly across the regions. In Alaska, precipitation projections suggested increasing precipitation and a widening of the projected temperature from a range of 2 to nearly 5 ºC in the 2060s to 3 to 8 ºC in the 2090s, with the NCARCCSM3 model projecting the greatest warming in Alaska. In the Mediterranean, Prairie, Dry Subtropical, and Subtropical, precipitation ratios widened and temperature increased from the 2060s to the 2090s, in contrast to the Marine region where the precipitation ratios across the models remained similar but temperature increased in 2090. By the 2090, the models forced by the A2 scenario almost invariably projected a greater warming than the projections associated with A1B, which in turn produced greater warming than the projections associated with B1.

Consistent with expectations, the models all projected the greatest warming for high latitudes (Alaska, Figure 6a) and the least warming for the narrow West Coast ecoregions (Figures 6b and 6c). Though MIROC32MR generally projected the greatest warming, notably in the southern and mid-continental regions (Figures 6d–h), it was not always the warmest projection in each region. NCARCCSM3 projected similar increases for Alaska and on the West Coast, both NCARCCSM3 and CGCM31MR projected slightly greater warming than MIROC32MR. CSIROMK35 generally projected the least warming.

There was much less agreement among the models on projected changes in precipitation, and the trends varied greatly with location. In the Mediterranean ecoregion (Figure 6b), CSIROMK35 projected precipitation increases of 30 to 40% (A1B and A2 scenarios) by 2090, greater than projected for the Marine ecoregion. NCARCCSM3 projected decreases of 13% with the A1B, but only 8% with the A2 in the Marine region (Figure 6b). In these coastal regions MIROC32MR generally projected decreases similar to those projected by CGCM31MR in the Mediterranean region and slight increases in the Marine ecoregion.

MIROCMR32 projected the greatest increase in precipitation for Alaska (with the A2 forcing, Figure 6a), but in the southern and midcontinental regions (Figures 6d–h), and particularly in the Subtropical ecoregions (Figures 6g, 6h), the model projected large decreases where other models either projected no change or small increases. Among other models, in the southern and mid-continental regions, the NCARCCSM3 and CSIROMK35 generally projected increases in precipitation, and the CGCM31MR was most conservative, projecting modest increases in most regions and slight decreases in the Dry Subtropical ecoregion (Figure 6h).

Comparison of Simulated Interannual Variability

The following discussion attempts to sample all the available data by comparing some results obtained with each model and each GHG scenario for each ecoregion, climate variable, and season. The selection of graphs representative of the different regions and seasons, and are used to highlight some specific strengths and weaknesses, where differences among the results may indicate problems with particular variables or GCMs.

The leftmost panels of Figures 7 and 8 (together with those of graphs a, b, and c in Figures 11–14) show how the different GCMs were able to capture observed interannual variability in seasonal and annual temperature and precipitation. In each figure, observed data for 1961-2008 (black line) are superimposed on the results of the GCM simulations, comprising the 20C3M scenario (historical simulated) for the period of 1961-2000 (1961-1999 for NCARCCSM3) and the three future emissions scenarios for the 2001-2008 (2000-2008 for NCARCCSM3)

Although there clearly were some important differences, the amplitudes of the variations around the simulated means for the 1961-2008 period were generally comparable to the amplitudes of the interpolated observed data (shown in black), and the differences among seasons were captured well. This result was also seen in the differences in patterns of variability between T_{max} and T_{min}, seen both in summer (Figures 7a, 7b and 13a, 13b) and winter (Figures 7c, 7d and 14a, 14b). However, some GCMs tended to exaggerate the observed variability (notably NCARCCSM3 for the Marine ecoregion in winter seen in Figures 14a, 14b).

The quality of agreement in amplitude of variation was poorer for precipitation, both between the simulated historical and the observed interpolated data and among models. Figures 8a–d show CSIROMK35 generally exaggerated observed variability year round in the Prairie ecoregion. Figure 11c shows NCARCCSM3 exaggerated the annual variability for the Dry Temperate ecoregion, but MIROC32MR appeared to underestimate variability.

Conversely, in the Subtropical ecoregion (Figure 12c), MIROC32MR greatly overestimated observed variability in summer. In the Dry Subtropical during fall, NCARCCSM3 and CSIROMK35 both overestimated variability (Figure 13c), but in the Marine ecoregion during winter (when mean precipitation amounts were large and interannual variability was correspondingly large), all the GCMs seemed to generate variability similar to the observed interpolated data (Figure 14c).

The results overall suggested considerable consensus among the models, particularly regarding simulation of the interannual variability of observed temperature means, but even to some extent with the observed precipitation data. Hence, the GCMs appeared to capture many of the observed characteristics of these climate variables, which in turn suggests that the future scenarios can be treated as plausible projections of future climate, as determined by different scenarios of future GHG emissions.

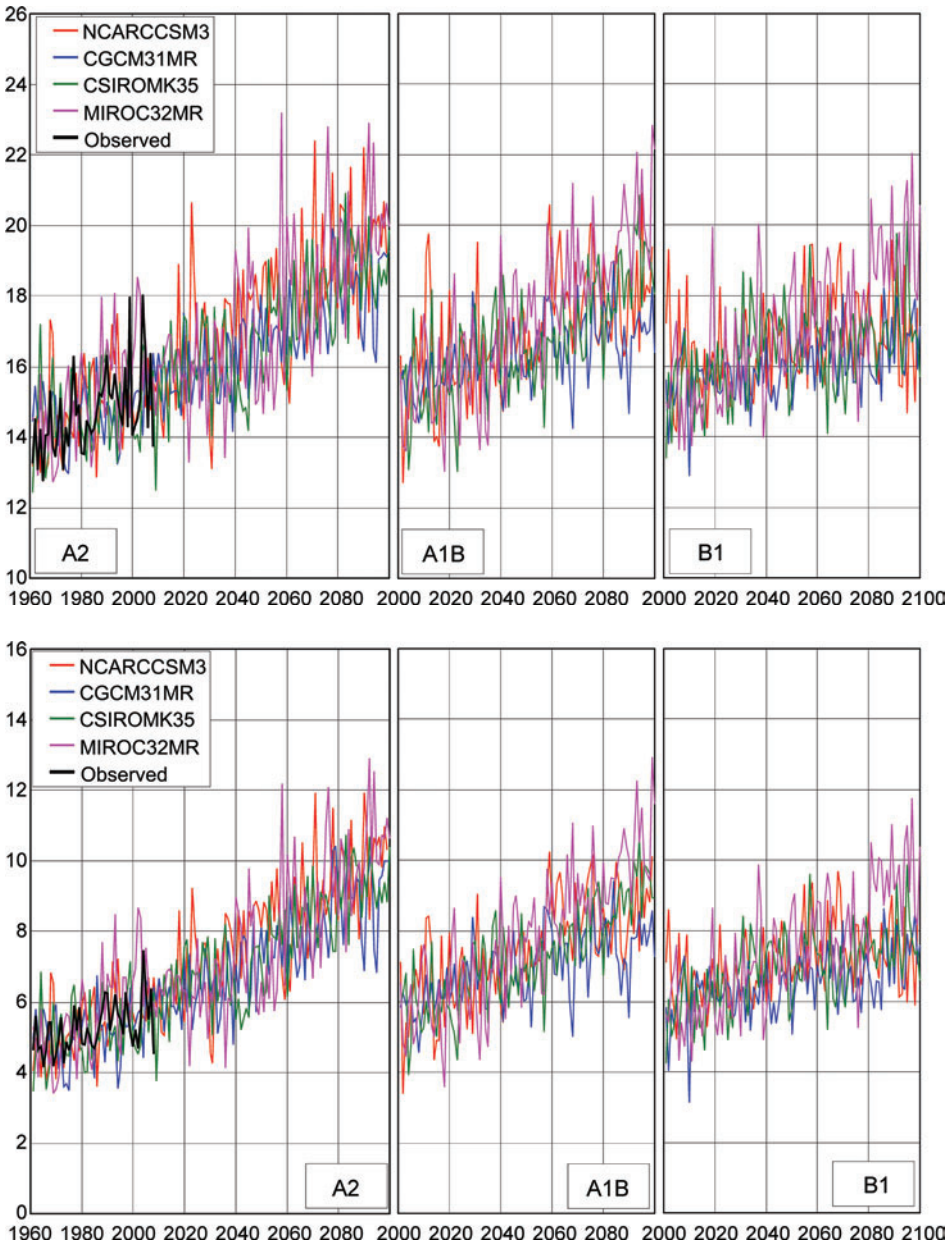

Figure 7a, b. Projections of spatially averaged summer mean daily maximum (a, upper) and minimum temperature (b, lower) (°C) for Alaska for four greenhouse gas forcing scenarios, relative to interpolated observed data for 1961–2008. The simulated historical data for the period 1961-2000 (20C3M scenario for each general circulation model) and the observed data are shown only in the leftmost panels, but are common to all three future projections. CGCM31MR = Third Generation Coupled Global Climate Model, version 3.1, medium resolution; CSIROMK35 = Commonwealth Scientific and Industrial Research Organisation Climate System Model, Mark 3.5; MIROC32MR = Model for Interdisciplinary Research on Climate, version 3.2 medium resolution; NCARCCSM3 = Community Climate System Model, version 3.0.

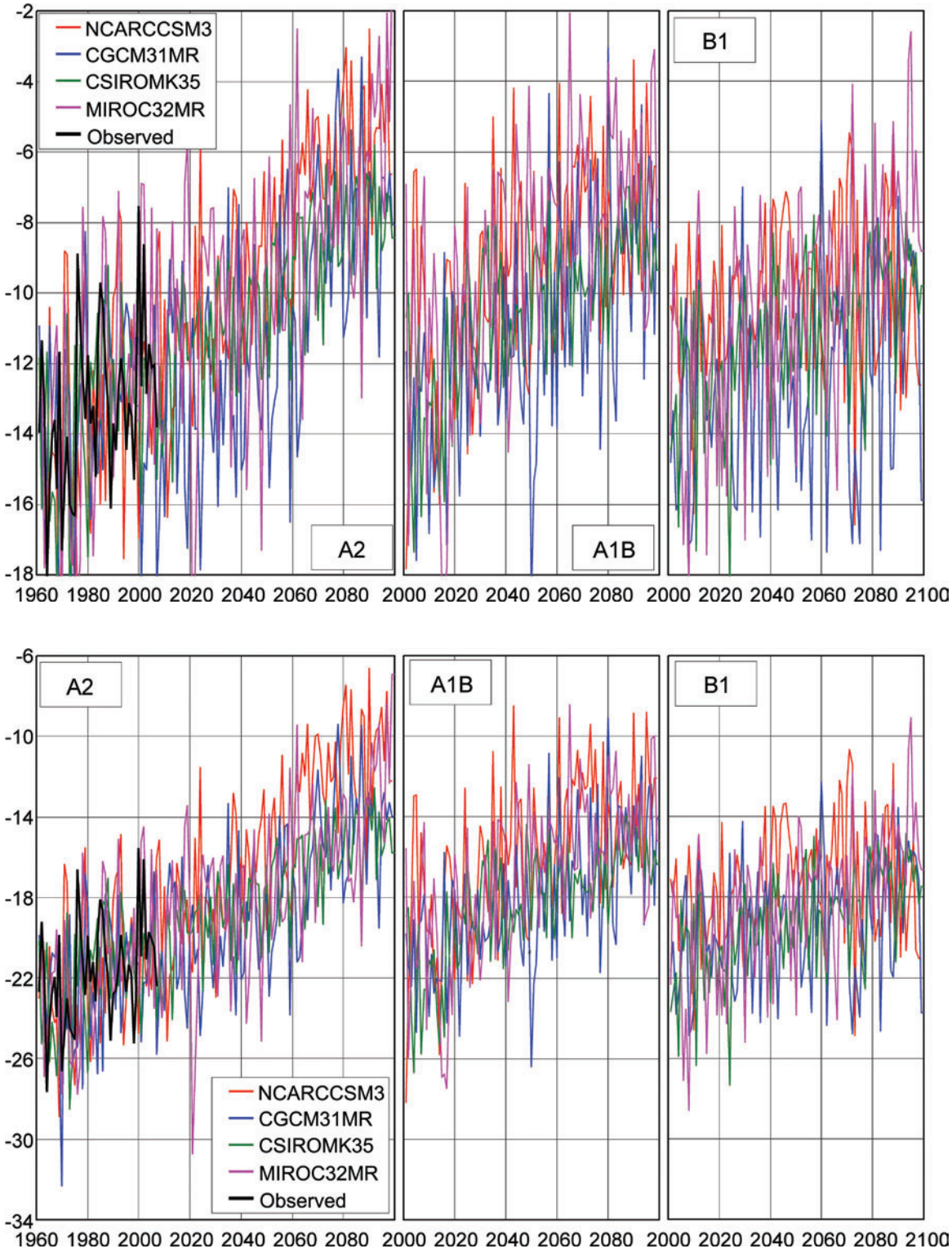

Figure 7c, d. Projections of spatially averaged winter mean daily maximum (c, upper) and minimum temperature (d, lower) (°C) for Alaska for four greenhouse gas forcing scenarios, relative to interpolated observed data for 1961–2008. The simulated historical data for the 1961-2000 period (20C3M scenario for each general circulation model) and the observed data are shown only in the leftmost panels, but are common to all three future projections.

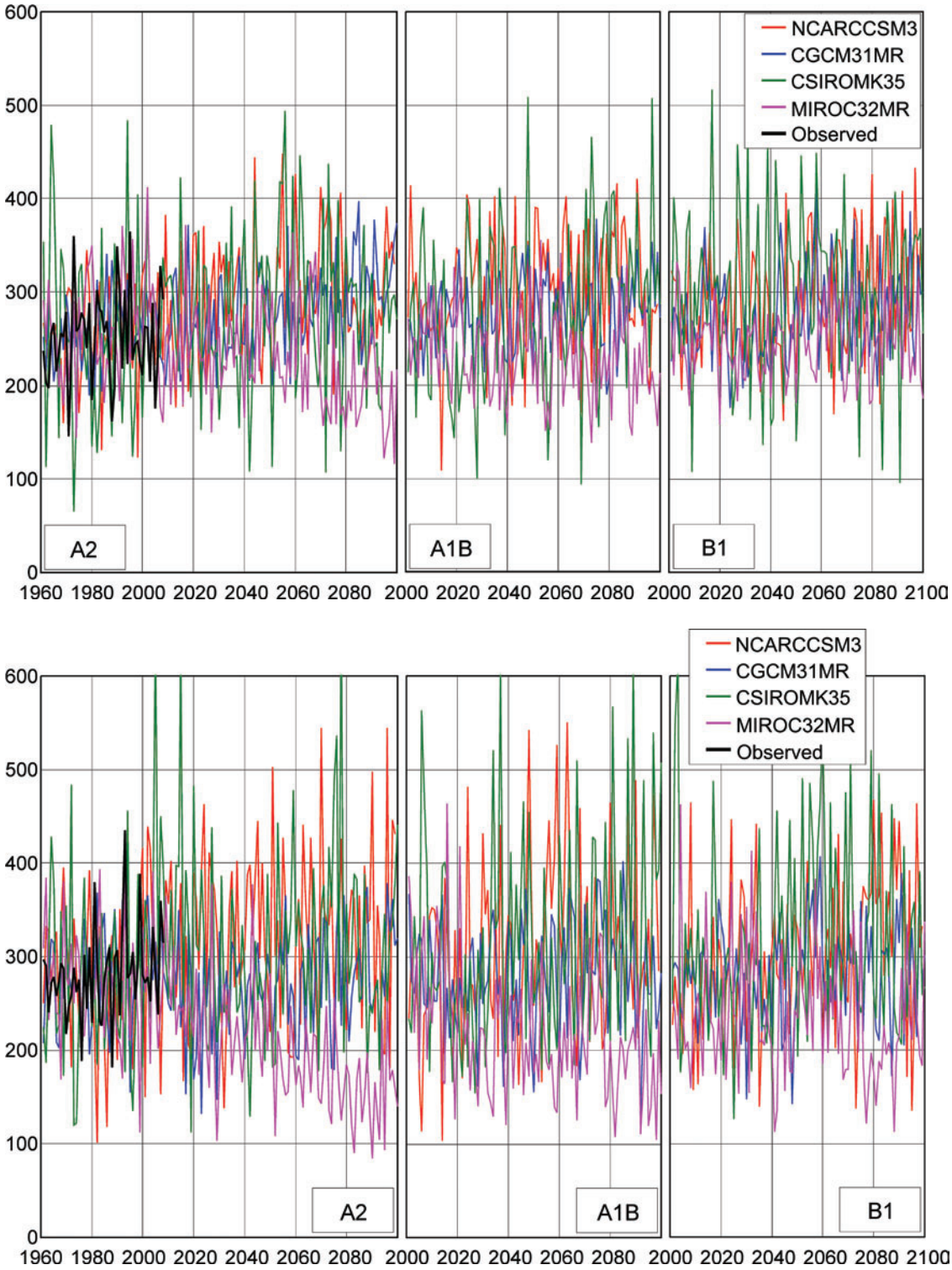

Figure 8a, b. Projections of spatially averaged spring (a, upper) and summer (b, lower) total seasonal precipitation (mm) for the Prairie region for four greenhouse gas forcing scenarios, relative to interpolated observed data for 1961–2008. The simulated historical data for the period 1961-2000 (20C3M scenario for each general circulation model) and observed data are shown only in the leftmost panels, but are common to all three future projections. CGCM31MR = Third Generation Coupled Global Climate Model, version 3.1, medium resolution; CSIROMK35 = Commonwealth Scientific and Industrial Research Organisation Climate System Model, Mark 3.5; MIROC32MR = Model for Interdisciplinary Research on Climate, version 3.2 medium resolution; NCARCCSM3 = Community Climate System Model, version 3.0.

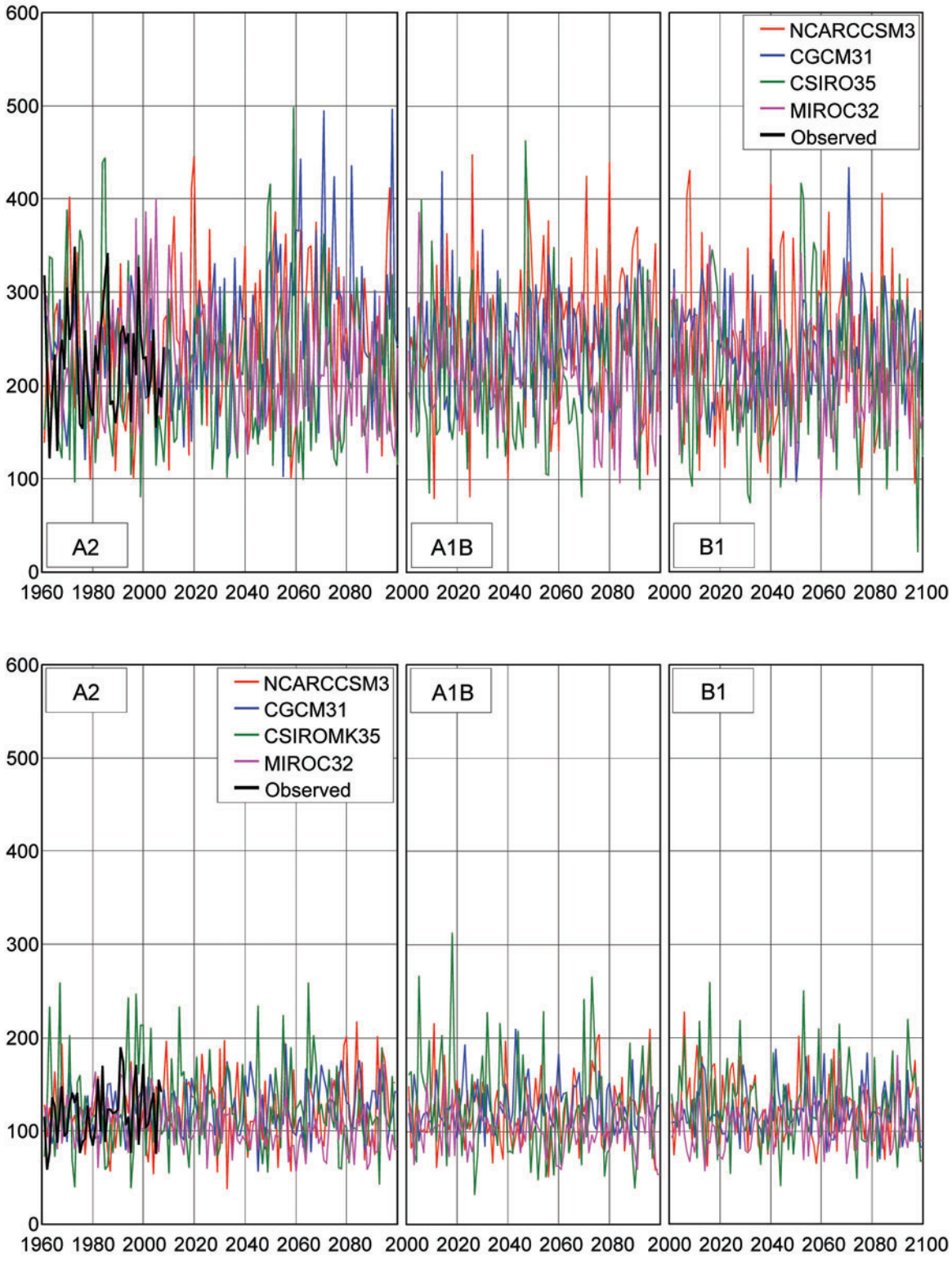

Figure 8c, d. Projections of spatially averaged fall (c, upper) and winter (d, lower) total seasonal precipitation (mm) for the Prairie region for four greenhouse gas forcing scenarios, relative to interpolated observed data for 1961–2008. The simulated historical data for the 1961-2000 period (20C3M scenario for each general circulation model) and observed data are shown only in the leftmost panels, but are common to all three future projections.

Projected Climate Trends 2001–2100

Alaska was projected to experience the largest increases in temperature within the continental United States over the next 90 years (Figure 6a). Summer temperatures (both daily minima and maxima) were projected to increase by 3–5 °C (Figures 7a and 7b), while the increases for winter temperatures were larger, in the range 4–8 °C (Figures 7c and 7d). Clearly, there was some divergence among the models, with MIROC32MR and NCARCCSM3 both projected greater increases (winter daily minima by as much as 12 °C and maxima by up to 10 °C by 2100 with the A2 scenario) than the CGCM31MR and CSIROMK35 projections, which were still in the range 4–6 °C and 4–7 °C, for winter T_{max} and T_{min}, respectively, by 2100. Variation in summer projections was less across all scenarios and models than the winter projections, likely reflecting the corresponding variations in the seasonal historical temperatures. Projections for winter mean daily maximum remain within the historical range of variability well into the 21st century (Figure 7c).

With few exceptions, all four models showed good agreement in the projected changes in means and interannual variation in precipitation in the Prairie region up to 2100 (Figure 8). The NCARCCSM3, and in particular the CSIROMK35, generally projected greater extremes. MIROC32MR was the only GCM to show a distinct pattern of decreasing precipitation across all scenarios, particularly in spring and summer with the A2 forcing scenario (Figure 8a and b), a trend that recurred in other regions (notably for annual precipitation in the Dry Temperate region [Figure 11c] and summer precipitation in the Subtropical region [Figure 12c]). Winter precipitation showed little to no change (Figure 8d) whereas spring precipitation showed an increase in the mean of 9 mm to 23 mm by 2079-2100 (Table 8). When projections for all four models within each scenario were averaged for the Prairie region, the general pattern was for a slight increase in annual precipitation of 14 to 42 mm by 2070–2099, mainly in spring. There was little obvious dependence on the GHG forcing scenario as the precipitation projections for all models in each season encompassed each other (Figure 8).

Vapor pressure projections for the Mediterranean region provide a good comparison of the results for this variable from different GCMs found throughout the downscaled data set (Figure 9). All four models within all three future scenarios projected steady increasing values for vapor pressure reflecting the projected trends in temperature (Figures 3d, 3e, and 3f). Although individual model projections within each season tracked each other; projections tended to be the highest by 2100 for the A2 scenario. Vapor pressure increased the greatest in summer and the least in winter.

Projections by the four models of changes in summer and winter solar radiation for the Continental region were very similar in their projected amplitudes of interannual variability, particularly in summer (Figure 10a), when it is almost impossible to rank them. For winter, NCARCCSM3 produced the greatest extremes and CGCM31MR the smallest, with MIROC32MR tended higher than the mean and CSIROMK35 tended lower (Figure 10b). The substantial interannual variability obscures changes that can be seen in the 10-year moving averages of the same data (Figure 10c and 10d), such as the pattern of increasing summer radiation with CGCM31MR and MIROC32MR, but little change projected by NCARCCSM3 and CSIROMK35. These trends were strongest with the A2 scenario, which has the highest emission levels by 2100, but barely detectable with B1, the lowest emission levels. Three models projected a trend of decreasing winter radiation (seen in Figure 10d), with the A2 resulting in the largest declines; MIROC32MR exceptionally projected an initial increase followed by steady decline back to initial levels in all three future scenarios.

Projections by individual model for mean daily minimum temperature for the Dry Temperature region tracked each other closely within each scenario and show the influence of the GHG forcing in that the greatest temperature increases were associated with A2 and the least with B1 (Figure 11a and 11b, similar patterns seen in Figure 6f). For maximum temperature, the individual model projections separated early in the 21st century with the MIROC projection increasing above all other models in all three future scenarios (Figure 11a). The comparison of the simulated with the observed precipitation data showed that NCARCCSM3 exhibited high variability and trended above the other model projections (Figure 11c). When annual precipitation means of the 1980-2009 period were compared with the 2070-2100 period, precipitation was projected to increase for the B1 scenario (7.4 mm) and the A2 scenario (2.7 mm), and to decrease for the A1B scenario (7.7 mm). Obviously there was great variation over the 21st century within each projection.

Projections by the four models of changes in annual solar radiation for the Dry Temperate region were very similar in their projected amplitudes of interannual variability (Figure 11d). MIROC32MR tended higher than the mean but the projections within each scenario encompassed each other. When the model results are averaged by scenario, summer radiation declines only

slightly and to the same extent in all scenarios. As with the Mediterranean region (Figure 9), vapor pressure for the Dry Temperate region increases but annually only a small amount (Figure 11e). Scenario A2 shows the greatest increase, with the MIROC32 model showing the smallest changes. Wind speed for the Dry Temperate region showed little change by scenario. This pattern was seen consistently in all other regions, in the means or variability, and no consistent sensitivity to the level of GHG. Hence, there do not appear to be large or consistent differences among the four GCMs with respect to wind speed.

Similar to the annual temperature changes in Dry Temperate region (Figure 11a), the summer mean daily maximum and minimum temperatures for the Subtropical region projected by individual models showed the influence of the GHG forcing with the warmest temperatures at the end of the 21st occurring in the A2 scenario, then A1B and finally B1 (Figure 12). The summer mean daily minimum temperatures for the Subtropical region projected by individual models within each scenario tracked each other closely (Figure 12b); but greater variation of the model projections within each of the scenarios was seen for the mean daily maximum temperature, with the MIROC projection rising above all of the other model projections in the A2 and A1B scenarios (Figure 12a). The Subtropical region encompasses the southeastern parts of the United States and annual precipitation projection varied by model and scenario, with the CGCM31MR and the CSIROMK35 projecting little change across all scenarios; but the MIROC32MR projecting large declines in annual precipitation when the 2071-2100 period is compared to the 1961-1990 period (Figures 5d, 5e, and 5f) Projections for summer precipitation declined in the MIROC32MR projections for scenarios A2 and A1B, but changed minimally in the other models (Figure 12c). When averaged across models by scenarios, summer precipitation declined for the A2 and A1B scenarios, showing a slight increase in the B1 scenario (Table 9). A major influence in these composite projections was the MIROC projection for A2 and A1B (Figure 12c). These precipitation patterns were also seen in the summer vapor pressure (Figure 12e). Wind speed projections for the Subtropical region, as with other regions, showed very little sensitivity to model or to scenario (Figure 12f).

Fall mean daily maximum and minimum temperatures for the dry Subtropical region increased in all scenarios, with the largest increases in the A2 scenario and the smallest changes in the B1 scenario (Figure 13a). For maximum temperature, the MIROC32MR projections tended to be the highest; however for minimum temperature, the projections encompassed one another within each scenario. Projections for fall precipitation had high variability, reflecting the historical variability (Figure 13c). This region spans from central Texas west to the California border and when compared to the 1961-1990 period, the spatial patterns of annual precipitation projections for 2070-2100 varied greatly within the region by model, more than by scenario. For example, NCARCCSM3 projected little change to some increases in precipitation across all scenarios, with great spatial variability (Figures 5d, 5e, 5f). MIRCO32MR consistently projected declines across the region. Projections for fall solar radiation showed little sensitivity to scenario, similar to other regions, but were more variable, than annual solar radiation for the Dry Temperate region (Figure 11d) or summer solar radiation for the Subtropical region (Figure 12c). Vapor pressure projections for the fall season showed sensitivity to scenario; however wind speed showed little sensitivity to scenario or model.

Winter projections for the Marine region reflected general patterns seen in other regions, winter maximum and minimum temperatures were sensitive to the scenario, precipitation projections had great variability, and little changes were seen in solar radiation or wind speed (Figure 14). NCARCCSM3 projected much greater interannual variability, particularly for minimum temperature in winter. Increases in winter temperature were greater for minimum temperature than maximum, a pattern seen in the Alaska region (Figure 7c and 7d).

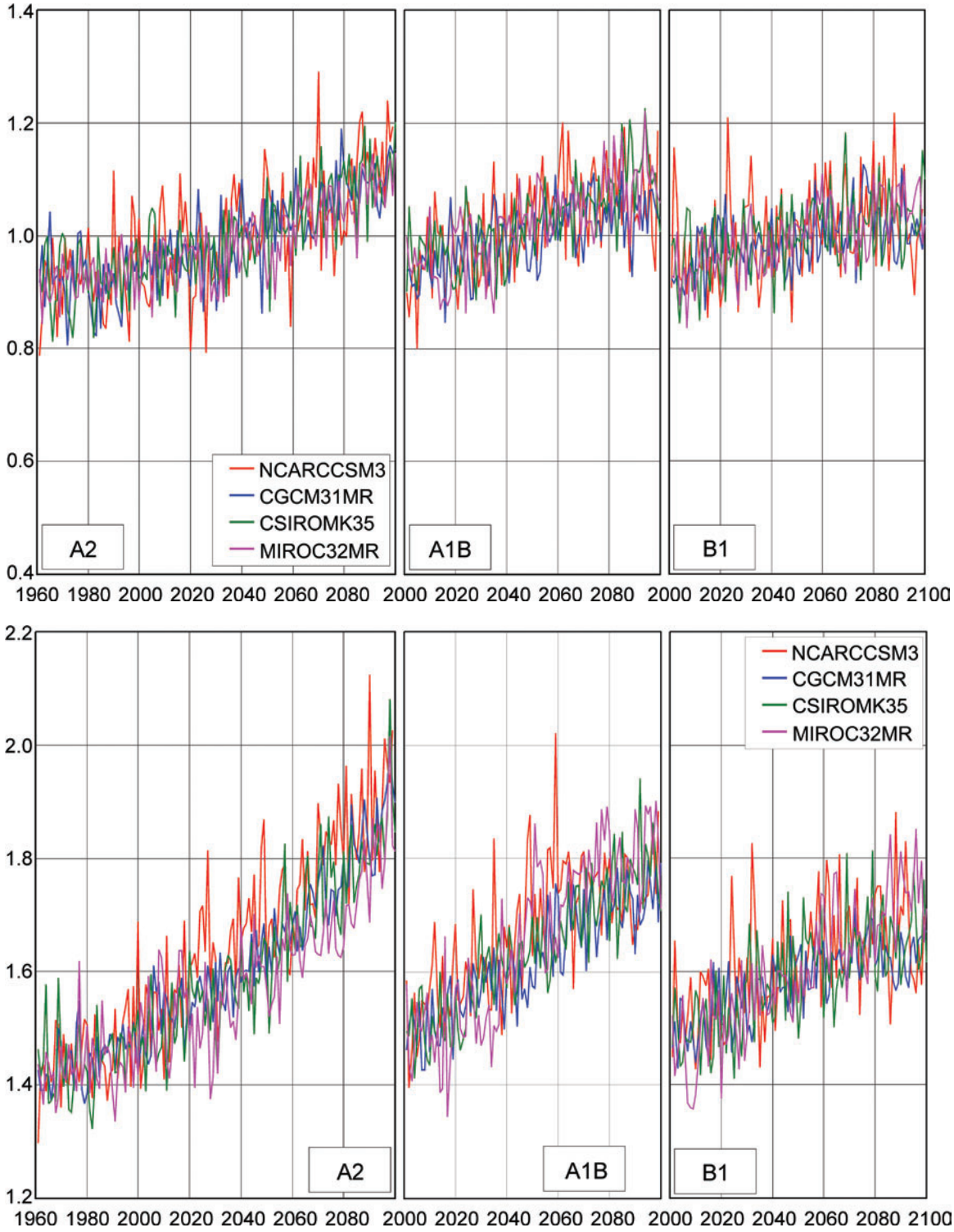

Figure 9a, b. Projections of spatially averaged spring (a, upper) and summer (b, lower) mean vapor pressure (kPa) for the Mediterranean region for four greenhouse gas forcing scenarios. The simulated historical data for the 1960-2000 period (20C3M scenario for each general circulation model) are shown only in the leftmost panels, but are common to all three future projections. CGCM31MR = Third Generation Coupled Global Climate Model, version 3.1, medium resolution; CSIROMK35 = Commonwealth Scientific and Industrial Research Organisation Climate System Model, Mark 3.5; MIROC32MR = Model for Interdisciplinary Research on Climate, version 3.2 medium resolution; NCARCCSM3 = Community Climate System Model, version 3.0.

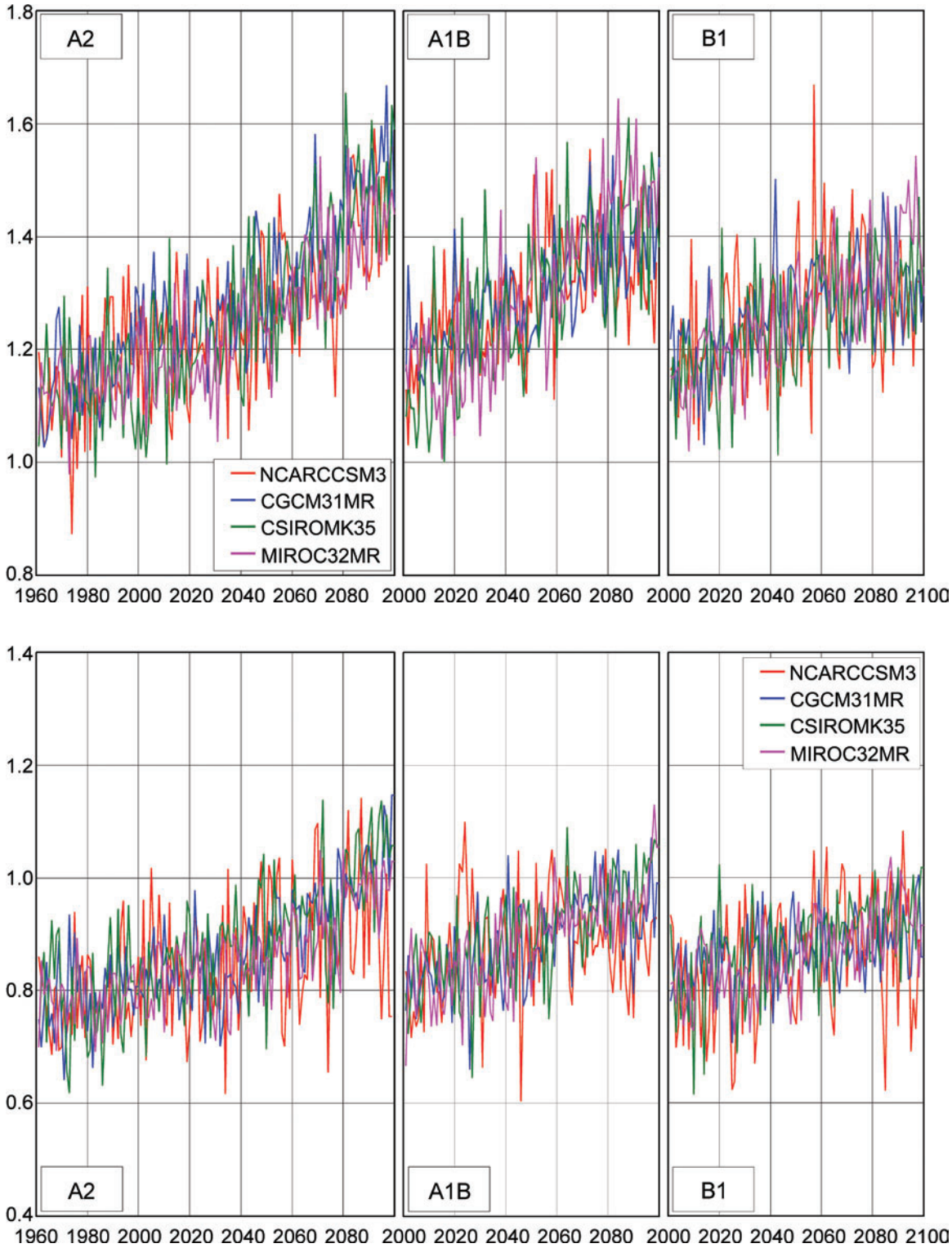

Figure 9c, d. Projections of spatially averaged fall (c, upper) and winter (d, lower) mean vapor pressure (kPa) for the Mediterranean region for four greenhouse gas forcing scenarios. The simulated historical data for the 1960-2000 period (20C3M scenario for each GCM) are shown only in the leftmost panels, but are common to all three future projections.

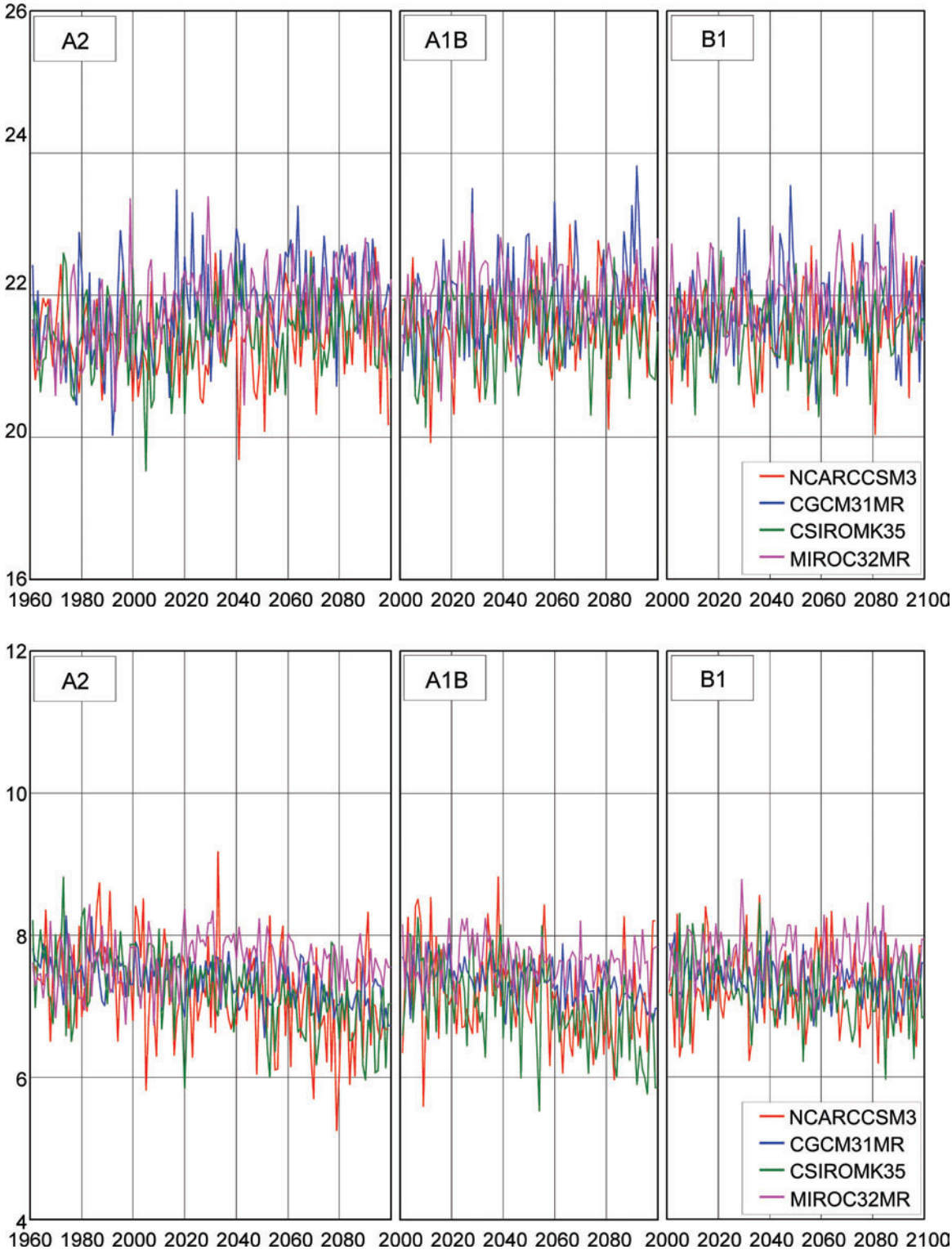

Figure 10a, b. Projections of spatially averaged summer (a, upper) and winter (b, lower) mean daily global solar radiation (MJ m^{-2} d^{-1}) for the Continental region for four greenhouse gas forcing scenarios. The simulated historical data for the 1960-2000 period (20C3M scenario for each general circulation model) are shown only in the leftmost panels, but are common to all three future projections. CGCM31MR = Third Generation Coupled Global Climate Model, version 3.1, medium resolution; CSIROMK35 = Commonwealth Scientific and Industrial Research Organisation Climate System Model, Mark 3.5; MIROC32MR = Model for Interdisciplinary Research on Climate, version 3.2 medium resolution; NCARCCSM3 = Community Climate System Model, version 3.0.

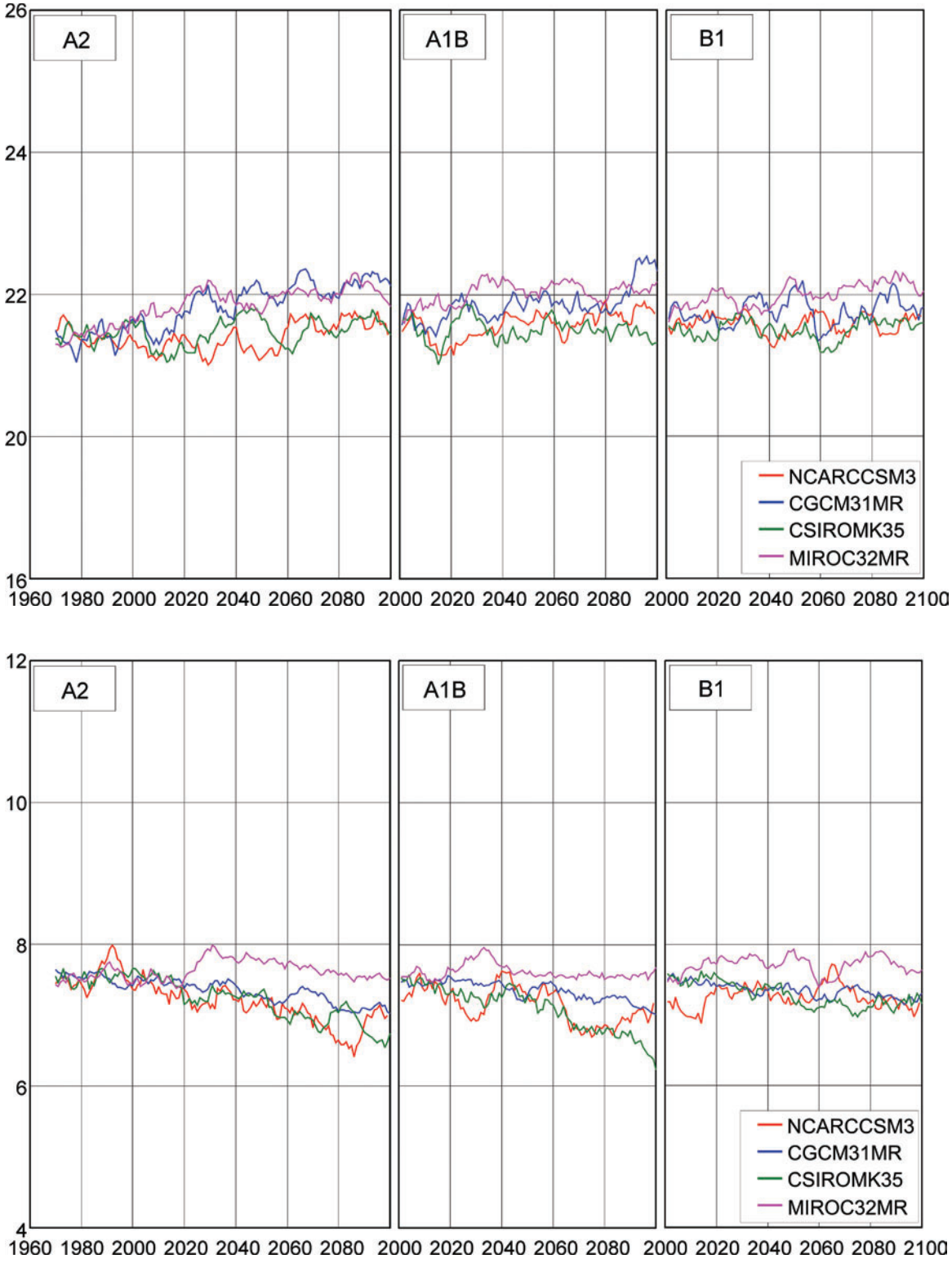

Figure 10c, d. Projections of spatially averaged summer (c, upper) and winter (d, lower) mean daily global solar radiation (MJ m^{-2} d^{-1}) for the Continental region for four greenhouse gas forcing scenarios. Annual data have been smoothed with a 10-year moving average. The simulated historical data for the 1960-2000 period (20C3M scenario for each general circulation model) are shown only in the leftmost panels, but are common to all three future projections.

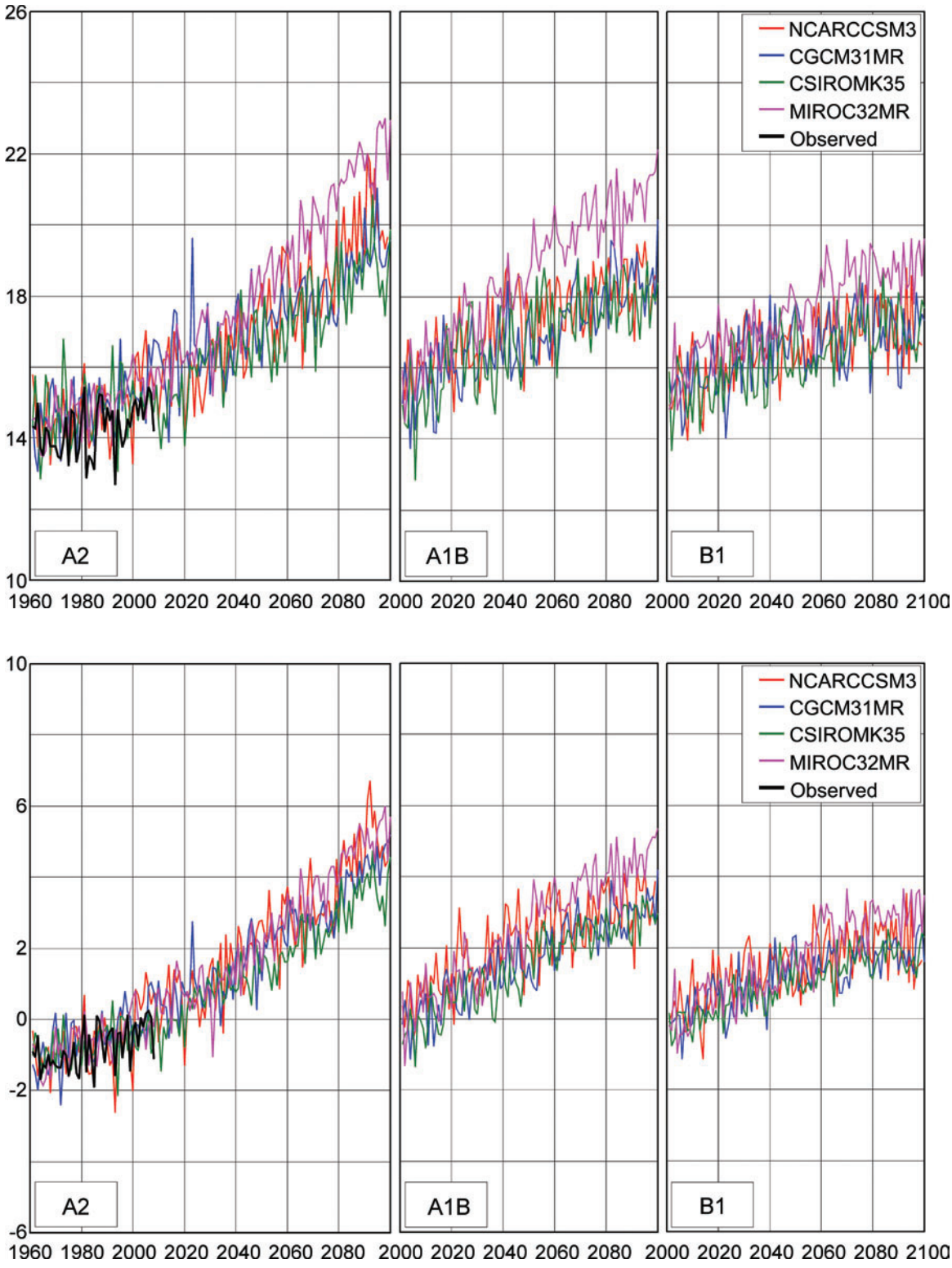

Figure 11a, b. Projections of spatially averaged annual mean daily maximum (a, upper) and minimum (b, lower) temperature (°C) for the Dry Temperate region for four greenhouse gas forcing scenarios, relative to interpolated observed data for 1961–2008. The simulated historical data for the 1960-2000 period (20C3M scenario for each general circulation model) and observed data are shown only in the leftmost panels, but are common to all three future projections. CGCM31MR = Third Generation Coupled Global Climate Model, version 3.1, medium resolution; CSIROMK35 = Commonwealth Scientific and Industrial Research Organisation Climate System Model, Mark 3.5; MIROC32MR = Model for Interdisciplinary Research on Climate, version 3.2; NCARCCSM3 = Community Climate System Model, version 3.0.

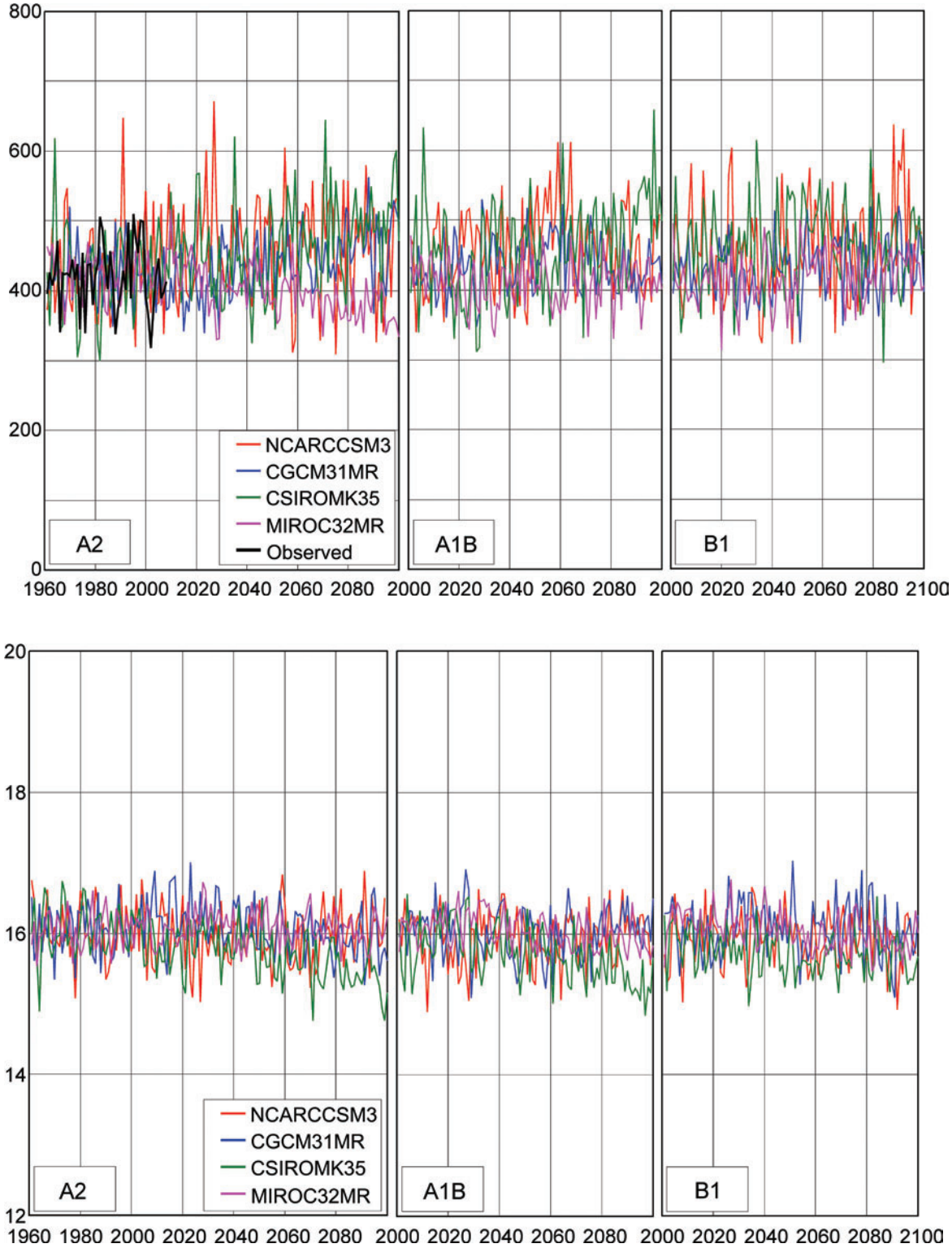

Figure 11c, d. Projections of spatially averaged annual total precipitation (mm) (c, upper) and daily global solar radiation (d, lower) (MJ m^{-2} d^{-1}) for the Dry Temperate region, for four greenhouse gas forcing scenarios. Precipitation projections are also compared with the interpolated observed data for 1961-2008. The simulated historical data for the 1960-2000 period (20C3M scenario for each general circulation model) and observed data (precipitation only) are shown only in the leftmost panels, but are common to all three future projections.

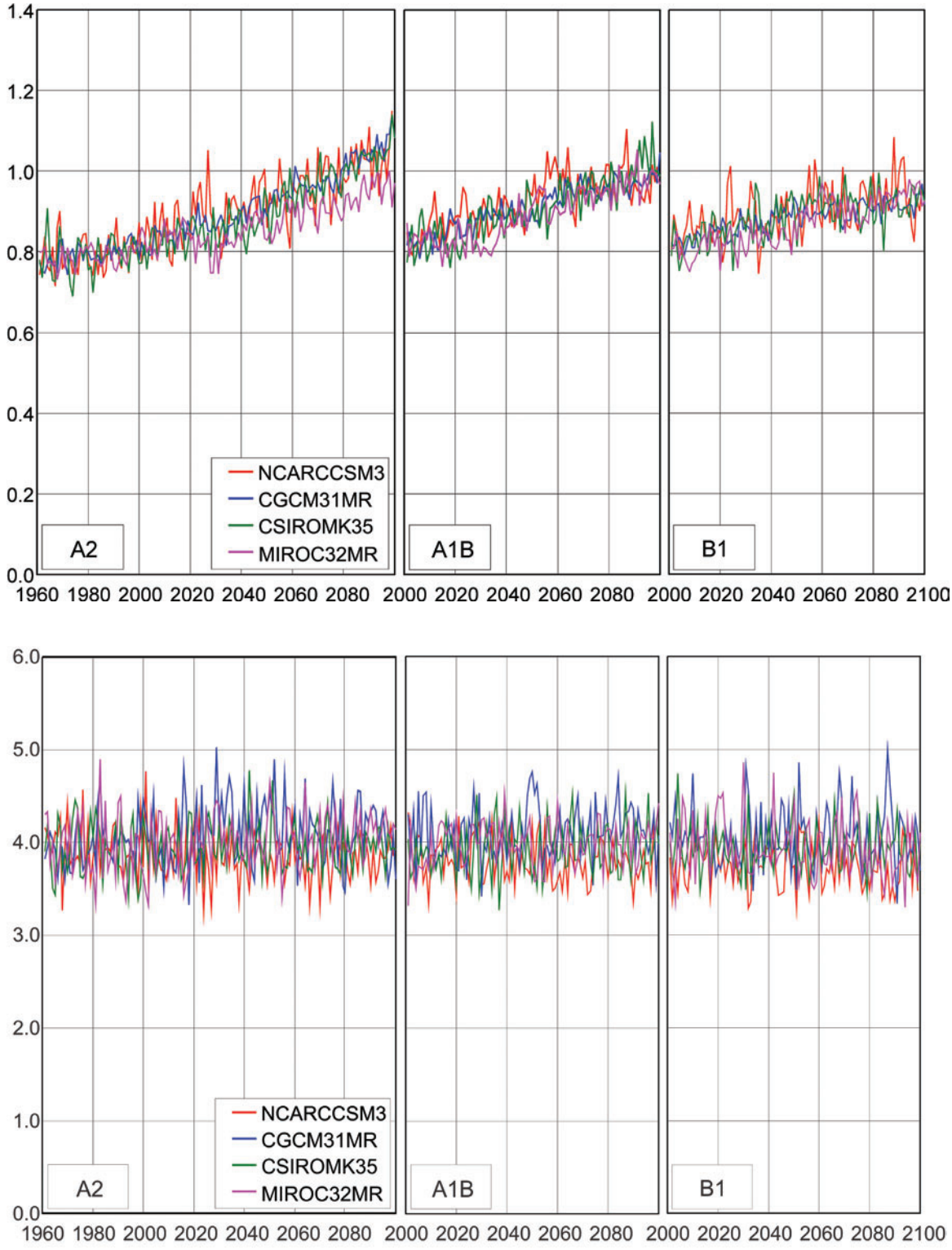

Figure 11e, f. Projections of spatially averaged annual mean vapor pressure (kPa) (e, upper) and wind speed (m s^{-1}) (f, lower) for the Dry Temperate region, for four greenhouse forcing scenarios. The simulated historical data for the 1960-2000 period (20C3M scenario for each GCM) are shown only in the leftmost panels, but are common to all three future projections.

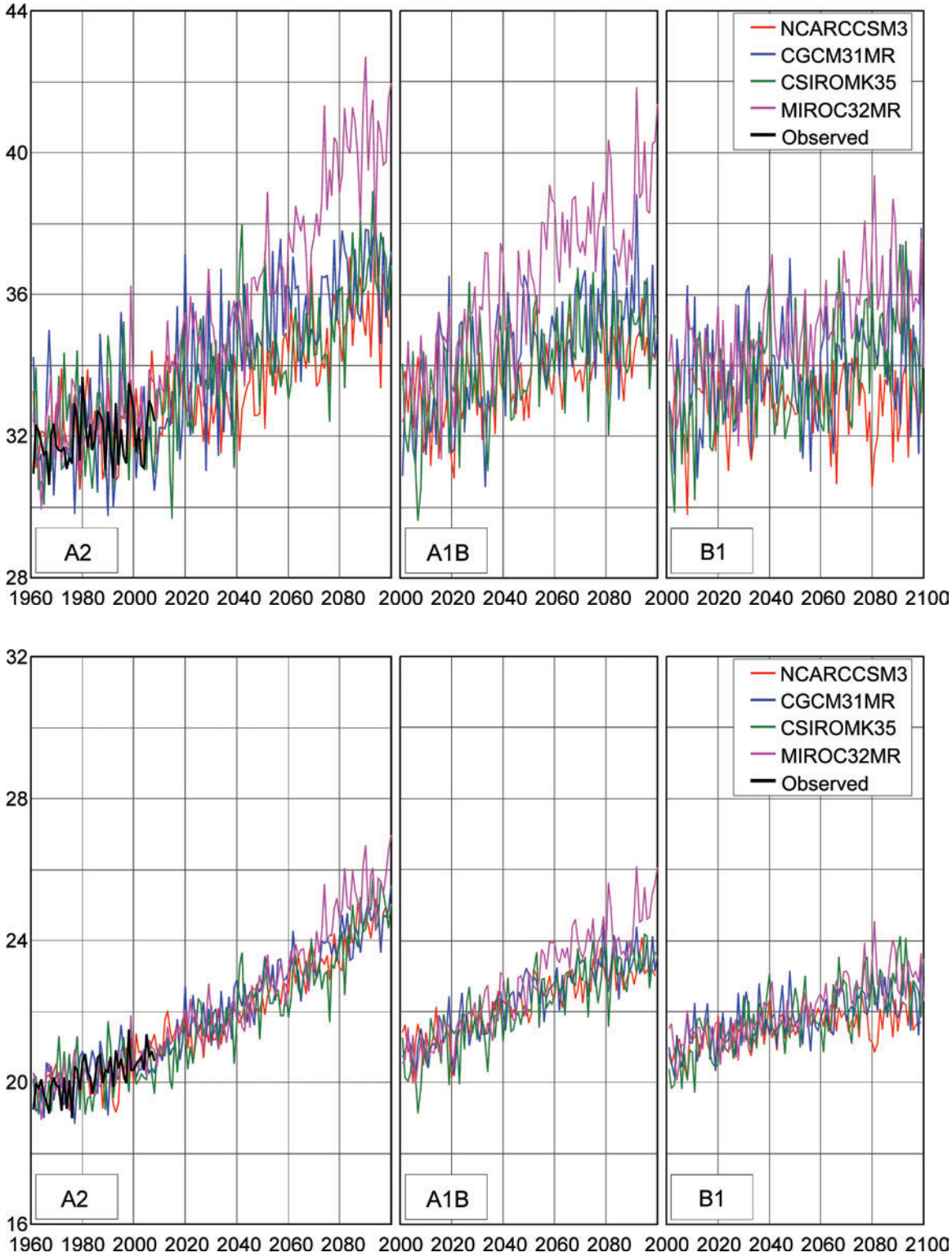

Figure 12a, b. Projections of spatially averaged summer (June, July, August) mean daily maximum and minimum temperature (°C) for the Subtropical region for four greenhouse forcing scenarios, relative to interpolated observed data for 1961–2008. The simulated historical data for the 1960-2000 period (20C3M scenario for each GCM) and observed data are shown only in the leftmost panels, but are common to all three future projections. CGCM31MR = Third Generation Coupled Global Climate Model, version 3.1, medium resolution; CSIROMK35 = Commonwealth Scientific and Industrial Research Organisation Climate System Model, Mark 3.5; MIROC32MR = Model for Interdisciplinary Research on Climate, version 3.2; NCARCCSM3 = Community Climate System Model, version 3.0.

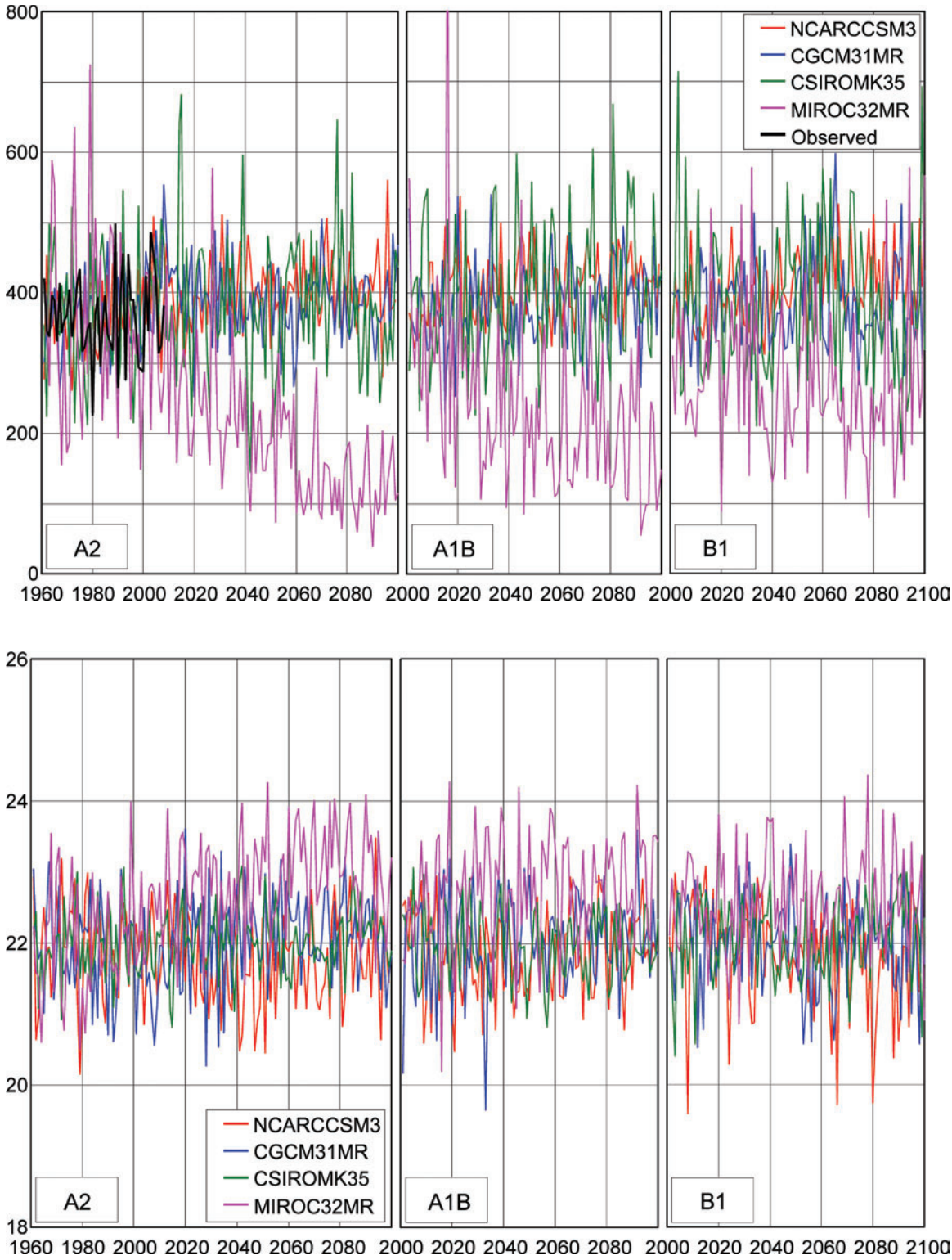

Figure 12c, d. Projections of spatially averaged summer (June, July, August) total precipitation (mm) and daily global solar radiation (MJ m^{-2} d^{-1}) for the Subtropical region, for four greenhouse forcing scenarios. Precipitation projections are also compared to interpolated observed data for 1961–2008. The simulated historical data for the 1960-2000 period (20C3M scenario for each GCM) and observed data are shown only in the leftmost panels, but are common to all three future projections.

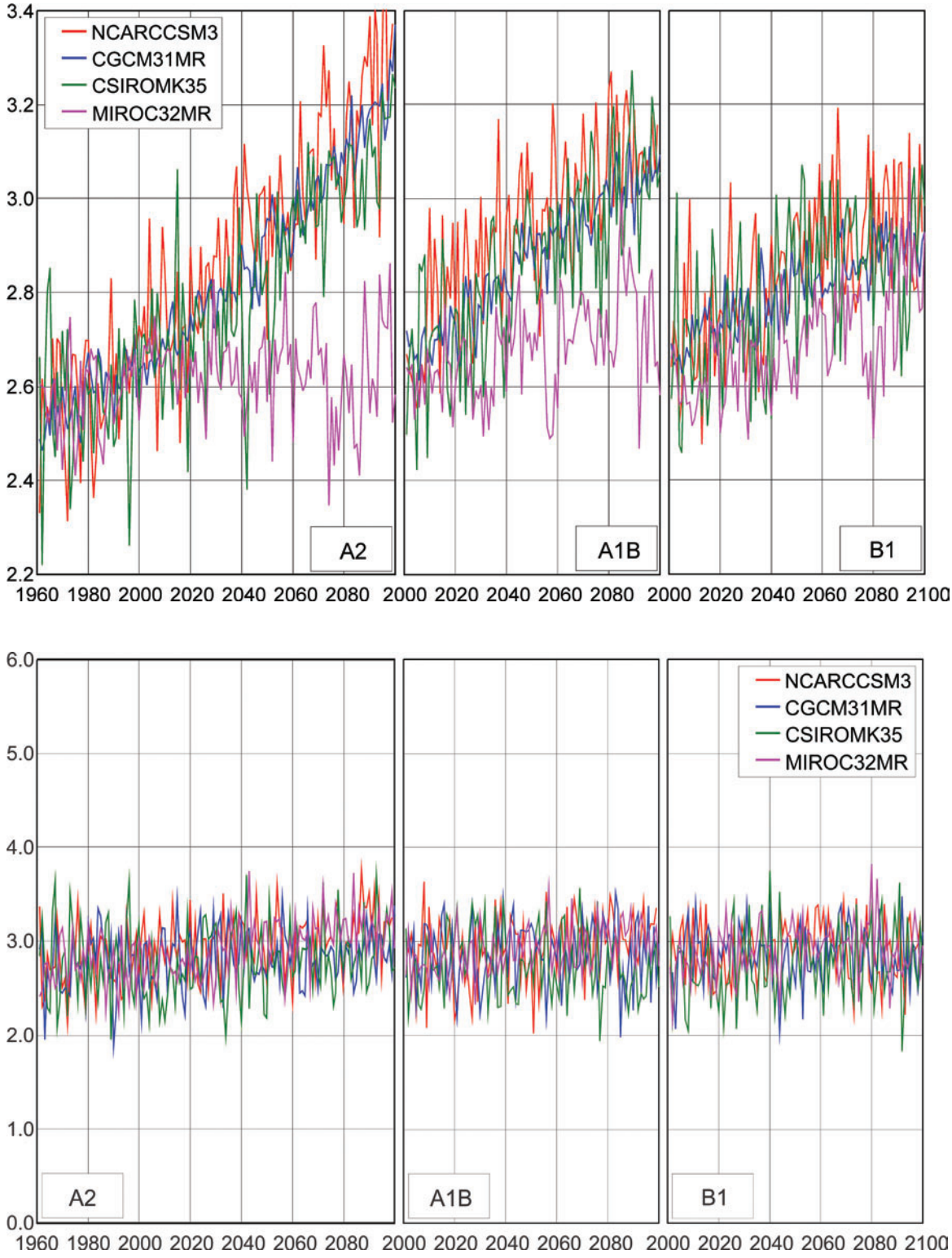

Figure 12e, f. Projections of spatially averaged summer (June, July, August) mean vapor pressure (kPa) (e, upper) and wind speed (m s^{-1}) (f, lower) for the Subtropical region, for four greenhouse gas forcing scenarios. The simulated historical data for the 1960-2000 period (20C3M scenario for each GCM) are shown only in the leftmost panels, but are common to all three future projections.

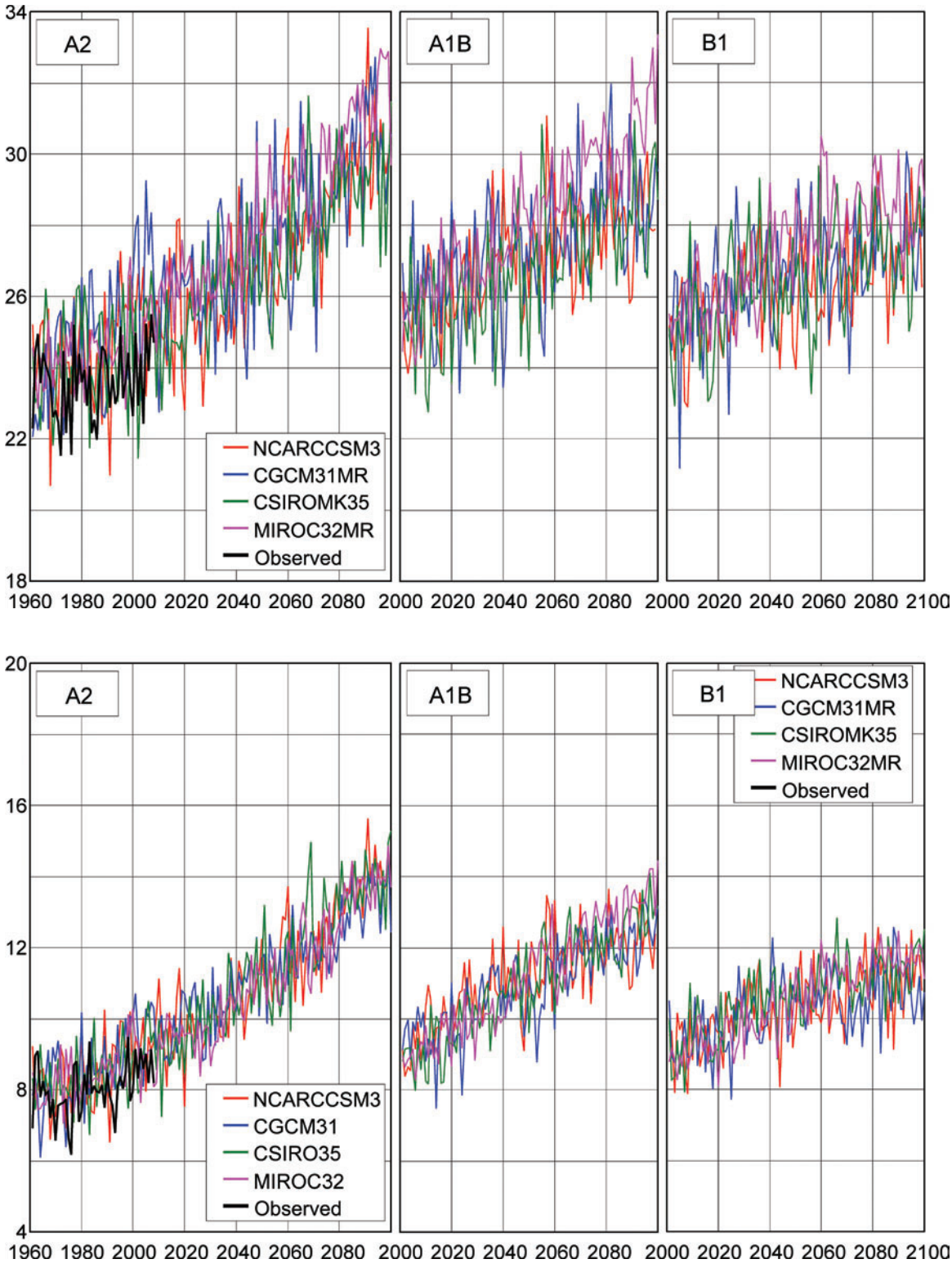

Figure 13a, b. Projections of spatially averaged fall (September, October, November) mean daily maximum (a, upper) and minimum (b, lower) temperature (°C) for the Dry Subtropical region for four greenhouse gas forcing scenarios, relative to interpolated observed data for 1961–2008. The simulated historical data for the 1960-2000 period (20C3M scenario for each GCM) and observed data are shown only in the leftmost panels, but are common to all three future projections. CGCM31MR = Third Generation Coupled Global Climate Model, version 3.1, medium resolution; CSIROMK35 = Commonwealth Scientific and Industrial Research Organisation Climate System Model, Mark 3.5; MIROC32MR = Model for Interdisciplinary Research on Climate, version 3.2; NCARCCSM3 = Community Climate System Model, version 3.0.

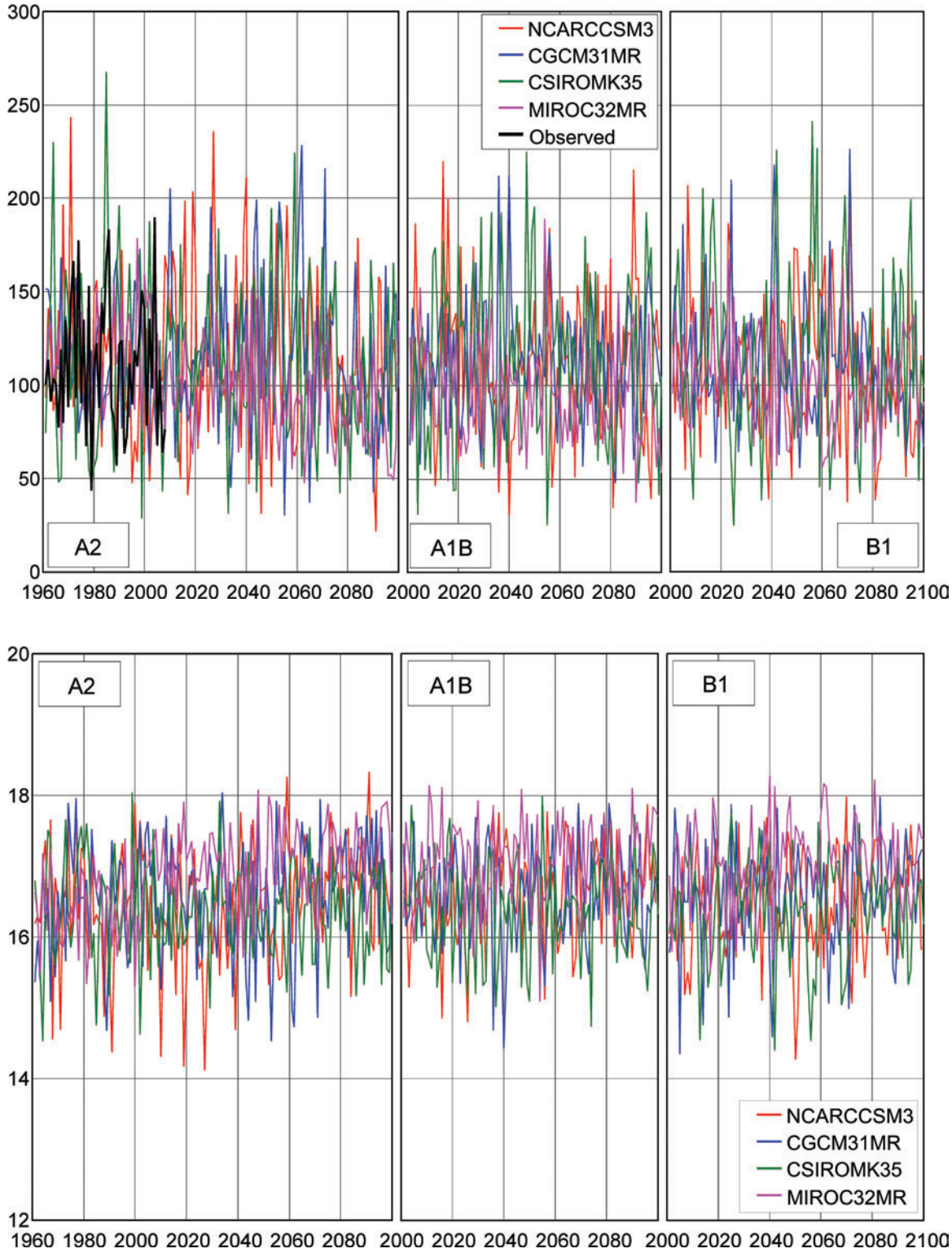

Figure 13c, d. Projections of spatially averaged fall (September, October, November) total precipitation (mm) (c, upper) and daily global solar radiation (MJ m^{-2} d^{-1}) (d, lower) for the Dry Subtropical region, for four greenhouse gas forcing scenarios. The simulated historical precipitation projections (20C3M scenario) are compared to interpolated observed data for 1961–2008. The simulated historical data for the 1960-2000 period (20C3M scenario for each GCM) and observed data are shown only in the leftmost panels, but are common to all three future projections

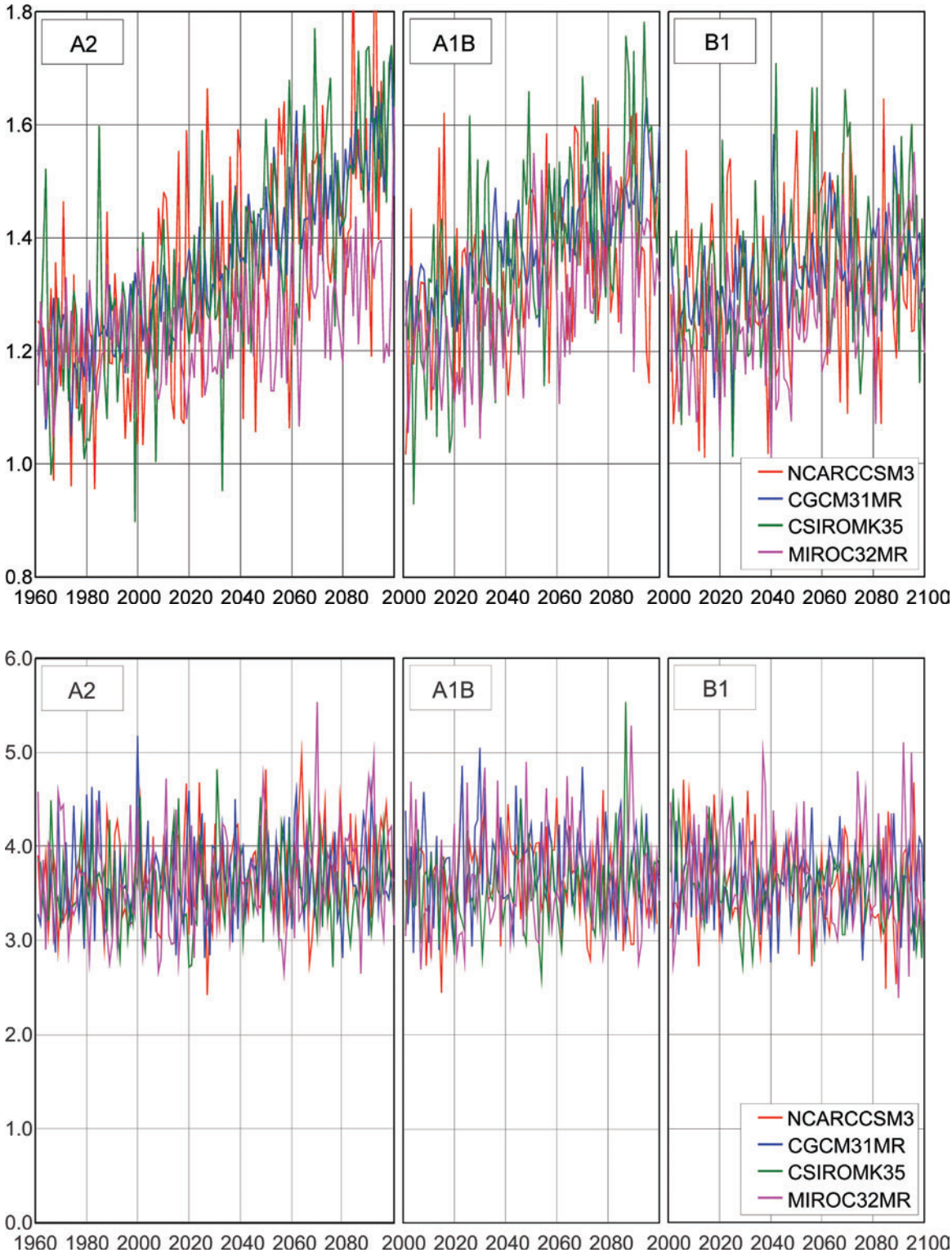

Figure 13e, f. Projections of spatially averaged fall (September, October, November) mean vapor pressure (kPa) (e, upper) and wind speed (m s^{-1}) (f, lower) for the Dry Subtropical region, for four greenhouse gas forcing scenarios. The simulated historical data for the 1960-2000 period (20C3M scenario for each GCM) are shown only in the leftmost panels, but are common to all three future projections.

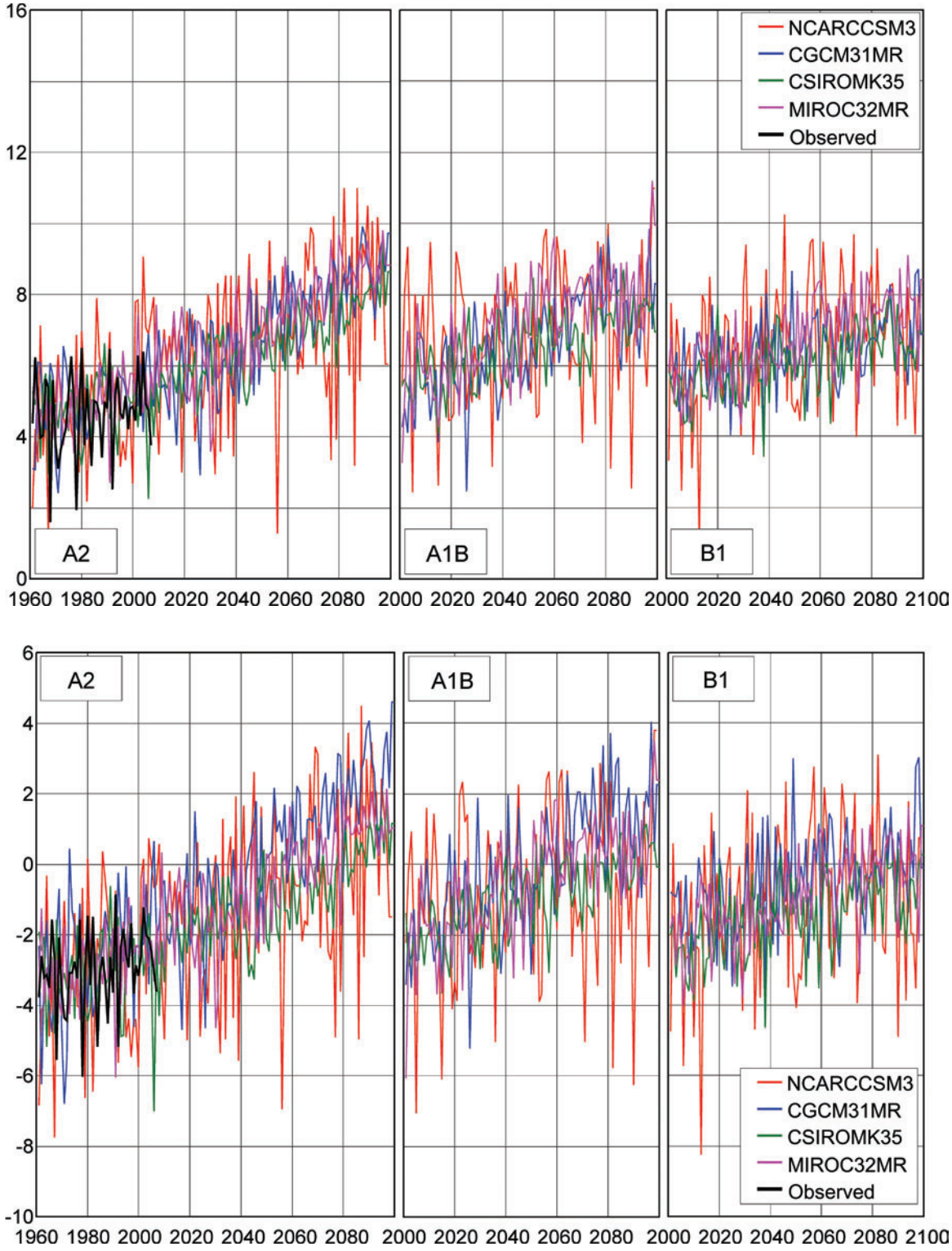

Figure 14a, b. Projections of spatially averaged winter (December, January, February) mean daily maximum (a, upper) and minimum (b, lower) temperature (°C) for the Marine region for four greenhouse gas forcing scenarios, compared to interpolated observed data for 1961–2008. The simulated historical data for the 1960-2000 period (20C3M scenario for each GCM) and observed data are shown only in the leftmost panels, but are common to all three future projections. CGCM31MR = Third Generation Coupled Global Climate Model, version 3.1, medium resolution; CSIROMK35 = Commonwealth Scientific and Industrial Research Organisation Climate System Model, Mark 3.5; MIROC32MR = Model for Interdisciplinary Research on Climate, version 3.2; NCARCCSM3 = Community Climate System Model, version 3.0.

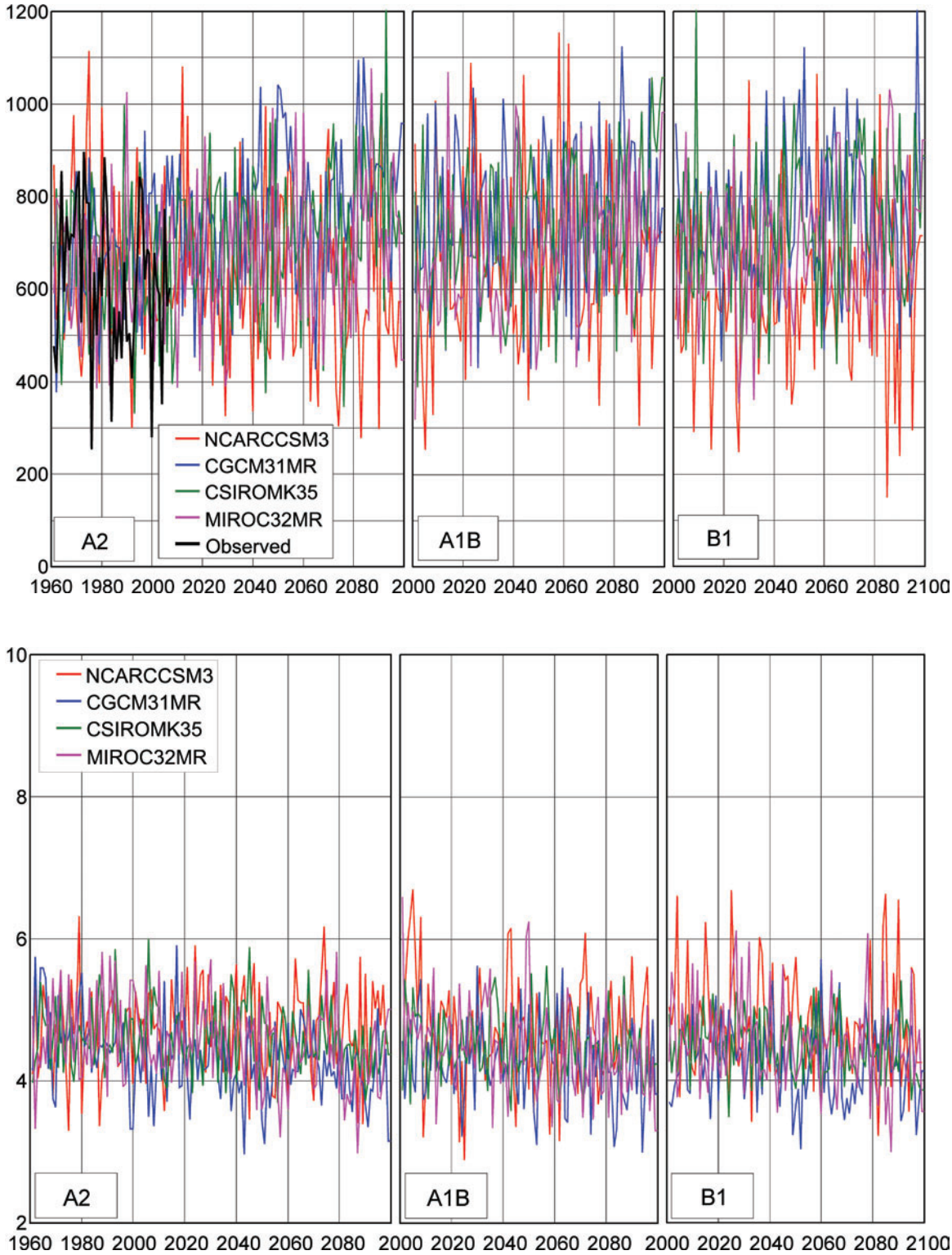

Figure 14c, d. Projections of spatially averaged winter (December, January February) total precipitation (mm) (c, upper) and daily global solar radiation (MJ m^{-2} d^{-1}) (d, lower) for the Marine region, for four greenhouse gas forcing scenarios. The simulated historical data for precipitation (20C3M scenario for each GCM) are also compared to interpolated observed data for 1961–2008. The simulated historical data for the 1960-2000 period (20C3M) and observed data are shown only in the leftmost panels, but are common to all three future projections.

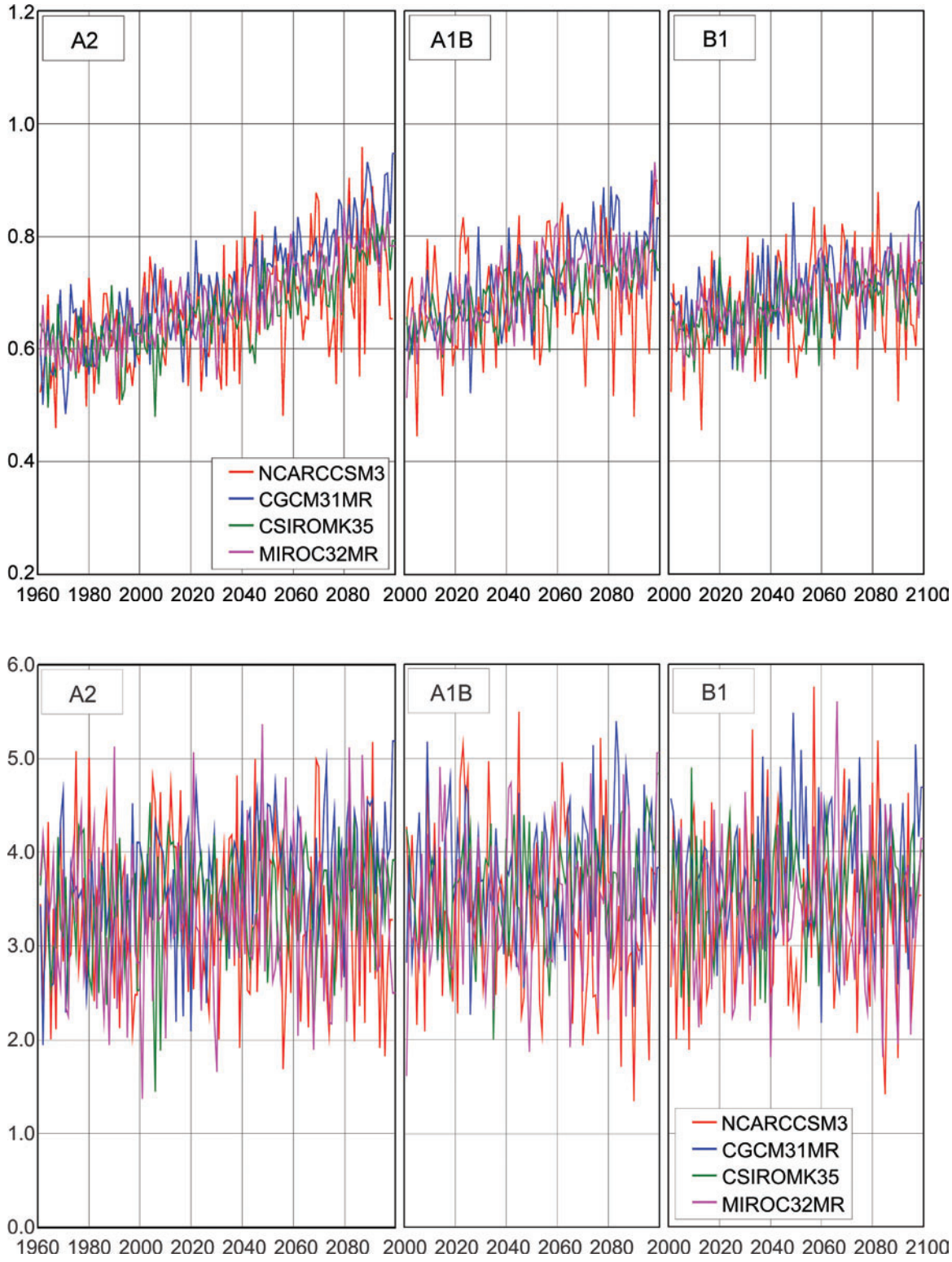

Figure 14e, f. Projections of spatially averaged winter (December, January, February) mean vapor pressure (kPa) (e, upper) and wind speed (m s^{-1}) (f, lower) for the Marine region, for four greenhouse gas forcing scenarios. The simulated historical data for the 1960-2000 period (20C3M scenario for each GCM) are shown only in the leftmost panels, but are common to all three future projections.

Regional Outlook

The data shown in Tables 4–11 deserve careful study; some key results are summarized that could be interpreted as a "national climate outlook" for the United States, somewhat analogous to a national weather forecast based on multiple sources of information. When ranges for future projections are reported in the following paragraphs, they generally range from the minimum change (obtained with the B1 scenario) to the maximum change (obtained from the A2 scenario), expressed as a change from "present-day," *circa*. 2000. It also is important to note use of the word "will" is merely a convenient simplification; the outlook presented here was generated only by a suite of imperfect models projecting an uncertain future.

Alaska

Projected temperature increases for Alaska were the largest of those for the eight regions. Annual mean T_{min} was projected to increase by about 3.0 to 5.0 ºC and T_{max} by 2.5 to 4.0 ºC by 2100 (Table 4). Winter T_{min} increased the most (4.0–7.5 ºC), and spring/summer T_{max} the least (2.5–4.0 ºC). Interannual variability was projected to decline in all seasons except for summer, where increases of up to 26% occurred with the most extreme A2 emissions scenario. Precipitation was projected to increase year-round by 10–20%, accompanied by increases in interannual variability, particularly in spring and summer. Related to these increases in precipitation, mean vapor pressure was projected to increase by 10 to 25% in general (more in spring and summer), and solar radiation declined by 6 to 10% year round. Mean wind speeds were projected to increase very slightly, while they became less variable, particularly in fall and winter.

Continental Ecoregion

Projected increases in T_{min} and T_{max} were relatively consistent year round, ranging from 2.0 to 4.5 ºC by 2099 (Table 5). Interannual variability, particularly for T_{min}, was projected to increase under the A2 by 20 to 30%, but projected changes for A1B and B1 were smaller and often negative. Annual precipitation was projected to increase by 7 to 8%, mostly in spring, when increases were as much as 10% according to the A1B scenario. Interannual variation also was projected to increase, particularly in winter and particularly with the A2 forcing scenario. Summer and fall radiation levels were projected to increase by 1 to 2%, balanced by proportionately larger decreases in winter radiation, for very little net change annually, but interannual variation was projected to decrease year-round. Vapor pressure was strongly influenced by the projected increases in temperature under each forcing scenario, with increases of 10 to 25% year-round, reflecting also the projected increases in annual precipitation. Interannual variability in vapor pressure was projected to increase quite dramatically according to the A2, compared to relatively little change with the B1. Changes in vapor pressure variability were projected to be greatest in spring, but the patterns for other seasons were inconsistent. Mean wind speeds were projected to increase, by as much as 5% year-round with the A2. Wind speed variability was projected to decline slightly in general, but all scenarios indicated greater variability during fall.

Marine Ecoregion

This region was projected to warm by 2.5 to 3.5 ºC, by 2070-2099 (Table 6). Projected changes in T_{min} and T_{max} were very similar; although it appeared summer maxima increased more than the annual mean (in the range 2.5–4.2 ºC). Projected changes in interannual variability were inconsistent, with greater variability expected for summer under A2, but smaller increases or reductions otherwise. Much of the increased variability was traced to the contribution of the NCARCCSM3 model, which projected much greater interannual variability, particularly for T_{min} in winter, than did the other models, although all four GCMs agreed quite strongly in the general trends (Figure 14b). Precipitation was projected to increase by 5–8% annually, mainly in winter and fall, with smaller decreases projected for spring and summer. Summer precipitation in this region already was very low (about 120 mm), so the projected decreases, on the order of 10 to 20%, could be ecologically very significant. Interannual variability of precipitation was projected to increase slightly with A1B and A2. The CSIROMK35 model was markedly more variable in its projections of future summer precipitation.

Consistent with these projections of reduced summer precipitation, solar radiation during spring and summer was projected to increase by as much as 5% under A1B and A2, but decrease in winter. Also consistent with reduced summer precipitation, interannual variability in solar radiation was projected to decrease by 5 to 10%, particularly in summer and fall. Vapor pressure also was projected to increase, particularly in summer and fall, with increases by 2070-2099 in the range 10 to 20% compared to the present day. Changes in variability of vapor pressure were less consistent, showing large increases, particularly in summer and fall for A2. Projections for wind speed showed slight increases on average, except for general decreases in spring. There was a suggestion of decreasing variability on average, also particularly in spring.

Mediterranean Ecoregion

The models projected rather similar increases in T_{min} and T_{max} throughout the year (MIROC32MR tended to be slightly higher, and CSIROMK35 slightly lower than the mean for T_{max} and NCARCCSM3 somewhat higher for summer T_{min}), with annual mean increases of 0.8 to 0.9 ºC by 2010–2039 gradually diverging to a range of about 2.0 to 3.5 ºC by 2070–2099 (Table 7). Summer was projected to warm the most, in the range of 2.2 to 4.0 ºC toward the end of the century. Winter and spring were projected to increase the least. Interannual variability was noticeably greater with NCARCCSM3 than with other models during winter, and all models suggested fall T_{min} was particularly variable. Projected changes in temperature variability, however, did not show consistent patterns: with the A2 there was a general increase (by 50% annually), but the other scenarios produced much smaller increases, including decreases with the A1B.

Precipitation was projected to increase in winter with all scenarios, while other seasons showed slight decreases, suggesting little change overall in annual amounts. Interannual variability of summer precipitation decreased by 20 to 30%, but there were no clear trends for other seasons. Annual precipitation variability increased by 15 to 20% according to the models for the A2 and B1 scenarios. Solar radiation in spring was projected to increase marginally, with general decreases in other seasons and a slight reduction in interannual variability. Vapor pressure was projected to increase with temperature, particularly in summer and fall, but the projected changes in variability were inconsistent among the three emissions scenarios. Mean wind speeds showed little projected change and small, but inconsistent, reductions in interannual variability.

Prairie Ecoregion

Projections for T_{min} and T_{max} generally were similar throughout the year, with annual averages increasing 2 to 3 ºC in the B1 scenario, 3 to 4 ºC with the A1B and 4 to 5 ºC with the A2, by 2070–2099 (Table 8). Increases projected by MIROC32MR were higher than the average, particularly for T_{max}, and projections by NCARCCSM3 were lower, with a tendency to more extreme interannual variation, particularly for T_{min}. Interannual variability was projected to increase by 15 to 40% in most seasons according to the A2, but less consistent and smaller changes occurred with the other emissions scenarios. Annual precipitation was projected to increase by 3 to 5% by 2070-2099, particularly in spring, with little change in interannual variability. MIROC32MR projected a general decrease in precipitation, particularly in the second half of the 21st century and particularly in summer that corresponded with projections for the Subtropical and Dry Subtropical regions and, to some extent, the Continental region. Over the same period solar radiation was projected to change little, but there were suggestions of decreases in spring that would be consistent with the increased precipitation. Vapor pressure was projected to increase with temperature by around 13% under B1, to 20 to 25% under A2. Wind speeds were generally projected to increase slightly, particularly in spring and summer, while projections for variability showed slight increases in summer, but small and inconsistent changes in other seasons.

Subtropical Ecoregion

T_{min} was projected to increase quite steadily, rising 2 to 4 ºC by 2070–2099, with spring, summer, and fall tending to warm more than fall and winter. The pattern was very similar for T_{max}, with comparable or even slightly larger increases (Table 9) (though it should be noted this trend was the result of the very large increases projected by MIROC32MR shown in Figure 12b). Inter-annual variation in temperature was projected to increase year round with the A2, but trends in temperature variability with A1B and B1 were generally much smaller or even negative. Mean precipitation was projected to decline, particularly under the A2, but this again was traced to MIROC32MR which projected major decreases, particularly in summer, although the other three models projected relatively little change (Figure 12c). Overall the projected annual precipitation change was about 5% decrease with A2 and 1 to 2% increase with A1B and B1, with no clear seasonality. Solar radiation was projected to increase slightly in all scenarios and all seasons (except B1 spring), but interannual variability generally declined. Consistent with the projected temperature increases, mean vapor pressure also increased, by about 18% with A2, compared to 15% with A1B and 10% with B1 (Figure 12e). Mean wind speed was projected to increase slightly under all scenarios, with consistent agreement that the general trend will be reduced interannual variation (see also Figure 12f), particularly under the A2 emissions scenario.

Dry Temperate Ecoregion

Temperatures were projected to increase by 2.5 to 4.5 ºC by 2070-2099, with little difference in the annual mean increase for both T_{min} and T_{max} (Table 10). Seasonally, summer temperatures were projected to increase by as

much as 5 ºC with the A2, and spring temperatures increased by 2 to 4 ºC. Interannual variability in temperature was projected to increase dramatically in summer with the A2, particularly as simulated by MIROC32MR and NCARCCSM3. The MIROC32MR also projected lower summer precipitation than the model mean for all three GHG scenarios, consistent with the Subtropical region. Summer precipitation variability was markedly higher with the NCARCCSM3 and CSIROMK35, but projected means showed very little change from present-day either in amounts or interannual variation. Similarly there was little projected change in solar radiation annually, though winter and spring were consistently projected to have decreases of 1 to 2% as summer shows balancing increases of about 1%. Projected changes in interannual variability of solar radiation were inconsistent in sign, but generally small.

Depending on the GHG scenario, vapor pressure was projected to increase by 15 to 25% annually by 2070–2099, with larger proportionate increases occurring in winter (20–30%). Interannual variability in vapor pressure was projected to increase dramatically with the A2 (Figure 11e), but much less with A1B and B1. Wind speed projections showed inconsistent changes both seasonally and annually, with a suggestion of general increases in variability in summer and decreases in fall and winter.

Dry Subtropical Ecoregion

Projected temperature increases in this region (Table 11)were similar to those for the Subtropical ecoregion (Table 9), ranging from 2.5 to 4.5 C for T_{min} and slightly less for T_{max}. Increases in summer/fall maxima were somewhat greater than the annual averages, with MIROC32MR higher than other models particularly in summer and winter. Temperature variability was projected to increase by 25 to 40% with the A2 scenario. In comparison, the A1B and B1 showed very little overall change in variability (Figure 13a, b). Precipitation in this region was projected to change very little year round (about 5% decrease annually with A2, but no substantial change with A1B and B1), although there was a suggestion that summer precipitation might increase slightly under all scenarios. Given the relatively low present-day annual precipitation (~400 mm) and the high evaporative demand, even small changes may be significant ecologically and for land management. Solar radiation was projected to increase slightly, but decrease in summer, presumably related to the general changes in precipitation. Conversely, vapor pressure was projected to increase by 12 to 20% correlated with the projected warming, with less consistent changes in seasonal and annual variability. Wind speeds were projected to change little with the B1, but A1B and A2 led to progressively larger increases, particularly in summer and fall.

Tables 4–11. Summaries of future projections for each climate variable by ecoregion. These data are area-weighted means obtained for each climate variable according to each climate scenario. That is, they are the means of the four values projected by each GCM and therefore represent a "best estimate," assuming that all GCMs are equally skillful (or equally plausible). Each two-page table contains results for six climate variables for a single ecoregion derived from the classification of Bailey (1995) within the conterminous 48 states, while the Alaska region comprises the state of Alaska in entirety. Each table is split into two parts: (a) maximum and minimum temperature and precipitation and (b) global solar radiation incident on a horizontal surface, vapor pressure, and windspeed.

Some further notes on how to interpret these tables: For each variable, data are organized across the page, in three sets of five columns. Each set is for a single GHG emissions scenario, in the order A2, A1B, B1, with each column containing the averages of the four GCM projections of monthly values for spring, summer, fall, and winter, and for the entire year, respectively. The lines of data are labeled in the left-most column, as follows:

The 30-year period (1980-2009) was selected as a baseline for comparison of model results because it represents current climate and immediately precedes the three consecutive 30-year periods reported as projections for the future (starting with 2010). It is important to distinguish this from the 1961–1990 period used as the baseline for combining the scenario data with observed climate normals. Although the changes between the periods of 1961–1990 and of 1980–2009 are likely to be small, there is evidence of a general warming trend over the 1961 through 2009 period (IPCC 2007). This is visible in many of the graphs (both in the historical trends and in most of the GCM projections). The 1980–2009 baseline mean values differ slightly among the three emissions scenarios because data for the nine years 2001–2009 originate from the different GHG scenario simulations and, hence, lead to different calculated means. The following three lines, labeled Change by 2010–2039, Change by 2040–2069, and Change by 2070–2099, respectively, give the average net changes in the projected 30-year means relative to 1980–2009. A positive value indicates an increase, and a negative value a decrease. The units of these changes are indicated with the variable name in the line directly above. In particular, note that precipitation changes are reported in millimeters relative to baseline (1980-2009). Following the mean changes for the three 30-year periods are two lines labeled 100-year forcing and 100-year variability (%). Here we are looking at the changes over 100 years, comparing two 30-year periods, 1970-1999 and 2070-2099. The 100-year forcing is the changes in the 30-year means, and the 100-year variability is the change in the 30-year standard deviations (S.D.). The change in S.D. is reported as a percentage relative to 100% for 1970–1999.

Table 4. Climate change projection summary for Alaska (mean of four general circulation models).

Climate Variable	A2 Emissions Scenario					A1B Emissions Scenario					B1 Emissions Scenario				
Mean Daily T_{min} (°C)	Spring	Summer	Fall	Winter	Year	Spring	Summer	Fall	Winter	Year	Spring	Summer	Fall	Winter	Year
Baseline 1980-2009	-10.07	5.67	-7.90	-21.04	-8.30	-10.14	5.61	-7.86	-20.91	-8.29	-10.28	5.66	-7.90	-21.10	-8.38
Change by 2010-2039	1.22	0.81	1.44	1.70	1.25	1.11	0.84	1.05	1.55	1.07	1.39	0.69	1.08	1.40	1.12
Change by 2040-2069	2.51	2.02	2.65	4.10	2.77	2.81	1.90	2.86	4.31	2.92	2.35	1.58	2.19	2.91	2.23
Change by 2070-2099	4.66	3.68	4.84	7.43	5.10	3.95	3.07	4.14	5.92	4.24	3.04	2.03	2.82	3.79	2.90
100-year forcing	5.26	4.06	5.22	8.10	5.66	4.47	3.41	4.55	6.73	4.81	3.43	2.41	3.19	4.41	3.38
100-year variability (%)	-6.67	26.40	-32.08	-28.65	-18.51	-12.80	2.65	-29.50	-27.25	-21.84	1.74	4.97	-28.92	-13.95	-16.08
Mean Daily T_{max} (°C)	Spring	Summer	Fall	Winter	Year	Spring	Summer	Fall	Winter	Year	Spring	Summer	Fall	Winter	Year
Baseline 1980-2009	-0.01	15.22	-0.32	-12.65	0.59	-0.06	15.19	-0.28	-12.51	0.61	-0.17	15.28	-0.31	-12.69	0.54
Change by 2010-2039	0.87	0.78	1.18	1.10	0.95	0.73	0.76	0.88	0.93	0.76	0.98	0.62	0.90	0.85	0.82
Change by 2040-2069	1.76	1.96	2.18	2.90	2.16	2.02	1.75	2.37	3.10	2.27	1.69	1.49	1.80	1.96	1.72
Change by 2070-2099	3.42	3.63	4.08	5.54	4.12	2.93	2.99	3.48	4.43	3.43	2.22	1.95	2.38	2.73	2.31
100-year forcing	3.82	3.98	4.40	5.94	4.55	3.28	3.32	3.84	4.97	3.88	2.46	2.37	2.71	3.10	2.68
100-year variability (%)	-5.75	25.05	-28.33	-30.34	-19.79	-13.56	4.36	-24.39	-27.35	-22.97	-2.16	10.86	-28.33	-13.03	-20.85
Total Precipitation (mm)	Spring	Summer	Fall	Winter	Year	Spring	Summer	Fall	Winter	Year	Spring	Summer	Fall	Winter	Year
Baseline 1980-2009	85	178	168	109	540	85	180	167	111	543	86	176	167	109	537
Change by 2010-2039	6	8	8	6	28	6	7	5	5	22	5	12	8	4	30
Change by 2040-2069	13	16	17	13	58	12	21	19	10	63	8	17	12	7	45
Change by 2070-2099	23	29	36	24	112	18	27	25	19	87	13	18	19	12	62
100-year forcing	25	32	38	26	121	20	30	27	23	100	16	18	20	15	69
100-year variability (%)	26.12	32.02	18.46	6.62	11.05	23.81	18.66	-1.29	9.44	5.18	8.40	27.97	3.27	8.61	7.47

Table 4. Continued

Climate Variable	A2 Emissions Scenario					A1B Emissions Scenario					B1 Emissions Scenario				
Mean Daily Global Solar Radiation (MJ m^{-2})	Spring	Summer	Fall	Winter	Year	Spring	Summer	Fall	Winter	Year	Spring	Summer	Fall	Winter	Year
Baseline 1980-2009	12.80	16.55	4.03	1.28	8.66	12.87	16.74	4.00	1.28	8.72	12.88	16.79	4.04	1.29	8.75
Change by 2010-2039	-0.45	-0.21	-0.20	-0.04	-0.22	-0.47	-0.58	-0.09	-0.04	-0.29	-0.43	-0.44	-0.19	-0.04	-0.27
Change by 2040-2069	-1.04	-0.51	-0.34	-0.11	-0.50	-1.13	-0.96	-0.38	-0.10	-0.64	-0.89	-0.57	-0.27	-0.07	-0.45
Change by 2070-2099	-1.79	-0.41	-0.58	-0.18	-0.74	-1.53	-0.56	-0.42	-0.16	-0.67	-1.12	-0.45	-0.37	-0.10	-0.51
100-year forcing	-2.07	-0.70	-0.63	-0.20	-0.90	-1.74	-0.66	-0.49	-0.18	-0.77	-1.33	-0.50	-0.40	-0.12	-0.59
100-year variability (%)	3.68	24.29	-27.19	-29.72	14.76	-5.06	14.97	-20.92	-23.27	20.13	5.51	23.93	-21.85	-11.15	24.49
Mean Vapor Pressure (kPa)	Spring	Summer	Fall	Winter	Year	Spring	Summer	Fall	Winter	Year	Spring	Summer	Fall	Winter	Year
Baseline 1980-2009	0.349	1.009	0.434	0.135	0.482	0.347	1.005	0.436	0.137	0.482	0.345	1.009	0.433	0.135	0.481
Change by 2010-2039	0.022	0.058	0.035	0.013	0.031	0.025	0.059	0.027	0.011	0.030	0.026	0.048	0.031	0.011	0.029
Change by 2040-2069	0.052	0.151	0.072	0.031	0.076	0.057	0.139	0.079	0.033	0.077	0.046	0.114	0.059	0.022	0.060
Change by 2070-2099	0.102	0.282	0.142	0.061	0.146	0.086	0.231	0.119	0.048	0.121	0.063	0.149	0.080	0.030	0.080
100-year forcing	0.113	0.308	0.151	0.066	0.159	0.096	0.254	0.130	0.054	0.133	0.070	0.176	0.088	0.034	0.092
100-year variability (%)	39.64	59.90	14.88	3.14	37.82	21.96	25.48	12.56	-3.16	14.65	37.40	26.32	-7.93	5.45	10.829
Mean Windspeed (m s^{-1})	Spring	Summer	Fall	Winter	Year	Spring	Summer	Fall	Winter	Year	Spring	Summer	Fall	Winter	Year
Baseline 1980-2009	4.42	3.16	3.52	4.24	3.85	4.40	3.14	3.53	4.28	3.85	4.43	3.09	3.52	4.25	3.83
Change by 2010-2039	0.09	0.14	-0.05	-0.08	0.01	0.12	0.24	-0.11	-0.12	0.01	0.09	0.14	-0.07	-0.05	0.02
Change by 2040-2069	-0.08	0.20	-0.18	0.03	-0.02	-0.09	0.29	-0.10	0.06	0.02	0.05	0.20	-0.02	0.07	0.07
Change by 2070-2099	-0.05	0.28	-0.16	0.09	0.03	0.00	0.19	-0.09	0.09	0.03	0.03	0.30	-0.08	-0.02	0.05
100-year forcing	0.00	0.28	-0.19	0.08	0.04	0.04	0.17	-0.12	0.12	0.06	0.10	0.23	-0.12	-0.03	0.05
100-year variability (%)	6.44	0.15	-8.35	-17.54	-10.41	10.95	3.35	-4.32	-5.17	-8.88	4.61	15.60	-11.70	-7.69	-8.79

Table 5. Climate change projection summary for Continental Ecoregion (mean of four general circulation models).

Climate Variable	A2 Emissions Scenario					A1B Emissions Scenario					B1 Emissions Scenario				
Mean Daily T_{min} (°C)	Spring	Summer	Fall	Winter	Year	Spring	Summer	Fall	Winter	Year	Spring	Summer	Fall	Winter	Year
Baseline 1980-2009	2.75	14.80	5.11	-8.45	3.54	2.79	14.89	5.12	-8.50	3.56	2.91	14.89	5.18	-8.32	3.64
Change by 2010-2039	1.00	1.08	1.16	1.10	1.10	1.13	1.18	1.31	1.43	1.28	0.61	0.93	0.91	0.74	0.82
Change by 2040-2069	2.34	2.54	2.63	2.63	2.52	2.40	2.45	2.60	2.76	2.55	1.67	1.64	1.78	1.92	1.77
Change by 2070-2099	3.87	4.29	4.35	4.28	4.21	3.23	3.29	3.39	3.91	3.46	1.99	2.20	2.21	2.39	2.21
100-year forcing	4.07	4.50	4.67	4.71	4.48	3.48	3.60	3.72	4.29	3.76	2.35	2.50	2.60	2.95	2.59
100-year variability (%)	17.22	17.80	25.65	-6.08	26.31	-17.73	-10.29	4.27	-10.09	-7.63	-11.76	-21.56	6.12	-15.03	-15.21
Mean Daily T_{max} (°C)	Spring	Summer	Fall	Winter	Year	Spring	Summer	Fall	Winter	Year	Spring	Summer	Fall	Winter	Year
Baseline 1980-2009	15.51	27.60	17.15	2.21	15.60	15.55	27.78	17.18	2.16	15.66	15.68	27.83	17.21	2.31	15.74
Change by 2010-2039	1.06	1.17	1.16	0.77	1.05	1.14	1.24	1.41	1.07	1.23	0.68	1.01	1.06	0.44	0.82
Change by 2040-2069	2.36	2.80	2.80	2.13	2.52	2.49	2.51	2.65	2.24	2.47	1.59	1.46	1.84	1.53	1.62
Change by 2070-2099	4.01	4.55	4.50	3.69	4.20	3.25	3.39	3.49	3.34	3.37	1.94	2.23	2.39	1.99	2.15
100-year forcing	4.21	4.65	4.85	3.99	4.41	3.49	3.67	3.86	3.59	3.64	2.30	2.56	2.79	2.39	2.50
100-year variability (%)	23.32	13.30	30.83	20.34	40.54	-11.59	1.92	5.01	10.74	5.43	2.18	-5.47	4.24	2.37	-1.64
Total Precipitation (mm)	Spring	Summer	Fall	Winter	Year	Spring	Summer	Fall	Winter	Year	Spring	Summer	Fall	Winter	Year
Baseline 1980-2009	288	311	252	203	1054	289	304	253	204	1050	287	300	254	203	1044
Change by 2010-2039	9	-1	6	5	17	11	3	7	3	26	7	1	-1	2	12
Change by 2040-2069	18	-11	4	16	28	11	7	8	8	35	23	23	11	8	65
Change by 2070-2099	18	-5	18	23	55	28	10	6	23	70	29	10	2	15	58
100-year forcing	25	7	18	24	74	36	16	8	25	85	35	12	5	15	67
100-year variability (%)	15.89	4.81	17.79	27.27	19.52	0.60	-2.87	0.24	34.85	-3.04	5.66	-6.56	-3.41	23.17	1.56

Table 5. Continued

Climate Variable	A2 Emissions Scenario					A1B Emissions Scenario					B1 Emissions Scenario				
Mean Daily Global Solar Radiation (MJ m^{-2})	Spring	Summer	Fall	Winter	Year	Spring	Summer	Fall	Winter	Year	Spring	Summer	Fall	Winter	Year
Baseline 1980-2009	17.28	21.44	11.12	7.54	14.35	17.25	21.51	11.13	7.52	14.36	17.27	21.55	11.10	7.50	14.36
Change by 2010-2039	0.00	0.19	0.00	-0.12	0.02	0.03	0.17	0.08	-0.08	0.04	0.07	0.13	0.12	-0.02	0.07
Change by 2040-2069	-0.05	0.31	0.15	-0.25	0.04	0.05	0.27	0.10	-0.25	0.05	-0.09	0.15	0.12	-0.13	0.01
Change by 2070-2099	0.06	0.35	0.16	-0.48	0.02	-0.02	0.30	0.18	-0.44	0.00	-0.09	0.24	0.24	-0.17	0.05
100-year forcing	0.10	0.35	0.21	-0.48	0.05	-0.01	0.37	0.25	-0.45	0.04	-0.07	0.35	0.28	-0.21	0.09
100-year variability (%)	3.71	-9.87	-6.27	-9.73	-7.86	-14.85	-8.46	-9.60	-11.10	-25.85	-6.44	-9.74	-18.92	-9.96	-18.55
Mean Vapor Pressure (kPa)	Spring	Summer	Fall	Winter	Year	Spring	Summer	Fall	Winter	Year	Spring	Summer	Fall	Winter	Year
Baseline 1980-2009	0.86	1.93	1.07	0.37	1.06	0.86	1.93	1.07	0.37	1.06	0.87	1.92	1.07	0.38	1.06
Change by 2010-2039	0.058	0.110	0.074	0.024	0.066	0.063	0.127	0.084	0.030	0.076	0.039	0.092	0.054	0.014	0.050
Change by 2040-2069	0.131	0.222	0.172	0.061	0.146	0.126	0.252	0.181	0.063	0.155	0.097	0.211	0.136	0.045	0.123
Change by 2070-2099	0.203	0.403	0.296	0.107	0.252	0.184	0.353	0.238	0.098	0.218	0.116	0.242	0.145	0.055	0.140
100-year forcing	0.217	0.446	0.313	0.116	0.273	0.200	0.389	0.257	0.106	0.238	0.134	0.275	0.166	0.066	0.160
100-year variability (%)	47.46	26.72	23.77	38.97	56.39	16.81	5.42	16.50	20.76	14.93	17.76	-16.11	9.26	16.31	-4.96
Mean Windspeed (m s^{-1})	Spring	Summer	Fall	Winter	Year	Spring	Summer	Fall	Winter	Year	Spring	Summer	Fall	Winter	Year
Baseline 1980-2009	4.07	3.15	3.52	4.15	3.72	4.04	3.20	3.54	4.15	3.73	4.05	3.13	3.55	4.19	3.73
Change by 2010-2039	0.24	-0.06	0.01	0.14	0.08	0.00	0.02	-0.07	0.11	0.02	0.00	-0.02	-0.06	-0.05	-0.03
Change by 2040-2069	0.23	0.01	-0.02	0.26	0.13	0.14	-0.07	-0.06	0.11	0.04	0.12	0.02	-0.03	0.11	0.06
Change by 2070-2099	0.41	0.01	-0.01	0.28	0.18	0.23	-0.05	-0.05	0.13	0.07	0.05	0.02	-0.10	0.09	0.02
100-year forcing	0.44	0.00	0.01	0.33	0.19	0.23	0.00	-0.01	0.20	0.10	0.06	0.00	-0.04	0.18	0.05
100-year variability (%)	5.64	-8.38	23.57	5.51	-0.24	-1.18	-2.16	8.19	2.38	-6.17	-0.12	-1.59	14.14	6.17	5.96

Table 6. Climate change projection summary for Marine Ecoregion (mean of four general circulation models).

Climate Variable	A2 Emissions Scenario					A1B Emissions Scenario					B1 Emissions Scenario				
Mean Daily T_{min} (°C)	Spring	Summer	Fall	Winter	Year	Spring	Summer	Fall	Winter	Year	Spring	Summer	Fall	Winter	Year
Baseline 1980-2009	0.92	8.04	2.96	-2.50	2.35	0.90	8.01	2.98	-2.47	2.34	0.83	7.95	2.89	-2.58	2.27
Change by 2010-2039	0.58	0.90	0.78	0.80	0.78	0.91	1.05	0.77	1.01	0.95	1.02	0.83	0.75	0.95	0.88
Change by 2040-2069	1.67	2.20	1.96	2.13	1.97	1.83	2.36	2.07	2.16	2.11	1.35	1.74	1.61	1.80	1.62
Change by 2070-2099	2.90	3.80	3.33	3.29	3.34	2.40	3.26	3.04	2.82	2.88	1.79	2.26	2.17	2.23	2.11
100-year forcing	3.09	4.08	3.58	3.66	3.60	2.57	3.51	3.31	3.21	3.14	1.89	2.44	2.35	2.51	2.30
100-year variability (%)	-8.90	32.60	20.15	-8.35	21.21	-8.42	-6.10	-5.23	-2.92	-1.44	-14.26	-7.54	5.55	-14.49	-9.16
Mean Daily T_{max} (°C)	Spring	Summer	Fall	Winter	Year	Spring	Summer	Fall	Winter	Year	Spring	Summer	Fall	Winter	Year
Baseline 1980-2009	12.10	22.52	14.36	5.25	13.55	12.04	22.40	14.31	5.31	13.50	11.98	22.39	14.13	5.17	13.41
Change by 2010-2039	0.59	1.09	0.64	0.66	0.76	1.06	1.16	0.64	0.75	0.91	1.11	0.92	0.80	0.78	0.90
Change by 2040-2069	1.76	2.42	1.82	1.81	1.94	1.92	2.73	1.96	1.75	2.10	1.49	1.87	1.56	1.45	1.59
Change by 2070-2099	3.03	4.18	3.15	2.78	3.30	2.44	3.79	2.92	2.32	2.87	2.04	2.56	2.28	1.88	2.19
100-year forcing	3.27	4.53	3.45	3.08	3.59	2.62	4.01	3.16	2.67	3.11	2.16	2.78	2.34	2.09	2.35
100-year variability (%)	12.33	9.55	14.27	6.72	15.20	8.18	-10.67	3.70	18.57	-2.28	1.01	-1.72	5.21	-5.08	-3.92
Total Precipitation (mm)	Spring	Summer	Fall	Winter	Year	Spring	Summer	Fall	Winter	Year	Spring	Summer	Fall	Winter	Year
Baseline 1980-2009	344	117	418	656	1532	346	123	421	653	1539	348	120	425	664	1555
Change by 2010-2039	1	-13	22	24	37	-4	-3	22	42	66	-16	-7	15	-1	-5
Change by 2040-2069	-8	-14	37	43	54	-3	-19	43	70	91	-13	-10	35	44	56
Change by 2070-2099	-8	-19	47	71	95	1	-27	52	88	117	-13	-9	41	49	71
100-year forcing	-13	-21	52	71	88	-3	-24	60	86	118	-14	-8	53	58	87
100-year variability (%)	12.70	1.94	15.74	2.05	8.47	14.73	-10.91	7.28	-0.78	8.07	9.75	6.24	6.08	6.14	-2.26

Table 6. Continued

Climate Variable	A2 Emissions Scenario					A1B Emissions Scenario					B1 Emissions Scenario				
Mean Daily Global Solar Radiation (MJ m^{-2})	Spring	Summer	Fall	Winter	Year	Spring	Summer	Fall	Winter	Year	Spring	Summer	Fall	Winter	Year
Baseline 1980-2009	14.95	22.48	9.63	4.63	12.92	14.87	22.32	9.56	4.68	12.86	14.90	22.39	9.48	4.61	12.84
Change by 2010-2039	0.09	0.34	-0.15	-0.04	0.06	0.30	0.32	-0.12	-0.19	0.07	0.23	0.28	0.06	0.02	0.14
Change by 2040-2069	0.28	0.52	-0.11	-0.15	0.14	0.26	0.76	-0.08	-0.20	0.18	0.33	0.46	-0.02	-0.15	0.16
Change by 2070-2099	0.26	0.80	-0.03	-0.23	0.20	0.18	1.06	0.00	-0.32	0.23	0.51	0.70	0.13	-0.19	0.29
100-year forcing	0.33	0.95	0.03	-0.25	0.27	0.18	1.05	-0.02	-0.29	0.24	0.54	0.75	0.03	-0.23	0.27
100-year variability (%)	1.32	-6.53	-14.09	-6.57	-6.29	1.29	-20.49	-8.37	-0.69	-8.06	0.62	-6.37	-13.09	9.13	-8.22
Mean Vapor Pressure (kPa)	Spring	Summer	Fall	Winter	Year	Spring	Summer	Fall	Winter	Year	Spring	Summer	Fall	Winter	Year
Baseline 1980-2009	0.768	1.202	0.954	0.627	0.887	0.765	1.205	0.954	0.627	0.887	0.762	1.199	0.953	0.623	0.884
Change by 2010-2039	0.028	0.056	0.044	0.031	0.040	0.046	0.073	0.053	0.042	0.054	0.049	0.051	0.047	0.035	0.045
Change by 2040-2069	0.082	0.156	0.128	0.089	0.113	0.090	0.148	0.129	0.091	0.115	0.069	0.122	0.097	0.072	0.090
Change by 2070-2099	0.148	0.277	0.224	0.144	0.198	0.123	0.230	0.200	0.124	0.169	0.090	0.156	0.130	0.095	0.118
100-year forcing	0.157	0.293	0.237	0.157	0.211	0.130	0.249	0.213	0.138	0.182	0.094	0.169	0.142	0.104	0.127
100-year variability (%)	5.95	63.26	45.20	27.77	70.73	4.65	28.06	16.73	27.36	35.58	2.31	8.17	16.08	7.85	11.98
Mean Windspeed (m s^{-1})	Spring	Summer	Fall	Winter	Year	Spring	Summer	Fall	Winter	Year	Spring	Summer	Fall	Winter	Year
Baseline 1980-2009	3.41	3.30	2.99	3.36	3.26	3.45	3.27	3.01	3.34	3.27	3.43	3.29	3.00	3.36	3.27
Change by 2010-2039	-0.01	0.07	0.10	0.07	0.06	-0.13	0.03	0.04	0.18	0.04	-0.13	0.03	0.01	0.10	0.00
Change by 2040-2069	-0.04	0.11	0.12	0.19	0.09	-0.05	0.15	0.13	0.17	0.09	-0.18	0.04	0.09	0.22	0.04
Change by 2070-2099	-0.02	0.18	0.06	0.16	0.10	-0.08	0.12	0.11	0.22	0.09	-0.24	0.05	0.07	0.15	0.01
100-year forcing	-0.08	0.22	0.07	0.19	0.10	-0.10	0.14	0.14	0.22	0.09	-0.27	0.09	0.09	0.18	0.02
100-year variability (%)	-13.33	-0.40	-7.64	-1.30	-8.49	-10.30	-7.08	-6.16	9.04	-6.53	-3.42	4.55	0.26	0.81	-8.98

Table 7. Climate change projection summary for Mediterranean Ecoregion (mean of four general circulation models).

Climate Variable	A2 Emissions Scenario					A1B Emissions Scenario					B1 Emissions Scenario				
Mean Daily T_{min} (°C)	Spring	Summer	Fall	Winter	Year	Spring	Summer	Fall	Winter	Year	Spring	Summer	Fall	Winter	Year
Baseline 1980-2009	3.59	11.31	6.08	0.01	5.24	3.57	11.26	6.04	-0.03	5.20	3.52	11.21	5.96	-0.12	5.14
Change by 2010-2039	0.62	1.00	0.75	0.59	0.76	0.90	1.12	0.90	0.85	0.95	0.89	0.91	0.87	0.82	0.87
Change by 2040-2069	1.68	2.28	2.08	1.74	1.94	1.79	2.43	2.09	1.87	2.05	1.34	1.75	1.62	1.51	1.55
Change by 2070-2099	3.05	3.91	3.52	2.92	3.36	2.39	3.36	3.10	2.51	2.84	1.71	2.24	2.20	1.98	2.03
100-year forcing	3.21	4.21	3.83	3.22	3.61	2.54	3.61	3.37	2.77	3.06	1.80	2.44	2.38	2.15	2.19
100-year variability (%)	20.68	39.80	21.98	18.11	53.18	12.31	-7.38	-11.97	18.65	13.81	-4.67	5.48	1.47	1.05	6.63
Mean Daily T_{max} (°C)	Spring	Summer	Fall	Winter	Year	Spring	Summer	Fall	Winter	Year	Spring	Summer	Fall	Winter	Year
Baseline 1980-2009	17.86	28.91	21.36	11.67	19.94	17.89	28.85	21.32	11.70	19.93	17.80	28.82	21.15	11.60	19.83
Change by 2010-2039	0.77	1.12	0.70	0.61	0.81	1.12	1.13	0.90	0.79	0.99	0.90	0.89	1.05	0.69	0.88
Change by 2040-2069	2.02	2.40	2.13	1.80	2.08	2.01	2.49	2.09	1.76	2.10	1.43	1.74	1.58	1.39	1.54
Change by 2070-2099	3.58	3.93	3.47	2.85	3.47	2.49	3.42	3.08	2.38	2.85	1.80	2.19	2.24	1.87	2.04
100-year forcing	3.81	4.26	3.76	3.13	3.74	2.75	3.69	3.33	2.68	3.11	1.97	2.42	2.32	2.08	2.20
100-year variability (%)	17.49	25.15	13.21	7.38	30.78	8.20	-7.48	-6.90	26.74	6.41	3.43	2.47	-10.60	8.49	-2.04
Total Precipitation (mm)	Spring	Summer	Fall	Winter	Year	Spring	Summer	Fall	Winter	Year	Spring	Summer	Fall	Winter	Year
Baseline 1980-2009	178	32	167	347	723	179	32	170	338	718	179	33	170	339	721
Change by 2010-2039	-5	-8	-12	11	-10	-17	-3	0	-1	-16	-4	-7	-8	19	-1
Change by 2040-2069	-16	-11	-15	3	-40	-14	-5	-7	35	6	0	-8	-5	22	8
Change by 2070-2099	-27	-9	-4	42	2	1	-10	-17	42	16	-2	-4	0	45	36
100-year forcing	-35	-9	-2	49	-1	-6	-11	-12	40	8	-9	-4	5	44	31
100-year variability (%)	6.52	-24.72	4.73	15.79	18.80	10.17	-36.36	-20.30	-1.51	3.59	-8.54	-18.26	6.34	18.92	20.68

Table 7. Continued

Climate Variable	A2 Emissions Scenario					A1B Emissions Scenario					B1 Emissions Scenario				
Mean Daily Global Solar Radiation (MJ m^{-2})	Spring	Summer	Fall	Winter	Year	Spring	Summer	Fall	Winter	Year	Spring	Summer	Fall	Winter	Year
Baseline 1980-2009	19.82	25.93	14.06	8.39	17.05	19.82	25.93	14.03	8.46	17.06	19.79	25.93	14.02	8.44	17.04
Change by 2010-2039	0.21	0.06	-0.02	0.03	0.06	0.29	-0.03	0.03	-0.04	0.06	0.22	0.00	0.10	-0.10	0.05
Change by 2040-2069	0.38	0.00	0.02	0.03	0.11	0.36	-0.04	0.03	-0.16	0.05	0.24	-0.03	-0.04	-0.13	0.02
Change by 2070-2099	0.65	-0.15	-0.08	-0.11	0.08	0.20	-0.02	0.03	-0.17	0.01	0.25	-0.09	-0.01	-0.20	-0.01
100-year forcing	0.76	-0.13	-0.08	-0.13	0.11	0.31	0.00	-0.01	-0.12	0.05	0.32	-0.06	-0.06	-0.17	0.01
100-year variability (%)	-3.62	-5.80	-8.29	-6.23	0.98	-3.97	-14.48	-15.00	-18.50	-3.47	-1.70	-1.97	-11.20	7.53	0.81
Mean Vapor Pressure (kPa)	Spring	Summer	Fall	Winter	Year	Spring	Summer	Fall	Winter	Year	Spring	Summer	Fall	Winter	Year
Baseline 1980-2009	0.934	1.473	1.173	0.802	1.095	0.931	1.470	1.165	0.798	1.090	0.929	1.465	1.165	0.794	1.088
Change by 2010-2039	0.031	0.081	0.041	0.029	0.047	0.043	0.083	0.054	0.049	0.058	0.044	0.071	0.042	0.040	0.049
Change by 2040-2069	0.083	0.184	0.128	0.090	0.121	0.099	0.208	0.143	0.104	0.139	0.078	0.151	0.119	0.081	0.107
Change by 2070-2099	0.153	0.334	0.246	0.162	0.225	0.141	0.288	0.232	0.141	0.201	0.101	0.202	0.155	0.110	0.142
100-year forcing	0.162	0.358	0.271	0.178	0.242	0.147	0.309	0.248	0.153	0.214	0.105	0.218	0.172	0.118	0.153
100-year variability (%)	7.53	65.67	35.32	37.31	54.33	13.94	13.81	7.57	-1.39	16.95	11.24	18.85	10.73	8.83	13.86
Mean Windspeed (m s^{-1})	Spring	Summer	Fall	Winter	Year	Spring	Summer	Fall	Winter	Year	Spring	Summer	Fall	Winter	Year
Baseline 1980-2009	3.62	3.63	2.81	2.90	3.24	3.64	3.64	2.83	2.86	3.24	3.64	3.65	2.83	2.84	3.24
Change by 2010-2039	0.00	0.04	0.09	-0.11	0.01	-0.05	0.00	0.03	-0.02	0.00	-0.16	-0.01	0.02	0.00	-0.03
Change by 2040-2069	0.08	0.13	0.08	-0.02	0.06	-0.06	0.02	0.07	0.01	0.01	0.03	0.01	-0.01	0.09	0.03
Change by 2070-2099	0.07	0.16	0.09	-0.04	0.07	0.03	0.03	-0.02	-0.01	0.00	-0.08	-0.03	-0.02	0.05	-0.01
100-year forcing	0.06	0.18	0.08	0.00	0.08	0.03	0.05	-0.01	-0.02	0.01	-0.08	0.01	0.00	0.03	-0.01
100-year variability (%)	-6.53	-0.16	0.18	2.66	-14.11	-0.11	0.99	0.17	10.37	9.61	-12.33	2.53	-6.83	5.55	-12.01

Table 8. Climate change projection summary for Prairie Ecoregion (mean of four general circulation models).

Climate Variable	A2 Emissions Scenario					A1B Emissions Scenario					B1 Emissions Scenario				
Mean Daily T_{min} (°C)	Spring	Summer	Fall	Winter	Year	Spring	Summer	Fall	Winter	Year	Spring	Summer	Fall	Winter	Year
Baseline 1980-2009	6.22	18.13	7.53	-6.28	6.38	6.25	18.27	7.55	-6.36	6.42	6.29	18.30	7.53	-6.27	6.44
Change by 2010-2039	0.87	1.22	1.12	0.96	1.06	1.14	1.36	1.31	1.32	1.30	0.69	1.05	1.07	0.76	0.91
Change by 2040-2069	2.17	2.68	2.77	2.34	2.48	2.27	2.54	2.65	2.50	2.49	1.50	1.63	1.90	1.80	1.72
Change by 2070-2099	3.66	4.57	4.55	3.89	4.18	2.98	3.49	3.62	3.55	3.41	1.80	2.21	2.40	2.40	2.21
100-year forcing	3.80	4.78	4.91	4.38	4.46	3.17	3.83	4.00	3.96	3.73	2.02	2.59	2.76	2.90	2.55
100-year variability (%)	27.94	34.75	35.07	-7.48	36.13	-6.49	13.35	1.76	-8.01	-5.36	1.08	-2.32	10.48	-14.87	-9.71
Mean Daily T_{max} (°C)	Spring	Summer	Fall	Winter	Year	Spring	Summer	Fall	Winter	Year	Spring	Summer	Fall	Winter	Year
Baseline 1980-2009	18.92	30.95	20.34	5.09	18.81	18.98	31.20	20.37	5.04	18.89	19.04	31.28	20.26	5.09	18.90
Change by 2010-2039	1.00	1.50	1.22	0.82	1.15	1.14	1.52	1.55	1.16	1.36	0.74	1.17	1.35	0.66	1.00
Change by 2040-2069	2.22	2.91	2.92	2.21	2.56	2.43	2.61	2.76	2.45	2.56	1.45	1.48	2.20	1.72	1.73
Change by 2070-2099	3.90	4.79	4.71	3.85	4.33	3.19	3.60	3.88	3.49	3.54	1.82	2.17	2.77	2.31	2.27
100-year forcing	4.04	4.91	5.07	4.24	4.56	3.39	3.97	4.28	3.82	3.85	2.07	2.61	3.05	2.69	2.59
100-year variability (%)	15.26	20.78	27.28	14.83	39.52	-5.79	6.84	1.28	11.84	3.29	0.81	1.86	7.11	3.47	4.46
Total Precipitation (mm)	Spring	Summer	Fall	Winter	Year	Spring	Summer	Fall	Winter	Year	Spring	Summer	Fall	Winter	Year
Baseline 1980-2009	261	284	228	120	891	258	273	228	121	881	260	271	231	120	881
Change by 2010-2039	3	-6	5	1	4	10	-4	-3	2	5	12	-3	-9	-1	1
Change by 2040-2069	21	-13	8	-3	15	13	10	4	-7	20	22	24	-1	0	46
Change by 2070-2099	9	-5	9	0	14	25	15	3	-1	42	23	17	-7	-2	33
100-year forcing	15	7	9	2	33	28	17	4	2	50	28	17	-3	0	42
100-year variability (%)	-2.42	10.70	5.68	12.84	2.53	0.93	15.03	-1.33	13.92	-10.87	4.57	8.35	-6.56	3.75	4.10

Table 8. Continued

Climate Variable	A2 Emissions Scenario					A1B Emissions Scenario					B1 Emissions Scenario				
Mean Daily Global Solar Radiation (MJ m^{-2})	Spring	Summer	Fall	Winter	Year	Spring	Summer	Fall	Winter	Year	Spring	Summer	Fall	Winter	Year
Baseline 1980-2009	18.34	22.88	12.61	8.87	15.67	18.33	22.93	12.60	8.88	15.68	18.33	22.94	12.54	8.85	15.67
Change by 2010-2039	-0.04	0.10	-0.01	-0.05	0.00	-0.08	0.12	0.12	-0.05	0.03	-0.05	0.07	0.16	-0.02	0.04
Change by 2040-2069	-0.19	0.07	0.04	-0.10	-0.04	-0.04	0.10	0.08	-0.11	0.01	-0.14	0.01	0.18	-0.06	0.00
Change by 2070-2099	-0.09	0.06	0.09	-0.31	-0.06	-0.10	0.07	0.17	-0.26	-0.03	-0.18	0.04	0.28	-0.09	0.01
100-year forcing	-0.06	0.06	0.13	-0.30	-0.04	-0.09	0.12	0.20	-0.24	0.00	-0.17	0.11	0.25	-0.10	0.02
100-year variability (%)	-9.81	-6.54	-16.19	-12.25	-9.02	-14.08	-7.75	-21.69	-9.25	-25.36	-5.87	-7.11	-21.35	-8.32	-11.53
Mean Vapor Pressure (kPa)	Spring	Summer	Fall	Winter	Year	Spring	Summer	Fall	Winter	Year	Spring	Summer	Fall	Winter	Year
Baseline 1980-2009	1.094	2.203	1.238	0.469	1.251	1.095	2.182	1.239	0.470	1.246	1.093	2.179	1.244	0.469	1.246
Change by 2010-2039	0.055	0.100	0.075	0.023	0.063	0.075	0.104	0.075	0.033	0.072	0.057	0.096	0.049	0.019	0.056
Change by 2040-2069	0.152	0.216	0.177	0.062	0.151	0.134	0.245	0.175	0.059	0.153	0.114	0.222	0.126	0.047	0.127
Change by 2070-2099	0.220	0.375	0.295	0.109	0.250	0.193	0.346	0.243	0.097	0.220	0.128	0.250	0.127	0.061	0.142
100-year forcing	0.234	0.421	0.313	0.119	0.271	0.208	0.372	0.262	0.109	0.237	0.140	0.272	0.151	0.072	0.159
100-year variability (%)	25.88	28.85	4.28	30.42	35.09	8.26	14.22	15.36	2.20	5.90	15.73	5.14	7.29	10.39	11.990
Mean Windspeed (m s^{-1})	Spring	Summer	Fall	Winter	Year	Spring	Summer	Fall	Winter	Year	Spring	Summer	Fall	Winter	Year
Baseline 1980-2009	4.75	3.85	4.06	4.53	4.30	4.71	3.86	4.10	4.53	4.29	4.72	3.84	4.11	4.56	4.30
Change by 2010-2039	0.27	0.03	0.17	0.07	0.13	0.08	0.17	0.00	0.05	0.08	0.05	0.12	0.07	-0.05	0.05
Change by 2040-2069	0.34	0.17	0.14	0.18	0.20	0.23	0.14	0.19	0.10	0.17	0.18	0.11	0.07	0.12	0.13
Change by 2070-2099	0.55	0.38	0.32	0.20	0.37	0.29	0.15	0.18	0.07	0.18	0.11	0.21	-0.03	0.04	0.08
100-year forcing	0.58	0.41	0.34	0.23	0.39	0.27	0.19	0.23	0.11	0.20	0.10	0.23	0.03	0.10	0.11
100-year variability (%)	4.48	17.44	8.04	5.69	5.12	-11.18	12.89	-0.38	-4.47	-11.19	2.24	21.88	13.55	-0.45	9.81

Table 9. Climate change projection summary for Subtropical Ecoregion (mean of four general circulation models).

Climate Variable	A2 Emissions Scenario					A1B Emissions Scenario					B1 Emissions Scenario				
Mean Daily T_{min} (°C)	Spring	Summer	Fall	Winter	Year	Spring	Summer	Fall	Winter	Year	Spring	Summer	Fall	Winter	Year
Baseline 1980-2009	11.06	20.39	12.18	2.30	11.47	11.11	20.46	12.20	2.23	11.49	11.10	20.47	12.21	2.30	11.51
Change by 2010-2039	0.89	1.05	1.06	0.57	0.90	0.99	1.05	1.28	0.81	1.04	0.64	0.92	0.93	0.38	0.74
Change by 2040-2069	2.01	2.31	2.47	1.51	2.08	1.95	2.21	2.39	1.57	2.03	1.49	1.45	1.73	1.05	1.44
Change by 2070-2099	3.23	3.92	4.15	2.74	3.52	2.73	3.04	3.15	2.53	2.87	1.79	1.97	2.14	1.43	1.85
100-year forcing	3.39	4.10	4.44	3.00	3.73	2.95	3.29	3.46	2.73	3.10	1.99	2.24	2.47	1.70	2.10
100-year variability (%)	22.75	36.98	32.24	26.36	53.39	-1.67	2.43	7.16	3.85	9.85	4.22	-0.45	11.09	-0.13	3.11
Mean Daily T_{max} (°C)	Spring	Summer	Fall	Winter	Year	Spring	Summer	Fall	Winter	Year	Spring	Summer	Fall	Winter	Year
Baseline 1980-2009	24.49	32.39	25.32	14.77	24.23	24.58	32.56	25.40	14.71	24.31	24.61	32.64	25.43	14.77	24.35
Change by 2010-2039	0.97	1.20	1.06	0.54	0.95	0.96	1.06	1.20	0.69	0.98	0.57	0.99	0.89	0.33	0.71
Change by 2040-2069	2.06	2.72	2.51	1.51	2.20	2.06	2.32	2.30	1.62	2.07	1.32	1.26	1.57	1.06	1.31
Change by 2070-2099	3.40	4.42	4.16	2.85	3.72	2.68	3.22	3.17	2.58	2.91	1.65	1.92	2.13	1.50	1.81
100-year forcing	3.55	4.47	4.42	3.07	3.87	2.91	3.43	3.51	2.74	3.14	1.91	2.22	2.50	1.72	2.08
100-year variability (%)	20.75	9.47	37.75	15.99	37.14	-5.84	-2.47	7.12	1.34	-3.13	8.53	8.96	8.86	-3.31	6.17
Total Precipitation (mm)	Spring	Summer	Fall	Winter	Year	Spring	Summer	Fall	Winter	Year	Spring	Summer	Fall	Winter	Year
Baseline 1980-2009	354	376	287	334	1351	346	368	281	335	1329	347	363	280	334	1324
Change by 2010-2039	-16	-17	6	-3	-28	-4	-11	20	-5	2	10	-10	8	-8	4
Change by 2040-2069	-10	-44	5	-2	-49	-3	-16	12	-13	-20	16	10	20	-2	45
Change by 2070-2099	-13	-51	6	-28	-84	26	-13	5	-10	11	26	-7	17	-5	33
100-year forcing	-1	-42	8	-26	-61	30	-12	1	-7	13	30	-11	12	-4	29
100-year variability (%)	12.34	-16.95	-5.07	7.01	-3.34	1.82	-6.78	3.28	16.61	-13.07	22.02	2.78	1.17	19.33	-0.66

Table 9. Continued

Climate Variable	A2 Emissions Scenario					A1B Emissions Scenario					B1 Emissions Scenario				
Mean Daily Global Solar Radiation (MJ m^{-2})	Spring	Summer	Fall	Winter	Year	Spring	Summer	Fall	Winter	Year	Spring	Summer	Fall	Winter	Year
Baseline 1980-2009	19.36	21.94	14.38	10.19	16.47	19.37	22.02	14.42	10.17	16.50	19.44	22.03	14.45	10.14	16.52
Change by 2010-2039	0.07	0.18	0.04	0.07	0.09	0.09	0.09	-0.03	0.11	0.06	-0.07	0.16	0.01	0.17	0.06
Change by 2040-2069	0.01	0.28	0.12	0.17	0.14	0.21	0.11	0.07	0.24	0.16	-0.10	0.01	0.01	0.22	0.03
Change by 2070-2099	0.16	0.33	0.19	0.22	0.22	0.05	0.21	0.21	0.16	0.15	-0.13	0.11	0.14	0.30	0.10
100-year forcing	0.16	0.29	0.21	0.26	0.23	0.06	0.25	0.27	0.19	0.19	-0.05	0.15	0.23	0.30	0.16
100-year variability (%)	6.71	-19.87	-12.33	-17.43	-6.42	-13.49	-21.47	-2.09	-9.24	-24.03	5.84	1.10	-8.52	-9.85	-6.12
Mean Vapor Pressure (kPa)	Spring	Summer	Fall	Winter	Year	Spring	Summer	Fall	Winter	Year	Spring	Summer	Fall	Winter	Year
Baseline 1980-2009	1.474	2.629	1.672	0.825	1.649	1.473	2.619	1.672	0.824	1.647	1.469	2.617	1.671	0.828	1.645
Change by 2010-2039	0.071	0.103	0.092	0.030	0.074	0.085	0.120	0.116	0.039	0.090	0.069	0.088	0.083	0.015	0.065
Change by 2040-2069	0.176	0.221	0.217	0.075	0.173	0.158	0.247	0.219	0.073	0.174	0.144	0.205	0.175	0.051	0.145
Change by 2070-2099	0.266	0.372	0.356	0.138	0.283	0.253	0.352	0.282	0.125	0.254	0.172	0.250	0.190	0.065	0.170
100-year forcing	0.287	0.417	0.378	0.150	0.307	0.273	0.386	0.304	0.136	0.275	0.189	0.283	0.211	0.079	0.190
100-year variability (%)	39.20	25.70	25.95	29.56	61.96	15.04	3.64	20.35	17.93	19.95	21.78	6.77	8.91	11.03	19.647
Mean Windspeed (m s^{-1})	Spring	Summer	Fall	Winter	Year	Spring	Summer	Fall	Winter	Year	Spring	Summer	Fall	Winter	Year
Baseline 1980-2009	3.74	2.77	3.11	3.68	3.33	3.74	2.79	3.11	3.68	3.33	3.78	2.78	3.11	3.69	3.34
Change by 2010-2039	0.13	0.06	0.03	0.01	0.06	0.08	0.05	-0.02	-0.05	0.02	-0.10	0.04	0.00	-0.04	-0.02
Change by 2040-2069	0.17	0.13	0.07	0.02	0.09	0.11	0.09	0.07	0.05	0.08	0.07	0.12	-0.04	0.08	0.06
Change by 2070-2099	0.26	0.24	0.10	0.13	0.18	0.09	0.12	0.01	0.02	0.06	-0.01	0.09	-0.02	0.05	0.03
100-year forcing	0.27	0.24	0.15	0.19	0.21	0.11	0.14	0.06	0.09	0.10	0.05	0.10	0.03	0.13	0.08
100-year variability (%)	-6.32	-20.45	1.09	-2.86	-27.61	-8.37	-11.92	6.57	-3.94	-14.94	-2.69	4.19	5.37	-5.46	-20.64

Table 10. Climate change projection summary for Dry Temperate Ecoregion (mean of four general circulation models).

Climate Variable	A2 Emissions Scenario					A1B Emissions Scenario					B1 Emissions Scenario				
Mean Daily T_{min} (°C)	Spring	Summer	Fall	Winter	Year	Spring	Summer	Fall	Winter	Year	Spring	Summer	Fall	Winter	Year
Baseline 1980-2009	-1.13	10.30	0.20	-10.59	-0.32	-1.08	10.30	0.21	-10.60	-0.31	-1.14	10.33	0.11	-10.71	-0.36
Change by 2010-2039	0.74	1.20	0.96	0.98	1.00	1.25	1.39	1.08	1.33	1.28	1.04	1.06	1.03	0.99	1.04
Change by 2040-2069	2.27	2.77	2.53	2.59	2.52	2.36	2.81	2.49	2.65	2.58	1.66	1.86	1.89	2.14	1.89
Change by 2070-2099	3.88	4.63	4.16	4.14	4.22	3.07	3.80	3.58	3.62	3.52	2.12	2.46	2.53	2.84	2.49
100-year forcing	4.02	4.91	4.48	4.61	4.51	3.25	4.08	3.91	4.08	3.82	2.26	2.77	2.77	3.20	2.74
100-year variability (%)	1.14	76.08	30.36	0.44	47.74	-6.32	20.16	-14.51	0.17	-1.45	-21.79	7.72	-5.54	-5.79	-9.36
Mean Daily T_{max} (°C)	Spring	Summer	Fall	Winter	Year	Spring	Summer	Fall	Winter	Year	Spring	Summer	Fall	Winter	Year
Baseline 1980-2009	13.90	28.01	16.22	2.39	15.12	13.96	28.00	16.18	2.40	15.12	13.94	28.08	16.05	2.34	15.08
Change by 2010-2039	0.86	1.45	0.86	0.73	1.00	1.42	1.66	1.20	1.02	1.34	1.07	1.26	1.23	0.74	1.09
Change by 2040-2069	2.51	3.06	2.62	2.10	2.56	2.56	3.04	2.56	2.14	2.58	1.70	1.95	1.90	1.65	1.81
Change by 2070-2099	4.31	4.88	4.32	3.50	4.27	3.27	4.12	3.81	3.00	3.56	2.18	2.52	2.71	2.28	2.43
100-year forcing	4.48	5.23	4.73	3.85	4.57	3.51	4.46	4.18	3.36	3.86	2.39	2.94	2.94	2.58	2.70
100-year variability (%)	8.13	38.52	18.37	19.16	44.31	-3.83	5.19	-10.41	23.07	1.43	-13.36	8.34	-12.25	8.52	3.47
Total Precipitation (mm)	Spring	Summer	Fall	Winter	Year	Spring	Summer	Fall	Winter	Year	Spring	Summer	Fall	Winter	Year
Baseline 1980-2009	124	135	91	75	425	124	135	92	75	425	124	135	92	75	425
Change by 2010-2039	4	1	4	3	12	4	-2	2	2	6	6	0	-1	2	7
Change by 2040-2069	7	-2	2	6	12	6	5	4	7	22	10	5	4	6	25
Change by 2070-2099	6	3	3	12	24	10	0	2	11	23	10	6	0	8	24
100-year forcing	7	3	3	13	26	11	1	2	12	25	10	7	1	8	26
100-year variability (%)	10.52	4.74	12.62	13.86	2.72	-8.31	-2.21	5.72	4.77	-7.73	9.32	4.54	-1.26	20.03	7.40

Table 10. Continued

Climate Variable	A2 Emissions Scenario					A1B Emissions Scenario					B1 Emissions Scenario				
Mean Daily Global Solar Radiation (MJ m^{-2})	Spring	Summer	Fall	Winter	Year	Spring	Summer	Fall	Winter	Year	Spring	Summer	Fall	Winter	Year
Baseline 1980-2009	19.07	24.37	12.72	8.03	16.05	19.05	24.34	12.70	8.04	16.04	19.09	24.36	12.67	8.06	16.04
Change by 2010-2039	-0.08	0.16	-0.12	-0.13	-0.05	-0.08	0.16	0.01	-0.20	-0.03	-0.18	0.13	0.03	-0.12	-0.04
Change by 2040-2069	-0.15	0.19	-0.07	-0.35	-0.09	-0.21	0.21	-0.09	-0.39	-0.12	-0.24	0.15	-0.11	-0.31	-0.12
Change by 2070-2099	-0.23	0.15	-0.09	-0.61	-0.20	-0.37	0.25	-0.06	-0.56	-0.19	-0.37	0.11	0.00	-0.42	-0.17
100-year forcing	-0.21	0.24	-0.05	-0.67	-0.17	-0.36	0.30	-0.05	-0.60	-0.18	-0.34	0.18	-0.02	-0.45	-0.16
100-year variability (%)	-5.92	-7.60	-1.13	9.13	-4.91	-9.92	-11.01	-6.19	-3.68	-11.23	9.41	-2.49	-15.41	16.89	4.30
Mean Vapor Pressure (kPa)	Spring	Summer	Fall	Winter	Year	Spring	Summer	Fall	Winter	Year	Spring	Summer	Fall	Winter	Year
Baseline 1980-2009	0.693	1.361	0.795	0.376	0.806	0.695	1.360	0.794	0.375	0.806	0.691	1.357	0.791	0.373	0.803
Change by 2010-2039	0.031	0.095	0.045	0.023	0.049	0.048	0.075	0.043	0.033	0.050	0.046	0.078	0.041	0.024	0.047
Change by 2040-2069	0.093	0.174	0.112	0.064	0.110	0.092	0.190	0.114	0.067	0.116	0.076	0.155	0.098	0.053	0.096
Change by 2070-2099	0.154	0.303	0.193	0.111	0.191	0.131	0.265	0.173	0.095	0.166	0.095	0.194	0.116	0.072	0.119
100-year forcing	0.162	0.326	0.207	0.121	0.204	0.141	0.287	0.186	0.105	0.179	0.100	0.213	0.126	0.078	0.129
100-year variability (%)	7.40	70.45	60.86	36.83	60.65	0.12	28.34	23.56	20.04	19.55	7.07	24.35	30.44	18.72	25.574
Mean Windspeed (m s^{-1})	Spring	Summer	Fall	Winter	Year	Spring	Summer	Fall	Winter	Year	Spring	Summer	Fall	Winter	Year
Baseline 1980-2009	4.39	3.83	3.70	3.88	3.95	4.36	3.84	3.71	3.85	3.94	4.35	3.87	3.75	3.87	3.96
Change by 2010-2039	0.04	0.02	0.09	-0.01	0.04	-0.15	0.08	0.09	0.01	0.02	-0.14	0.03	0.02	-0.07	-0.03
Change by 2040-2069	0.01	0.13	0.06	0.02	0.05	-0.09	0.02	0.11	-0.02	0.01	-0.06	-0.06	0.02	0.03	-0.02
Change by 2070-2099	-0.01	0.20	0.07	-0.05	0.05	0.00	-0.01	0.06	0.03	0.03	-0.18	-0.07	-0.02	-0.02	-0.07
100-year forcing	0.02	0.19	0.04	-0.03	0.05	0.00	-0.01	0.05	0.02	0.02	-0.19	-0.03	0.01	-0.01	-0.06
100-year variability (%)	0.42	36.79	-18.66	-5.85	-16.26	-8.78	6.47	-22.23	-8.06	-20.87	5.37	9.38	-11.43	-3.67	-2.17

Table 11. Climate change projection summary for Dry Subtropical Ecoregion (mean of four general circulation models).

Climate Variable	A2 Emissions Scenario					A1B Emissions Scenario					B1 Emissions Scenario				
Mean Daily T_{min} (°C)	Spring	Summer	Fall	Winter	Year	Spring	Summer	Fall	Winter	Year	Spring	Summer	Fall	Winter	Year
Baseline 1980-2009	6.94	17.70	8.85	-1.52	7.98	6.99	17.78	8.81	-1.57	7.99	6.93	17.75	8.80	-1.68	7.94
Change by 2010-2039	0.83	1.19	0.94	0.61	0.91	1.10	1.20	1.18	0.93	1.12	0.83	1.05	1.00	0.76	0.92
Change by 2040-2069	2.12	2.67	2.55	1.75	2.27	2.10	2.47	2.48	1.85	2.23	1.53	1.74	1.84	1.39	1.62
Change by 2070-2099	3.66	4.31	4.31	3.12	3.86	2.86	3.51	3.61	2.73	3.18	1.88	2.17	2.35	1.96	2.09
100-year forcing	3.80	4.58	4.70	3.47	4.13	3.04	3.86	3.96	3.02	3.46	2.00	2.49	2.70	2.14	2.33
100-year variability (%)	34.37	49.86	24.38	26.23	80.63	4.26	19.20	-14.66	6.79	8.89	-3.43	3.24	-13.65	5.61	-6.87
Mean Daily T_{max} (°C)	Spring	Summer	Fall	Winter	Year	Spring	Summer	Fall	Winter	Year	Spring	Summer	Fall	Winter	Year
Baseline 1980-2009	24.05	33.81	24.90	13.90	24.15	24.25	33.96	24.90	13.95	24.25	24.21	33.96	24.80	13.81	24.18
Change by 2010-2039	1.14	1.33	0.99	0.80	1.08	1.22	1.18	1.39	0.93	1.20	0.64	1.05	1.25	0.72	0.92
Change by 2040-2069	2.74	2.83	2.70	2.29	2.63	2.51	2.43	2.69	2.33	2.49	1.59	1.70	2.01	1.63	1.74
Change by 2070-2099	4.61	4.38	4.75	3.85	4.41	3.33	3.51	3.92	3.24	3.51	2.13	1.99	2.76	2.33	2.31
100-year forcing	4.76	4.61	5.14	4.15	4.66	3.69	3.88	4.31	3.59	3.85	2.44	2.36	3.04	2.54	2.59
100-year variability (%)	8.05	13.41	20.84	23.85	33.54	-6.35	12.56	0.72	27.68	3.83	-0.55	6.34	-12.71	14.65	-9.14
Total Precipitation (mm)	Spring	Summer	Fall	Winter	Year	Spring	Summer	Fall	Winter	Year	Spring	Summer	Fall	Winter	Year
Baseline 1980-2009	85	144	115	69	412	82	139	114	67	402	82	141	116	67	405
Change by 2010-2039	-4	-1	-2	0	-6	2	9	-5	2	9	7	-3	-6	4	2
Change by 2040-2069	-4	-5	-1	-6	-15	2	17	-5	-6	8	7	13	-2	0	18
Change by 2070-2099	-10	2	-13	-6	-26	1	10	-7	-5	-1	-1	17	-12	-2	3
100-year forcing	-7	5	-12	-4	-18	1	8	-7	-5	-3	-1	18	-10	-2	5
100-year variability (%)	0.61	10.10	-6.59	-3.52	-11.55	18.17	10.79	0.53	-3.28	2.40	21.77	27.13	-6.18	0.04	1.83

Table 11. Continued

Climate Variable	A2 Emissions Scenario					A1B Emissions Scenario					B1 Emissions Scenario				
Mean Daily Global Solar Radiation (MJ m^{-2})	Spring	Summer	Fall	Winter	Year	Spring	Summer	Fall	Winter	Year	Spring	Summer	Fall	Winter	Year
Baseline 1980-2009	22.80	25.57	16.45	12.03	19.22	22.92	25.61	16.46	12.09	19.27	22.89	25.59	16.41	12.04	19.23
Change by 2010-2039	0.10	-0.06	0.04	0.02	0.02	-0.01	-0.10	0.16	-0.12	-0.01	-0.19	-0.04	0.19	-0.09	-0.03
Change by 2040-2069	0.17	-0.13	0.14	0.10	0.07	0.04	-0.19	0.20	0.01	0.02	-0.13	-0.09	0.15	0.00	-0.01
Change by 2070-2099	0.31	-0.24	0.31	-0.06	0.08	0.04	-0.25	0.25	-0.07	-0.01	0.00	-0.19	0.29	-0.04	0.02
100-year forcing	0.30	-0.27	0.31	-0.05	0.07	0.14	-0.24	0.25	0.01	0.04	0.09	-0.20	0.25	-0.01	0.03
100-year variability (%)	-19.79	-8.15	-8.29	-7.33	-14.80	-11.30	2.74	-10.13	-7.34	-15.68	-2.50	4.46	-13.54	-1.64	-8.70
Mean Vapor Pressure (kPa)	Spring	Summer	Fall	Winter	Year	Spring	Summer	Fall	Winter	Year	Spring	Summer	Fall	Winter	Year
Baseline 1980-2009	0.949	1.809	1.232	0.656	1.165	0.941	1.808	1.226	0.654	1.158	0.939	1.791	1.231	0.650	1.155
Change by 2010-2039	0.030	0.064	0.063	0.018	0.047	0.057	0.105	0.057	0.043	0.065	0.055	0.067	0.043	0.033	0.055
Change by 2040-2069	0.098	0.131	0.149	0.062	0.120	0.098	0.242	0.141	0.062	0.135	0.092	0.119	0.110	0.053	0.107
Change by 2070-2099	0.149	0.235	0.246	0.118	0.210	0.140	0.314	0.218	0.104	0.194	0.096	0.175	0.121	0.075	0.133
100-year forcing	0.160	0.255	0.272	0.132	0.230	0.143	0.332	0.239	0.117	0.207	0.097	0.176	0.146	0.083	0.144
100-year variability (%)	13.35	23.66	25.70	33.67	28.45	19.99	71.91	17.51	5.02	4.13	10.71	42.25	19.10	6.03	16.593
Mean Windspeed (m s^{-1})	Spring	Summer	Fall	Winter	Year	Spring	Summer	Fall	Winter	Year	Spring	Summer	Fall	Winter	Year
Baseline 1980-2009	4.45	3.88	3.57	3.58	3.88	4.48	3.90	3.59	3.56	3.89	4.51	3.91	3.64	3.60	3.91
Change by 2010-2039	0.16	0.14	0.07	0.00	0.09	0.13	0.11	0.03	-0.12	0.04	-0.08	0.08	-0.01	-0.07	-0.02
Change by 2040-2069	0.26	0.28	0.11	-0.04	0.15	0.04	0.17	0.11	-0.04	0.07	0.11	0.10	-0.02	0.01	0.05
Change by 2070-2099	0.24	0.45	0.18	-0.13	0.18	0.16	0.16	0.07	-0.09	0.07	-0.02	0.08	-0.06	-0.08	-0.02
100-year forcing	0.17	0.45	0.21	-0.18	0.16	0.13	0.19	0.11	-0.14	0.07	-0.02	0.12	0.02	-0.11	0.01
100-year variability (%)	0.01	15.30	2.26	8.23	1.68	-2.91	15.98	12.22	5.77	12.30	6.84	24.09	9.07	21.39	17.37

Discussion

Interpolated climate scenarios derived from state-of-the-art GCMs provide an effective and reasonable means for comparing standardized climate projections in assessments of the impacts of climate change at high spatial resolution. The suite of 12 climate scenarios presented here were downscaled from simulations carried out with four well-established GCMs, each forced by three GHG emissions scenarios developed for the IPCC: the A2 scenario, which provides the strongest GHG forcing; the B1 scenario, derived from a storyline with significant GHG mitigation, which provides the weakest forcing; and the A1B scenario, derived from an intermediate forcing scenario, which provides intermediate projections. The downscaled climate scenarios were developed in support of large-scale assessments of vulnerability to climate change, for the United States, the USDA FS RPA Assessment, and for Canada, as a contribution to the Canadian Council of Forest Ministers Climate Change Task Force. In both projects, a key objective was to follow recommendations on the selection and use of climate scenario data from the IPCC's AR4 (see http://www.ipcc-data.org/ddc_scen_selection.html). Each downscaled climate scenario comprised data for six monthly climate variables, reported as differences from or ratios in relation to mean values for 1961–1990. When combined with observed interpolated climatologies (data for 1961–1990 normals), these data sets should provide a solid basis for exploring the potential effects of climate change anywhere in Alaska, the conterminous United States and Canada.

Producing such a comprehensive data set requires an assessment of the quality and consistency of the data. With that in mind, an analysis was carried out to highlight both the consistencies and discrepancies among different GCMs and their differential responses to the three GHG forcing scenarios. To make this analysis more informative, the land area of the continental United States was divided into eight regions, comprising the entire state of Alaska and seven ecoclimatic divisions identified in the classification of Bailey (1995).

The results across models generally were highly consistent, particularly with respect to temperature and precipitation, both in terms of each model's response to the different forcing scenarios, and in agreement among the four models. This is not to say the models agreed completely in all cases, but in general, the different projections seemed plausible, and those from any single model rarely looked completely inconsistent with results from the other models. However, the divergence among model projections generally increased further into the future, and with increasing GHG forcing (i.e., from B1 to A1B to A2). Hence the uncertainty in projections of future climate must inevitably increase as the projected change from present-day conditions increases (consistent with many other assessments of climate scenarios).

Subjective comparisons for the period 1961–2008, for which both observed and modeled monthly temperature and precipitation data were available, strongly suggested the magnitude and periodicity of interannual variations produced by all four GCMs were consistent with observations in all seasons and all regions. There was less consistency among the models in their projections of changes in interannual variability over the 21st century, but time-dependent changes in amplitude and frequency generally were similar among models and seasonal differences appeared consistent.

Sources of Error and Uncertainty

Users of the data should keep in mind that general circulation models (GCM) provide imperfect but reasonably correct representations of observed climate, considered as variables averaged over large areas with little representation of the effects of surface topography. Furthermore, the global projections of future climate created by GCMs are based on an understanding of current global trends, such as eccentricities in the earth's orbit and observed rates of increase of atmospheric GHG--and the assumption that these trends will change only in predictable ways. For example, GCMs cannot capture future stochastic events, such as major volcanic eruptions, which could alter future climate at any time. Hence, the downscaled scenarios reported here should not be considered accurate predictions of future climate.

For each step in the process used for downscaling the data, there are areas of concern affecting the reliability of these projections. The concerns begin with the assumptions that underlie each GCM, which represent the physical and chemical processes occurring in the global atmosphere, in the oceans and on the land surface. These assumptions govern each GCM's responses to the SRES forcing scenarios, which are themselves based on a set of socio-economic assumptions that are unlikely to occur exactly as stated in reality. In addition, documentation for and availability of GCM output data were sometimes incomplete. For example, as discussed in the Methods section, humidity data generated by the NCARCCSM3 model forced by the A2 emissions scenario for the 2070s were missing from the PCMDI data portal and needed to be obtained elsewhere. Of these substitute data, humidity values for certain grid cells during the 2070s were

completely out of range and required correction. The latter problem was fixed in more recent simulations, but the metadata did not document why it occurred or how it was resolved.

Any process of downscaling GCM grid-level "averages" to a finer scale incorporates further assumptions (see the section 'Review of Spatial Downscaling of Global Climate Simulations" at the beginning of the Methods section). In the present study, GCM outputs were normalized and converted to change factors (relative to 1961–1990 simulated means) and downscaled by interpolation to a 5 arcminute grid. Clearly these downscaled change factors cannot be more accurate than the data from which they were derived. The interpolated change factors were applied to historical climatology for 1961–1990 to produce data that more closely resemble climatic observations.

Basing projections of future climate on interpolated weather station data provides a realistic context within which to assess the GCM results; however, station data also are subject to problems with data quality, measurement errors, and missing values. Further, observing stations are not uniformly distributed across a heterogeneous land surface. For example, there are relatively few stations to monitor climate at high elevations, resulting in larger errors in interpolated data in remote mountain regions. Hence, any baseline value is only an estimate of "truth." The implication is that the scenarios of future climate reported here must not be considered forecasts, but as a range of *plausible futures*. In particular, the influences of unpredictable climatic drivers, such as future volcanic eruptions, cannot be included in the GCM simulations, and the representation of biospheric feedbacks on GHG forcing, such as increased occurrence of forest fires, and accelerated oxidation of peatland soils, are represented very simplistically, if at all.

Carbon Dioxide Concentration Scenarios

The question might be posed: "Which projections of increases in atmospheric carbon dioxide (CO_2) concentration do the downscaled scenarios reported here represent?" This is not as easy to answer as it may seem because, although the original NetCDF files downloaded from PCMDI and other sites provide comprehensive metadata, most did not explicitly state whether the GHG forcing follows the ISAM or Bern-CC trajectories.

The individual scenarios of future climate developed by GCM modeling groups for the IPCC AR4 result from projections of how the world will change over the 21st century. As mentioned in the Methods section, the assumptions supporting these projections were documented by Nakićenović and others (2000) in the IPCC Special Report on Emissions (SRES) developed by Working Group III as part of the TAR. Two modeling groups developed separate global carbon cycle models (with components of GCMs, ocean carbon models, and dynamic vegetation models, including representations of historical land-use change effects, and climate change feedbacks on ocean and terrestrial processes) known as Bern-CC and ISAM. (See http://www.ipcc-data.org/ddc_co2.html and http://www.ipcc.ch/ipccreports/tar/wg1/122.htm#box37 for an overview of these models and their underlying assumptions.) These two models were used to project future global emissions of CO_2 and other GHGs for six SRES scenarios (four "marker scenarios" and two additional "illustrative scenarios"). The projected range of CO_2 concentrations for 2100 is from 550 to 970 ppm according to ISAM and from 540 to 960 ppm according to Bern-CC, which implies close agreement between the two modeling approaches. Of course, as mentioned above, none of these scenarios can be considered an accurate prediction of what may actually happen. In principle, all six scenarios, and underlying storylines of population growth and economic and technological development from which the concentration projections are derived, could be considered equally likely—depending on one's views of these possible paths for global society.

For all four GCMs considered in this report, however, the metadata refer to the "720 ppm stabilization experiment" and "550 ppm stabilization experiment" for the A1B and B1 projections, respectively. This implies closer agreement with the ISAM trajectories for A1B and B1, which reach 717 and 549 ppm in 2100, respectively, compared to 703 and 540 ppm according to Bern-CC. However, in the specific case of CGCM31MR, the metadata for A1B (see Appendix 1) state: "The CO_2 concentrations are from the Bern-CC model." Stabilization concentrations are not given in the metadata for the A2 projections—because, according to the A2 scenario, GHG emissions are assumed to continue growing and stabilization in 2100 is unlikely. In general, we recommend the ISAM trajectories be used where CO_2 concentration data are needed for an impacts assessment, though in practice either data set is likely to be acceptable.

Conclusions

The data sets are valuable for use in models and assessment frameworks that need climate variables as inputs. Twelve model/scenario combinations are presented to offer a variety of futures for assessing possible effects of a changing climate on natural resources, ecosystems,

human infrastructure, and communities. These data sets capture the trends of a projected climate and each should be considered a plausible outcome under a set of assumptions that we encourage the user to understand. Data are presented as grids and may be used in models to determine effects at scales similar to the grid-cell size. Reporting of spatial and temporal trends is meaningful across an aggregation of grid cells. For example, the timing of extreme values simulated for any given grid cell should be considered as a general indicator of future possibilities in that region, but not as a precise forecast of extreme events at that specific location.

Given the less predictable nature of precipitation and the known limitations in the capacity of GCMs to simulate precipitation patterns accurately, the agreement among the four GCMs in their simulations of observed data (when expressed at seasonal scales) was surprisingly good. Further, projections of future precipitation were generally similar among models and forcing scenarios, though MIROC32MR was a notable exception for the southern states, where it projected a future climate with substantially lower precipitation than the other GCMs. Consistency among model projections for temperature and precipitation probably also explained the good general agreement among models in projections of small changes in solar radiation, which typically were inversely related with the projected trends in precipitation. This is expected, because trends in simulated precipitation are related to vapor condensation as cloud and, hence, inversely related to solar radiation arriving at the earth's surface.

The different GCMs generally were similar in their projections of future changes in vapor pressure, although the MIROC32MR often showed relatively little change compared with other models, particularly during summer in the south. This difference is consistent with that model's projections of reduced summer precipitation in the same regions.

There was general agreement among the models that changes in mean wind speeds will be relatively small, but this result varied regionally and seasonally. There was some evidence that greater warming (i.e., as would result from the A1B or A2 emissions scenarios) would cause greater increases in wind speed in regions and seasons where some sensitivity occurs. In general, projected changes in interannual variability of wind speeds were small and the relationships were inconsistent across regions, seasons, and GHG forcing scenarios.

The climate projection data are available through the web for analysts who wish to use the data as input to climate change impact models, or for summaries at regional and national scales. The data are archived at http://www.fs.fed.us/rm/data_archive/.

References

Bailey, R. G. 1995. Description of the ecoregions of the United States (2nd ed.). Miscellaneous Publication No. 1391. Washington, DC: U.S. Department of Agriculture, Forest Service,.108 pp. + Map scale 1:7,500,000.

Conway, D.; Jones, P. D. 1998. The use of weather types and air flow indices for GCM downscaling. Journal of Hydrology 212–213(1–4): 348–361.

Coulson, D. P.; Joyce, L.A. 2010. Historical climate data (1940-2006) for the conterminous United States at the 5 arcminute grid spatial scale based on PRISM climatology. Fort Collins, CO: U.S. Department of Agriculture, Forest Service, Rocky Mountain Research Station. Available: http://www.fs.fed.us/rm/data_archive/dataaccess/US_HistClimateScenarios_grid_PRISM.shtml.

Daly, C.; Neilson, R. P.; Phillips, D. I. 1994. A statistical-topographic model for mapping climatological precipitation over mountainous terrain. Journal of Applied Meteorology 33: 140–158.

Fowler, H. J.; Blenkinsop, S.; Tebaldi, C. 2007. Linking climate change modeling to impacts studies: recent advances in downscaling techniques for hydrological modeling. International Journal of Climatology 27: 1547-1578.

Gibson, W.; Daly, C.; Kittel, T.; Nychka, D.; Johns, C.; Rosenbloom, N.; McNab, A.; Taylor, G. 2002. Development of a 103-year high-resolution climate data set of the conterminous United States. Proceedings of the 13th AMS Conference on Applied Climatology; May 13-16; Portland, OR. Washington, DC: American Meteorological Society,: 181-183. Available: http://ams.confex.com/ams/13ac10av/techprogram/programexpanded_99.htm or http://prism.oregonstate.edu/docs/index.phtml.

Hashmi, M. Z.; Shamseldin, A. Y.; Melville, B. W. 2009. Statistical downscaling of precipitation: state-of-the-art and application of Bayesian multi-model approach for uncertainty assessment. Hydrology and Earth System Sciences Discussions 6: 6535–6579. Available :http://www.hydrol-earth-syst-sci-discuss.net/6/6535/2009/hessd-6-6535-2009-discussion.html [28 July 2010].

Hijmans, R.; Cameron, S. E.; Parra, J.; Jones, P.; Jarvis, A. 2005. Very high resolution interpolated climate surface for global land areas. International Journal of Climatology 25: 1965–1978.

Houlder, D. J.; Hutchinson, M. F.; Nix, H. A.; McMahon, J. P. 2000. ANUCLIM user guide, Version 5.1. Centre for Resource and Environmental Studies, Australian National University, Canberra, Australia.

Hutchinson, M. F. 1995. Interpolating mean rainfall using thin plate smoothing splines. International Journal of GIS 9(4): 385–403.

Hutchinson M. F. 1998a. Interpolation of rainfall data with thin plate smoothing splines: I. Two dimensional smoothing of data with short range correlation. Journal of Geographic Information and Decision Analysis 2(2): 152–167.

Hutchinson M. F. 1998b. Interpolation of rainfall data with thin plate smoothing splines: II. Analysis of topographic dependence. Journal of Geographic Information and Decision Analysis 2(2): 168–185.

Hutchinson, M. F. 2010. ANUSPLIN Version 4.0. Available: http://fennerschool.anu.edu.au/publications/software/anusplin.php [28 July 2010].

Hutchinson, M. F.; Gessler, P. E. 1994. Splines-more than just a smooth interpolator. Geoderma 62: 45–67.

Hutchinson, M. F.; McKenney D. W.; Lawrence, K.; Pedlar, J. H.; Hopkinson, R. F.; Milewska, E.; Papadopol, P. 2009. Development and testing of Canada-wide interpolated spatial models of daily minimum–maximum temperature and precipitation for 1961–2003. Journal of Applied Meteorology and Climatology 48: 726–741.

[IPCC]Intergovernmental panel on Climate Change. 2007. Summary for policymakers. In: Solomon, S.; Qin, D.; Manning, M.; Chen, Z.; Marquis, M.; Averyt, K. B.; Tignor, M.; Miller, H. L., eds. Climate change 2007: The physical science basis. contribution of Working Group I to the Fourth Assessment Report of the Intergovernmental Panel on Climate Change.. Cambridge University Press, Cambridge, United Kingdom.

[IPCC-TGICA] Task Group on Data and Scenario Support for Impact and Climate Assessment; Intergovernmental Panel on Climate Change. 2007. General Guidelines on the Use of Scenario Data for Climate Impact and Adaptation Assessment. Version 2. Prepared by T.R. Carter on behalf of the Intergovernmental Panel on Climate Change, Task Group on Data and Scenario Support for Impact and Climate Assessment. Available at http://www.ipcc-data.org/guidelines/index.html, accessed 3/14/2011. 66 pp.

Jensen, M. E.; Burman , R. D.; Allen, R. G., eds. 1990. Evapotranspiration and irrigation water requirements. New York, NY: American Society of Civil Engineering.

Joyce, L. A. 2007. Climate change impacts on forestry. Chapter 14. In: Adams, D. M.; Haynes, R. W., eds. Resource and market projections for forest development: Twenty-five years' experience with the U.S. RPA timber assessment. Dordrecht, The Netherlands: Springer: 451–490.

Joyce, Linda A.; Price, David T.; Coulson, David P.; McKenney, Daniel W.; Siltanen, R. Martin; Papadopol, Pia; Lawrence, Kevin. (In process). Projecting climate change in the United States: A technical document supporting the Forest Service 2010 RPA Assessment. Fort Collins, CO: U.S. Department of Agriculture, Forest Service, Rocky Mountain Research Station.

Kang, B.; Ramírez, J. A. 2010, A coupled stochastic space-time intermittent random cascade model for rainfall downscaling, Water Resources Research 46. W10534, doi:10.1029/2008WR007692

Missing Kittel 1995 reference

Kittel, T. G. F.; Rosenbloom, N. A.; Royle, J. A.; Daly, C.; Gibson, W. P.; Fisher, H. H.; Thornton, P.; Yates, D. N.; Aulenbach, S.; Kaufman, C.; McKeown, R.; Bachelet, D.; Schimel, D. S. 2004. The VEMAP Phase 2 bioclimatic database. I: A gridded historical (20th century) climate dataset for modeling ecosystem dynamics across the conterminous United States. Climate Research 27:151-170.

Lawrence, K.; Hutchinson, M.; McKenney, D. 2007. Multi-scale Digital elevation models for Canada. Frontline Technical Report No. 109. Sault Ste. Marie, Ontario, Canada: Natural Resources Canada, Canadian Forest Service, Great Lakes Forestry Centre.

Mackey, B. G.; McKenney, D. W.; Yang, Y. Q.; McMahon, J. P.; Hutchinson, M. F. 1996. Site regions revisited: A climatic analysis of Hill's site regions for the province of Ontario using a parametric method. Canadian Journal of Forest Research 26: 333–354.

McKenney, D. W.; Hutchinson, M. F.; Kesteven, J. L.; Venier, L. A. 2001. Canada's plant hardiness zones revisited using modern climate interpolation techniques. Canadian Journal of Plant Science 81: 129–143.

McKenney, D. W.; Hutchinson, M. F.; Papadopol, P.; Price, D. T. 2004. Evaluation of alternative spatial models of vapour pressure in Canada. In: Proceedings of the American Meteorological Society 26th Conference on Agricultural Forest Meteorology; 23–26 August 2004; Vancouver, BC. Boston, MA: American Meteorological Society: 6.2.1–6.2.11. Available: http://ams.confex.com/ams/AFAPURBBIO/ techprogram/ paper_78201.htm [28 July 2010].

McKenney, D. W.; Papadapol, P.; Campbell, K.; Lawrence, K.; Hutchinson, M. 2006a. Spatial models of Canada- and North America-wide 1971/2000 minimum and maximum temperature, total precipitation and derived bioclimatic variables. Frontline Technical Note 106. Sault Ste. Marie, Ontario, Canada: Canadian Forestry Service, Great Lakes Forestry Centre. 9 pp.

McKenney, D. W.; Pedlar, J. H.; Papadopol, P.; Hutchinson, M. F. 2006b. The development of 1901–2000 historical monthly climate models for Canada and the United States. Agricultural and Forest Meteorology 138: 69–81.

McKenney, D. W.; Price, D. T.; Papadapol, P.; Siltanen, M; Lawrence, K. 2006c. High-resolution climate change scenarios for North America. Frontline Technical Note 107. Sault Ste. Marie, Ontario, Canada: Canadian Forestry Service, Great Lakes Forestry Centre. 6 pp.

McKenney, D.; Papadopol, P.; Lawrence, K.; Campbell, K.; Hutchinson, M. 2007. Customized spatial climate models for Canada. Frontline Technical Note No. 108. Sault Ste. Marie, Ontario, Canada: Great Lakes Forestry Centre, Natural Resources Canada, Canadian Forest Service. 7 pp.

Meehl, G. A.; Covey, C.; Delworth, T.; Latif, M.; McAvaney, B.; Mitchell, J. F. B.; Stouffer, R. J.; Taylor, K. E. 2007. The WCRP CMIP3 multimodel dataset: A New Era in Climate Change Research. Bulletin of the American Meteorological Society 88(9): 1383-1394.

Monteith, J. L.; Unsworth, M. H. 2008. Principles of environmental physics. Third Edition. Amsterdam: Academic Press, Elsevier. 418 pp.

Nakićenović, N.; Alcamo, J.; Davis, G.; de Vries, B.; Fenhann, J.; Gaffin, S.; Gregory, K.; Grübler, A.; Jung, T. Y.; Kram, T.; La Rovere, E. L.; Michaelis, L.; Mori, S.; Morita, T.; Pepper, W.; Pitcher, H.; Price, L.; Raihi, K.; Roehrl, A.; Rogner, H.-H.; Sankovski, A.; Schlesinger, M.; Shukla, P.; Smith, S.; Swart, R.; van Rooijen, S.; Victor, N.; Dadi, Z. 2000. Emissions scenarios. A special report of Working Group III of the Intergovernmental Panel on Climate Change. Cambridge University Press, Cambridge, United Kingdom. 599 pp. Available: http://www.grida.no/publications/other/ipcc_sr/?src=http://www.grida.no/climate/ipcc/ [28 July 2010].

New, M.; Lister, D.; Hulme, M.; Makin, I. 2002. A high-resolution data set of surface climate over global land areas. Climate Research 21(1): 1–25.

Price, D. T.; McKenney, D. W.; Nalder, I. A.; Hutchinson, M. F.; Kestevan, J. L. 2000. A comparison of statistical and thin-plate spline methods for spatial interpolation of Canadian monthly mean climate data. Agricultural and Forest Meteorology 101: 81–94.

Price, D. T.; McKenney, D. W.; Caya, D.; Flannigan, M. D.; Côté, H. 2001. Transient climate change scenarios for high resolution assessment of impacts on Canada's forest ecosystems. Final report to Climate Change Action Fund, June 2001. Available: http://www.cics.uvic.ca/scenarios/index.cgi?Other_Data#transienthighres [28 July 2010].

Price, D. T.; McKenney, D. W.; Papadopol, P.; Logan, T.; Hutchinson, M. F. 2004. High resolution future scenario climate data for North America. Pages 7.7.1–7.7.13 in Proc. Amer. Meteorol. Soc. 26th Conf. Agric. For. Meteorol., 23–26 August 2004, Vancouver, B.C., Am. Meteorol. Soc., Boston, MA. http://ams.confex.com/ams/AFAPURBBIO/techprogram/ paper_78202.htm accessed 28 July 2010.

Price, D. T.; Scott, D. 2006. Large scale modelling of Canada's forest ecosystem responses to climate change. Final Report on Climate Change Action Fund Project A636, Climate Change Impacts and Adaptation Program, June 2006. http://adaptation.nrcan.gc.ca/projdb/ pdf/116_e.pdf accessed 28 July 2010.

Price, D. T.; McKenney, D. W.; Joyce, Linda A.; Siltanen, R. M.; Papadopol, P.; Lawrence, K. (In process). High resolution interpolation of climate scenarios for Canada derived from general circulation models. Natural Resources Canada, Canadian Forest Service, Northern Forestry Center, Edmonton, Alberta. Inf. Rep. NOR-X-2011 135 p.

Randall, D. A.; Wood, R. A.; Bony, S.; Colman, R.; Fichefet, T.; Fyfe, J.; Kattsov, V.; Pitman, A.; Shukla, J.; Srinivasan, J.; Stouffer, R. J.; Sumi, A.; Taylor, K. E. 2007. Climate models and their evaluation. In: Solomon, S.; Qin, D.; Manning, M.; Chen, Z.; Marquis, M.; Averyt, K. B.; Tignor, M.; Miller, H. L., eds. Climate change 2007: The physical science basis. contribution of Working Group I to the Fourth Assessment Report of the Intergovernmental Panel on Climate Change.. Cambridge University Press, Cambridge, United Kingdom..

Rehfeldt, G. E. 2006. A spline model of climate for the western United States. Gen. Tech. Rep. RMRS-GTR-165. Fort Collins, CO: U.S. Department of Agriculture, Forest Service, Rocky Mountain Research Station. 21 p.

Semenov, M. A.; Barrow, E. M. 1997. Use of a stochastic weather generator in the development of climate change scenarios. Climatic Change 35: 397–414.

USDA Forest Service. (In press). Future Scenarios and Assumptions for the 2010 Resource Planning Act (RPA) Assessment. WO-GTR-XXX. Washington, DC: U.S. Department of Agriculture, Forest Service.

Wilby, R. L.; Dawson, C. W.; Barrow, E. M. 2002: SDSM—A decision support tool for the assessment of regional climate change impacts. Environmental Modelling and Software 17: 145–157.

Wilby, R. L.; Charles, S. P.; Zorita, E.; Timbal, B.; Whetton, P.; Mearns, L. O. 2004. Guidelines for use of climate scenarios developed from statistical downscaling methods. Supporting material of the Intergovernmental Panel on Climate Change, Task Group on Data and Scenario Support for Impacts and Climate Analysis (TGICA). 27 p. Available: http://www.ipcc-data.org/guidelines/dgm_no2_v1_09_2004.pdf accessed 28 July 2010.

Wilks, D. S.; Wilby, R. L. 1999. The weather generation game: A review of stochastic weather models. Progress in Physical Geography 23(3): 329–357.

Williams, J. W.; Jackson, S. T.; Kutzbach, J. E. 2007. Projected distributions of novel and disappearing climates by 2100 AD. Proceedings of the National Academy of Sciences 104(14): 5738–5742.

Appendix I

Examples of metadata embedded in the GCM NetCDF files downloaded from the data portal of the Program for Climate Model Diagnosis and Intercomparison (PCMDI) Climate Model Intercomparison Project 3 (CMIP3). These metadata were obtained directly from the data files used to create the input data for interpolation by ANUSPLIN (using ncdump –h <fname>), and hence can be considered sample documentation of the GCM simulation results used to create all of the climate scenario products described in this report.

NCAR-CCSM3.0

```
:table_id = “Table A1” ;
:title = “model output prepared for IPCC AR4” ;
:institution = “NCAR (National Center for Atmospheric \n”,
    “Research, Boulder, CO, USA)” ;
:source = “CCSM3.0, version beta19 (2004): \n”,
    “atmosphere: CAM3.0, T85L26;\n”,
    “ocean : POP1.4.3 (modified), gx1v3\n”,
    “sea ice   : CSIM5.0, T85;\n”,
    “land  : CLM3.0, gx1v3” ;
:contact = “ccsm@ucar.edu” ;
:project_id = “IPCC Fourth Assessment” ;
:Conventions = “CF-1.0” ;
:references = “Collins, W.D., and others, 2005:\n”,
    “ The Community Climate System Model, Version 3\n”,
    “ Journal of Climate\n”,
    “ \n”,
    “ Main website: http://www.ccsm.ucar.edu” ;
:acknowledgment = “ Any use of CCSM data should acknowledge the contribution\n”,
    “ of the CCSM project and CCSM sponsor agencies with the \n”,
    “ following citation:\n”,
    “ \’This research uses data provided by the Community Climate\n”,
    “ System Model project (www.ccsm.ucar.edu), supported by the\n”,
    “ Directorate for Geosciences of the National Science Foundation\n”,
    “ and the Office of Biological and Environmental Research of\n”,
    “ the U.S. Department of Energy.\’\n”,
    “In addition, the words \’Community Climate System Model\’ and\n”,
    “ \’CCSM\’ should be included as metadata for webpages referencing\n”,
    “ work using CCSM data or as keywords provided to journal or book\n”,
    “publishers of your manuscripts.\n”,
    “Users of CCSM data accept the responsibility of emailing\n”,
    “ citations of publications of research using CCSM data to\n”,
    “ ccsm@ucar.edu.\n”,
    “Any redistribution of CCSM data must include this data\n”,
    “ acknowledgement statement.” ;
:realization = 5 ;
:experiment_id = “720 ppm stabilization experiment (SRES A1B)” ;
:history = “Created from CCSM3 case b30.040e\n”,
    “ by strandwg@ucar.edu\n”,
    “ on Thu Dec  9 12:52:07 MST 2004\n”,
    “ \n”,
    “ For all data, added IPCC requested metadata” ;
:comment = “This simulation was initiated from year 2000 of \n”,
    “ CCSM3 model run b30.030e and executed on \n”,
    “ hardware bluesky.ucar.edu. The input external forcings are\n”,
    “ozone forcing: A1B.ozone.128x64_L18_1991-2100_c040528.nc\n”,
    “aerosol optics   : AerosolOptics_c040105.nc\n”,
```

```
“aerosol MMR  : AerosolMass_V_128x256_clim_c031022.nc\n”,
“carbon scaling   : carbonscaling_A1B_1990-2100_c040609.nc\n”,
“solar forcing: Fixed at 1366.5 W m-2\n”,
“GHGs         : ghg_ipcc_A1B_1870-2100_c040521.nc\n”,
“GHG loss rates   : noaamisc.r8.nc\n”,
“volcanic forcing : none\n”,
“DMS emissions: DMS_emissions_128x256_clim_c040122.nc\n”,
“oxidants     : oxid_128x256_L26_clim_c040112.nc\n”,
“SOx emissions: SOx_emissions_A1B_128x256_L2_1990-2100_c040608.nc\n”,
“ Physical constants used for derived data:\n»,
“ Lv (latent heat of evaporation): 2.501e6 J kg-1\n»,
“ Lf (latent heat of fusion     ): 3.337e5 J kg-1\n»,
“ r[h2o] (density of water      ): 1000 kg m-3\n»,
“ g2kg   (grams to kilograms    ): 1000 g kg-1\n»,
“ \n»,
“ Integrations were performed by NCAR and CRIEPI with support\n»,
“ and facilities provided by NSF, DOE, MEXT and ESC/JAMSTEC.» ;
```

MIROC3.2mr

```
:title = “CCSR/NIES/FRCGC  model output prepared for IPCC Fourth Assessment climate of the
20th Century experiment (20C3M)”
institution = “CCSR/NIES/FRCGC (Center for Climate System Research, Tokyo, Japan / National
Institute for
Environmental Studies, Ibaraki, Japan / Frontier Research Center for Global Change, Kanagawa,
Japan)”

:source = “MIROC3.2 (2004): atmosphere: AGCM (AGCM5.7b, T42 L20); ocean & sea ice: COCO
(COCO3.3, 256x192 L44); land: MATSIRO (T42)” ;
:contact = “Toru Nozawa (nozawa@nies.go.jp)”
:project_id = “IPCC Fourth Assessment” ;
:table_id = “Table A1 (8 October 2004)” ;
:experiment_id = “climate of the 20th Century experiment (20C3M)” ;
:realization = 3 ;
:cmor_version = 0.96f ;
:Conventions = “CF-1.0” ;
:history = “output from MIROC3.2  At 20:53:37 on 10/14/2004, CMOR rewrote data to comply with
CF standards and IPCC Fourth Assessment requirements” ;
:references = “K-1 Coupled GCM Description (K-1 Technical Report No.1) in preparation” ;
:comment = “This run was initiated after 300-year spin-up of the coupled model from an
arbitrary chosen initial condition (a snapshot result of a previous version of the model). The
preceding spinup was forced by fixed external conditions for the year 1850, including solar
and volcanic forcings, GHGs concentration, various aerosols emissions and land use, while all
those conditions were changed according to historical data during the 20C in the course of
this run.” ;
```

CGCM3.1mr

```
:title = “CCCma  model output prepared for IPCC Fourth Assessment 720 ppm stabilization
experiment (SRES A1B)” ;
:institution = “CCCma (Canadian Centre for Climate Modelling and Analysis, Victoria, BC,
Canada)” ;
:source = “CGCM3.1 (2004): atmosphere:  AGCM3 (GCM13d, T47L31); ocean: CCCMA
(OGCM3.1,192x96L29)” ;
:contact = “Greg Flato (Greg.Flato@ec.gc.ca)” ;
:project_id = “IPCC Fourth Assessment” ;
```

:table_id = “Table A1 (17 November 2004)” ;
:experiment_id = “720 ppm stabilization experiment (SRES A1B)” ;
:realization = 5 ;
:cmor_version = 0.96f ;
:Conventions = “CF-1.0” ;
:history = “ At 20:30:10 on 06/07/2005, CMOR rewrote data to comply with CF standards and IPCC Fourth Assessment requirements” ;
:comment = “This model run continues from the end of the 20th century simulation with GHG and aerosol loadings for the IPCC SRES A1B scenario as tabulated in the IPCC Third Assessment Report, Appendix II. The CO2 concentrations are from the Bern-CC model (Contribution of Working Group I to the Third Assesment Report of IPCC, p808) and the aerosol loadings are from O. Boucher, Laboratoire d\’Optique Atmospherique, France. For years 2101-2300, all GHG concentrations and the aerosol loading are held constant at the values obtained by extrapolation to year 2101.” ;

CSIRO Mk 3.5

:title = “CSIRO model output prepared for IPCC Fourth Assessment” ;
:institution = “CSIRO (CSIRO Atmospheric Research, Melbourne, Australia)” ;
:source = “CSIRO Mk3.5d (2005): atmosphere: spectral (T63L18); ocean: MOM2.2 (1.875x0.925L31)” ;
:contact = “Mark Collier (Mark.Collier@csiro.au), Martin Dix (Martin.Dix@csiro.au), Tony Hirst (Tony.Hirst@csiro.au)” ;
:project_id = “IPCC Fourth Assessment” ;
:experiment_id = “720 ppm stabilization experiment (SRES A1B)” ;
:realization = 1 ;
:Conventions = “CF-1.0” ;
:references = “Model described by Gordon and others The CSIRO Mk3 Climate System Model, 2002, www.dar.csiro.au/publications/gordon_2002a.pdf” ;
:comment = “SRES A1B experiment with CSIRO Mk 3.5d model, starting from year 2000 (model year 300) of 20C3M experiment. Radiative forcings held constant from year 2100.” ;
:history = “Date/Time stamp=year:2006:month:04:day:11:hour:06:minute:04:second:59:UTC. Processed from model output using tcl-nap version 8.4.” ;
:table_id = “Table A1a” ;

The Rocky Mountain Research Station develops scientific information and technology to improve management, protection, and use of the forests and rangelands. Research is designed to meet the needs of the National Forest managers, Federal and State agencies, public and private organizations, academic institutions, industry, and individuals. Studies accelerate solutions to problems involving ecosystems, range, forests, water, recreation, fire, resource inventory, land reclamation, community sustainability, forest engineering technology, multiple use economics, wildlife and fish habitat, and forest insects and diseases. Studies are conducted cooperatively, and applications may be found worldwide.

Station Headquarters
Rocky Mountain Research Station
240 W Prospect Road
Fort Collins, CO 80526
(970) 498-1100

Research Locations

Flagstaff, Arizona	Reno, Nevada
Fort Collins, Colorado	Albuquerque, New Mexico
Boise, Idaho	Rapid City, South Dakota
Moscow, Idaho	Logan, Utah
Bozeman, Montana	Ogden, Utah
Missoula, Montana	Provo, Utah

www.fs.fed.us/rmrs